

2013

Shrinkage and cracking behavior of HPC used for bridge deck overlays

Hasitha Bandara Seneviratne
Iowa State University

Follow this and additional works at: <https://lib.dr.iastate.edu/etd>

 Part of the [Civil Engineering Commons](#)

Recommended Citation

Seneviratne, Hasitha Bandara, "Shrinkage and cracking behavior of HPC used for bridge deck overlays" (2013). *Graduate Theses and Dissertations*. 13422.
<https://lib.dr.iastate.edu/etd/13422>

This Thesis is brought to you for free and open access by the Iowa State University Capstones, Theses and Dissertations at Iowa State University Digital Repository. It has been accepted for inclusion in Graduate Theses and Dissertations by an authorized administrator of Iowa State University Digital Repository. For more information, please contact digirep@iastate.edu.

Shrinkage and cracking behavior of HPC used for bridge deck overlays

by

Hasitha Bandara Seneviratne

A thesis submitted to the graduate faculty
in partial fulfillment of the requirement for the degree of

MASTER OF SCIENCE

Major: Civil Engineering (Civil Engineering Materials)

Program of Study Committee:

Kejin Wang, Major Professor

Sri Sritharan

R Christopher Williams

Iowa State University

Ames, Iowa

2013

Copyright © Hasitha Bandara Seneviratne, 2013. All rights reserved.

TABLE OF CONTENTS

LIST OF FIGURES	iv
LIST OF TABLES	ix
ACKNOWLEDGEMENT	xi
ABSTRACT	xii
CHAPTER 1. INTRODUCTION	1
1.1 Organization of Thesis	1
1.2 Problem Statement	1
1.3 Objective of thesis	2
CHAPTER 2. LITERATURE REVIEW	3
2.1 Shrinkage of Cement Concrete	3
2.2 Factors Effecting Shrinkage of Concrete	8
2.2.1 Effect of cementitious materials	8
2.2.2 Effect of aggregates	14
2.2.3 Effect of admixtures	17
2.2.4 Factors Influencing Drying Shrinkage and Restrained Cracking	18
2.3 Prediction Models for Creep	20
2.3.1 B3 model	20
2.3.2 Modified NCHRP 496 model	22
2. 4 Restrained Shrinkage	22
CHAPTER 3. MATERIALS AND EXPERIMENTS	26
3.1 Materials	26
3.2 Mix Proportions	28
3.3 Experiments	31
3.3.1 Autogenous shrinkage test	31
3.3.2 Free drying shrinkage test	32
3.3.3 Restrained ring shrinkage test	32
3.3.4 Strength and elastic modulus test	34
CHAPTER 4. RESULTS AND ANALYSIS	35
4.1 Autogenous Shrinkage	35
4.2 Free Drying Shrinkage	38

4.2.1 Mass loss of the specimens for free drying shrinkage test	38
4.2.2 Free drying shrinkage	41
4.3 Restrained Ring Shrinkage	45
4.4 Mechanical Strength Parameters.....	50
4.4.1 Compressive strength	50
4.4.2 Elastic modulus.....	53
4.4.3 Split tensile strength	55
4.5 Relationships among Test Results	57
4.5.1 Free drying shrinkage and mass loss of concrete	57
4.5.3 Restrained drying and free drying shrinkage stress of concrete	58
4.5.4 Relationships among strength parameters	60
4.6 Concrete Cracking Potential	61
4.7 Finite Element Analysis.....	64
4.7.1 Modeling stress due to creep in midas Civil.....	66
4.7.2 Results and observations	67
4.8 Summary of Results	70
CHAPTER 5. CONCLUSIONS AND RECOMMENDATIONS	72
5.1 Recommendations.....	73
Bibliography	75
Appendix	78
Test Measurements	78
Autogenous shrinkage measurements	78
Free shrinkage measurements.....	82
Restrained shrinkage measurements.....	86
Compressive strength	90
Elastic modulus.....	90
Split tensile strength	91
Prediction Models for Creep.....	91
B3 Model	91
Modified NCHRP 496 Model.....	95
Developing the finite element model in MIDAS 2013	96

LIST OF FIGURES

Figure 1 Plastic shrinkage cracking at the surface of concrete flatwork: (a) Surface Plastic shrinkage crack; and (b) plastic settlement cracks (Soroushian, 1998)	3
Figure 2 Chemical shrinkage (Tazawa, 1999)	4
Figure 3 Autogenous shrinkage (Tazawa E., 1999).....	5
Figure 4 Relation between calculated and measured autogenous shrinkage (Tazawa E., 1997).....	6
Figure 5 Distribution of solids and pores in hydrated cement paste (Mehta and Monteiro, 2003)	7
Figure 6 Schematic diagram of drying shrinkage	7
Figure 7 Influence of cement type on autogenous shrinkage (Tazawa, 1997)	8
Figure 8 Shrinkage of OPC and Expansive cements concrete (Satio, 1991).....	9
Figure 9 Creep (a) and drying shrinkage strains of HPC (Jianyong, 2001).....	9
Figure 10 Autogenous shrinkage (a) and drying shrinkage (b) of concrete with fly ash (Nakarai, 2009)	10
Figure 11 Development of restrained stress (Miyazawa, 2009)	10
Figure 12 Effect of curing and w/c ratio on drying shrinkage of silica fume concrete (Whiting, 2000).....	11
Figure 13 Effect of metakaolin on (a) early age (<24hrs), (b) after 24hrs and (c) total autogenous shrinkage (Brooks, 2001).....	12
Figure 14 Effect of metakaolin on (a) total shrinkage and (b) pure drying shrinkage of concrete (Brooks, 2001)	13
Figure 15 Effect of nano limestone and micro limestone on (a) drying shrinkage and (b) mass loss (Camiletti, 2013)	13
Figure 16 Effect of aggregate concentration on shrinkage of concrete (Powers, 1971).....	14
Figure 17 Relationship between shrinkage at 2 years and secant modulus of elasticity of concrete at 28 days (Reichard, 1964)	15
Figure 18 Drying shrinkage of HPC with and without SRA (Quangphu, 2008).....	18
Figure 19 Ring tests mold (a) cast specimen (b).....	23

Figure 20 An example of measuring ring strain vs. specimen age	23
Figure 21 Particle size distribution of coarse and fine aggregate	27
Figure 22 Mold, length comparator, and concrete specimens stored in the environment chamber.....	31
Figure 23 Length measurements of concrete specimens	32
Figure 24 Standard dimensions of the ring test setup (ASTM Standard C1581, 2008)	33
Figure 25 Ring steel mold (a) concrete ring specimen (b) and data logger setup (c)	33
Figure 26 Autogenous Shrinkage of Concrete (Group1).....	35
Figure 27 Autogenous Shrinkage of Concrete (Group 2).....	36
Figure 28 Autogenous Shrinkage of Concrete (Group 3).....	37
Figure 29 Autogenous Shrinkage of Concrete (Group 4).....	37
Figure 30 Autogenous Shrinkage of Concrete at 56 day for all mixes	38
Figure 31 Mass loss of Concrete (Group 1).....	39
Figure 32 Mass loss of Concrete (Group 2).....	39
Figure 33 Mass loss of Concrete (Group 3).....	40
Figure 34 Mass loss of Concrete (Group 4).....	40
Figure 35 Typical free drying shrinkage measurement of mix 5.....	41
Figure 36 Typical free drying shrinkage measurement of mix 11	41
Figure 37 Free Drying Shrinkage of Concrete (Group 1).....	42
Figure 38 Free Drying Shrinkage of Concrete (Group 2).....	43
Figure 39 Free Drying Shrinkage of Concrete (Group 3).....	43
Figure 40 Free Drying Shrinkage of Concrete, Group 4	44
Figure 41 Free Drying Shrinkage of Concrete at 56 days	44
Figure 42 Free Drying Shrinkage vs. Mass loss (%)	45
Figure 43 Typical result of restrained shrinkage Mix 10.....	46
Figure 44 Restrained Shrinkage of Group 1	46

Figure 45 Restrained Shrinkage of Group 2	47
Figure 46 Restrained Shrinkage of Group 3	48
Figure 47 Restrained Shrinkage of Group 4	48
Figure 48 Compressive strength of concrete Group 1-4.....	52
Figure 49 Elastic modulus of concrete Group 1-4.....	54
Figure 50 Split tensile strength of concrete Group 1-4.....	56
Figure 51 Free drying shrinkage vs. mass loss of concrete (a).....	57
Figure 52 Free drying shrinkage vs. mass loss of concrete (b).....	58
Figure 53 Ring stress vs. free drying shrinkage of c.....	60
Figure 54 Elastic modulus of concrete vs. compressive strength of concrete	61
Figure 55 Split tensile strength vs. compressive strength of concrete	61
Figure 56 Section of the deck and overlay in a slab and the finite element model of the slab	65
Figure 57 Typical axial tensile stress (σ_{xx}) pattern on the y axis.....	68
Figure 58 Axial stress (σ_{xx}) development with time in mix 1.....	68
Figure 59 Axial stress (σ_{xx}) development in the critical section for the 11 overlay mixes at 56 days.....	69
Figure 60 Mix 1 autogenous shrinkage results	78
Figure 61 Mix 2 autogenous shrinkage results	78
Figure 62 Mix 3 autogenous shrinkage results	79
Figure 63 Mix 4 autogenous shrinkage results	79
Figure 64 Mix 5 autogenous shrinkage results	79
Figure 65 Mix 6 autogenous shrinkage results	80
Figure 66 Mix 7 autogenous shrinkage results	80
Figure 67 Mix 8 autogenous shrinkage results	80
Figure 68 Mix 9 autogenous shrinkage results	81

Figure 69 Mix 10 autogenous shrinkage results	81
Figure 70 Mix 11 autogenous shrinkage results	81
Figure 71 Mix 1 free drying shrinkage results.....	82
Figure 72 Mix 2 free drying shrinkage results.....	82
Figure 73 Mix 3 free drying shrinkage results.....	82
Figure 74 Mix 4 free drying shrinkage results.....	83
Figure 75 Mix 5 free drying shrinkage results.....	83
Figure 76 Mix 6 free drying shrinkage results.....	83
Figure 77 Mix 7 free drying shrinkage results.....	84
Figure 78 Mix 8 free drying shrinkage results.....	84
Figure 79 Mix 9 free drying shrinkage results.....	84
Figure 80 Mix 10 free drying shrinkage results.....	85
Figure 81 Mix 11 free drying shrinkage results.....	85
Figure 82 Mix 1 restrained shrinkage results.....	86
Figure 83 Mix 2 restrained shrinkage results.....	86
Figure 84 Mix 3 restrained shrinkage results.....	87
Figure 85 Mix 4 restrained shrinkage result	87
Figure 86 Mix 5 restrained shrinkage results.....	87
Figure 87 Mix 6 restrained shrinkage results.....	88
Figure 88 Mix 7 restrained shrinkage results.....	88
Figure 89 Mix 8 restrained shrinkage results.....	88
Figure 90 Mix 9 restrained shrinkage results.....	89
Figure 91 Mix 10 restrained shrinkage results.....	89
Figure 92 Mix 11 restrained shrinkage results.....	89
Figure 93 Define unit system.....	97

Figure 94 Material property input window	97
Figure 95 Define (a) material and (b) section data	98
Figure 96 Time dependent material property: compressive strength.....	99
Figure 97 Time dependent material property: creep and shrinkage	100
Figure 98 Material link	101
Figure 99 Extrude elements	102
Figure 100 Overlay selected	103
Figure 101 All nodes parallel to x and y axes selected.....	103
Figure 102 Define supports.....	104
Figure 103 Define structure groups	104
Figure 104 Define construction stages.....	106
Figure 105 Compose construction stages	106
Figure 106 Define composite section for construction stages	106
Figure 107 Construction stage analysis control data	108

LIST OF TABLES

Table 1 Effect of various factors on concrete shrinkage (Meininger, 1966)	16
Table 2 Effect of coarse aggregate on drying shrinkage of concrete (Meininger, 1966)	16
Table 3 Factors affecting cracking.....	19
Table 4 Values of function $Q(t,t')$ for $m = 0.5$ and $n = 0.1$	21
Table 5 Theoretical analysis of effects of elastic strain rate and tensile creep on time to cracking (See, 2003)	25
Table 6 Materials used and their sources	26
Table 7 Chemical and physical properties of cementitious materials.....	27
Table 8 Gradations of coarse aggregates used	27
Table 9 Dosage of chemical admixtures	28
Table 10 HPC mixes to be used in this study	28
Table 11 Mix proportions for concrete	30
Table 12 Summary of restrained shrinkage	50
Table 13 Relationship between free drying shrinkage and moisture loss.....	58
Table 14 Rating range for concrete shrinkage	59
Table 15 Shrinkage Rating.....	59
Table 16 Concrete Shrinkage Potential.....	63
Table 17 Summary of input data for developing the model	66
Table 18 Max tensile stress (σ_{xx}) in the overlay concrete.....	69
Table 19 Stress ratio of concrete overlay.....	70
Table 20 Summary of Concrete Shrinkage.....	71
Table 21 Summary of Mechanical Properties.....	71
Table 22 Results of compressive strength test.....	90
Table 23 Results of elastic modulus test.....	90

Table 24 Results of Split tensile strength test.....	91
Table 25 Values of function $Q(t,t')$ for $m = 0.5$ and $n = 0.1$	92
Table 26 Summary of calculated creep coefficient.....	96

ACKNOWLEDGEMENT

First and foremost I want to thank Kejin Wang for providing the financial support for the successful completion of the research activities. Her support, experience and advice were instrumental in keeping me focused and in the right path to achieve my goals. Her advice helped me to improve my skills as a researcher and the exposure that she helped me gain experience in much more than one area of concrete testing.

I am grateful to Sri Sritharan for the support he gave prior to my arrival and during my stay at Iowa State University. I truly appreciate his patience with my efforts in the research work and for exposing me to the finite element analysis program MIDAS which would be a valuable asset for my future endeavors. Not to forget his advice as a committee member was extremely useful for me to accomplish my goals.

I am truly grateful to Chris Williams for serving as a committee member. Also for being one of the nicest persons I have met at ISU. I thoroughly enjoyed being in your classes as it was not only educative in subject matter but also in American history and culture.

My sincere thanks go out to everyone who has helped me to successfully complete my work. Bob Steffes, the manager at the PCC lab and Gilson Lomboy was very helpful and their advice helped me to acclimatize to the laboratory work. I have to mention Xuhao, Xin, Qizhe, Jianing Jinxin, Nishant and Jia Li who I shared the office space in Room 136 for making my stay fun and enjoyable experience.

Last but not least I would like to extend my sincere gratitude to my parents and family for being the strength behind me and motivating me all the way to achieve my goals at Iowa State University. None of this would have been possible if not for their continuous support in keeping me sane and focused at the task at hand.

ABSTRACT

High Performance Concrete (HPC) overlays have been used as a cheap and effective method of repair for bridge deck structures from wearing from traffic loadings. These HPC mixes usually consist of high amounts of cementitious materials and tend to have high tendency towards cracking induced by shrinkage. Accelerated corrosion of reinforcing steel and deterioration of deck surface are potential threats in bridge decks where cracks have occurred. Cracking potential of a mix under restraint is currently evaluated by ASTM C1581. The method looks into the rate at which the strain develops in a restrained condition to evaluate cracking potential. But a mix that develops shrinkage at a high rate may also develop strength at a higher rate, compensating the potential to cracking. This study involves investigating the use of simpler shrinkage measurements and strength characteristics to determine the cracking potential of a concrete mix.

For this investigation 11 HPC mixtures selected by the Iowa DOT which were composed of 3 cements, Type I, I/II and IP. Supplementary cementitious materials class c fly ash, slag and metakaolin were replaced by 20%, 15% and 5.6% respectively. Limestone coarse aggregate was used in 10 mixes and 1 mix with quartzite. Two gradations of coarse aggregate were used for limestone aggregates. The HPC mixes were investigated for free drying, restrained ring, elastic modulus, compressive and split tensile strength for a duration of 28 days. Average creep coefficient was calculated using the B-3 and AASHTO Report 496 (2009) models.

Restrained shrinkage and elastic modulus measured was used to calculate induced stress in full restraint which was then adjusted for creep. The stress calculated the restrained specimens were compared to the split tensile stress developed in time to check whether the stress level was above or below the strength of the mix. The results obtained showed close relationship to observed cracking in ring specimens and split tensile strength. Stress induced by free drying shrinkage under restrained conditions and restrained shrinkage samples showed a good correlation. This aids us in obtaining an understanding of restrained shrinkage through measuring free drying shrinkage, which is a relatively simple experiment to perform.

CHAPTER 1. INTRODUCTION

1.1 Organization of Thesis

The thesis contains five chapters. Chapter 1 provides an introduction into the problem of evaluating the cracking potential of concrete, a brief insight of the problem at hand and the objective of this thesis.

The second chapter covers a literature review of past studies of concrete shrinkage, its mechanisms and effects due to various different constituent materials. A general overview of volume change and an overview of structural, material and construction related effects on cracking potential is given. Some models used for estimating creep are also summarized.

Chapter 3 includes the methodology of the experiments and the experimental program conducted. It includes the description of all the cementitious materials, chemical admixtures, gradations of aggregates (coarse and fine) and the mix proportions used.

Chapter 4 discusses all the experimental results obtained. The results are summarized and analyzed to gain knowledge of possible solutions to the problem stated in section 1.2. This section includes all shrinkage test results and strength test results obtained throughout the duration of study. Further the section discusses relationships among test results obtained.

Chapter 5 concludes the thesis stating the conclusions and recommendations to the concrete mix design and testing methods that may be utilized in assessing cracking potential of concrete.

1.2 Problem Statement

The issue of volume change in concrete is inevitable. The processes that effect the volume change of concrete occur due to both chemical and physical reasons. Chemical processes are mainly the hydration of cement and physical means are drying and loading effects. Cracking induced by shrinkage of concrete is a major issue in pavement and bridge deck construction. The occurrence of cracking leads to accelerated damage and deterioration of the pavement structure due to traffic and chloride attack to reinforcement. Concrete

overlays have been adopted by state and federal governing bodies as a relatively cheap alternative to repair bridge decks.

1.3 Objective of thesis

The main objective of the work presented here is to perform a study of shrinkage cracking and cracking potential of a concrete mix. In order to understand the cracking behavior of a concrete mix experiments are conducted to determine the:

- The effects of different cements on shrinkage of HPC concrete mixes.
- The effects of supplementary cementitious materials and their combinations on shrinkage of HPC concrete mixes.
- Shrinkage cracking potential of restrained shrinkage specimens using existing test methods

CHAPTER 2. LITERATURE REVIEW

2.1 Shrinkage of Cement Concrete

There are five types of shrinkage; plastic, carbonation, chemical, autogenous and drying shrinkage. Carbonation shrinkage is a phenomenon that occurs at a low relative humidity and occurs mainly on the near surface level of the concrete. Carbonation shrinkage occurs by the reaction of $\text{Ca}(\text{OH})_2$ and CO_2 forming calcium carbonates. This results in a loss of alkalinity and has a greater influence towards forming desirable conditions for corrosion of reinforcement.

Plastic shrinkage is observed in concrete when the concrete is in a semifluid or plastic state (Wang, 2001) within the first few hours of placement. At the start of the reaction of the cement the water fills the spaces in between particles. The excess water rises to the surface and this is called bleeding water. The bleeding water forms a layer on the concrete surface. Plastic shrinkage is observed when the rate of evaporation of water exceeds the rate of water bleeding to the surface.

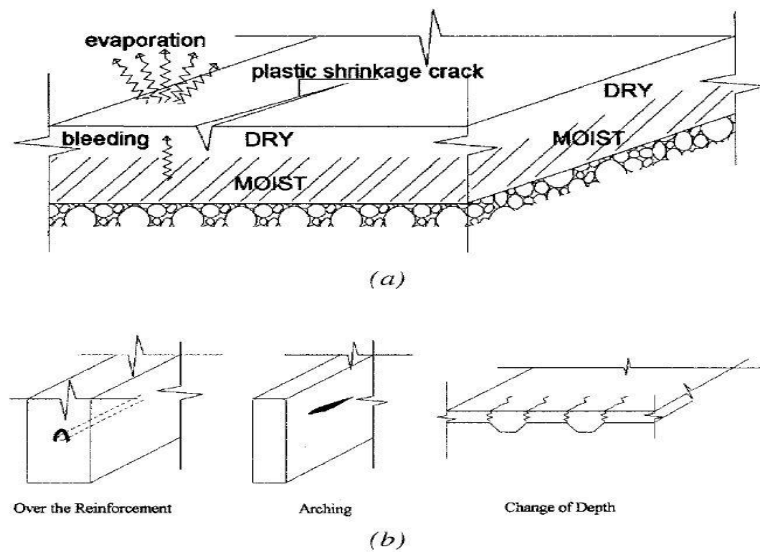


Figure 1 Plastic shrinkage cracking at the surface of concrete flatwork: (a) Surface Plastic shrinkage crack; and (b) plastic settlement cracks (Soroushian, 1998)

In a concrete mix design point of view, lower water cement ratio mixes have a greater tendency towards plastic shrinkage cracking due to the rapid setting and high rate of rigidity

development, low rate of bleeding and self-desiccation although early age tensile strength is high (Soroushian, 1998). The occurrence of plastic shrinkage can be controlled through applications of proper curing methods, wind barriers, wet burlap or providing shade from direct sunlight.

Chemical Shrinkage is the phenomena in which the absolute volume of hydration products is less than the total volume of unhydrated cement and water before hydration (Tazawa, 1999). Illustrated in Figure 2 is the absolute volume reduction known as chemical shrinkage where V_{w_i} and V_{c_i} are the initial volumes of cement and water. After the hydration process has started V_w and V_c are the volumes of the water and cement that have participated in the hydration reaction. The volume of the hydrated cement mixture is lesser than the total volume of reactants; the resulting loss of volume is the chemical shrinkage of cement.

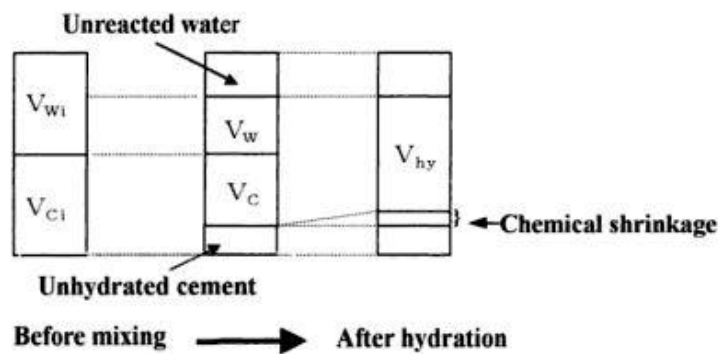


Figure 2 Chemical shrinkage (Tazawa, 1999)

Autogenous shrinkage holds a close relationship to chemical shrinkage but has a different process as it occurs after the solid skeleton has formed (Figure 3). Autogenous shrinkage is the macroscopic volume reduction of cementitious materials when cement hydrates after initial setting (Tazawa, 1999). It has also been defined as the phenomenon in which cementitious materials shrink at a constant temperature without any change in weight (Tazawa, 1995). The process of the autogenous shrinkage occurs by the removal of water in capillaries during the hydration of cement which is also known as self-desiccation. It is important to note that autogenous shrinkage occurs when there is no loss of moisture to the environment.

The issue of autogenous shrinkage is considered a significant factor in the case of high strength concretes incorporating high volumes of cementitious material, low water

cement ratios and silica fume (Jensen, 2001). The smaller capillaries and finer discontinuous microstructure of a high strength concrete compared to a normal strength concrete poses a favorable condition for higher autogenous shrinkage compared to normal strength concrete. Early observations of autogenous shrinkage (Davis, 1940) showed that the autogenous shrinkage of hardened cement concrete ranged from 50 to 100 μ strain in a period of 5 years and was considered insignificant compared to drying and thermal effects to volume change. However when sealed hydration of water cement pastes were investigated for self-desiccation, an appreciable amount of autogenous shrinkage was observed when the water cement ratio was below 0.4 (Powers, 1947).

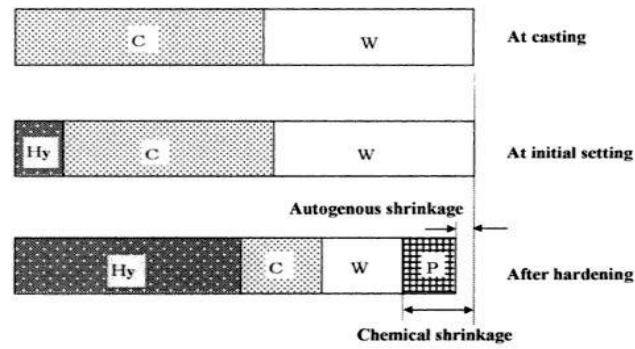


Figure 3 Autogenous shrinkage (Tazawa E., 1999)

Autogenous shrinkage can be expressed as a function of the degree of hydration and mineral composition of the cement. Tazawa and Miyazawa (1997) performed experiments to identify the influence of constituent composition on autogenous shrinkage of concrete, where 7 cement types were used. The constants of the model were obtained by the method of least squares for the observed autogenous shrinkage of the seven cements used. Method proposed by Copeland (1964) was used to calculate the degree of hydration.

$$\epsilon_{as} = -0.012\alpha_{C_3S}(t)(C_3S\%) - 0.070\alpha_{C_2S}(t)(C_2S\%) + 2.256\alpha_{C_3A}(t)(C_3A\%) + 0.859\alpha_{C_4AF}(t)(C_4AF\%)$$

The correlation between the estimated and measured values of autogenous shrinkage in Figure 4 shows that the model can be used to accurately estimate the autogenous shrinkage (ϵ_{as}) of a cement paste. The absolute values of the coefficients indicate that the mineral compounds C_3A and C_4AF have a one to two orders greater effect on autogenous shrinkage compared to C_3S and C_2S . Also the coefficients for C_3S and C_2S have a negative value indicating expansion. This indicates that the amount and hydration of C_3A and C_4AF have a greater effect towards the development of autogenous shrinkage than C_3S and C_2S .

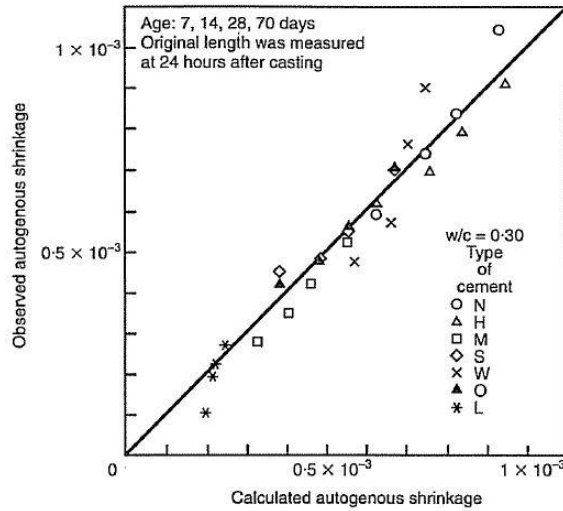


Figure 4 Relation between calculated and measured autogenous shrinkage (Tazawa E., 1997)

A concrete mix contains more water than what is required for the hydration of the cement. Water amounting to 25-30% of the mass of cement is required for the complete hydration of cement (Jennings, 2007). The excess amount of water is required for the requirement of making workable concrete [Neville (2002), Mehta and Monterio, (2003)]. The portion of water that is involved in the hydration of the cement gets chemically bonded to the cement and the rest of the water fills in the pores of the concrete structure. Drying shrinkage is the volume reduction in concrete due to migration of water to an environment that has a lower relative humidity compared to that of the initial concrete.

The drying mechanisms causing shrinkage are dependent on the internal pore spaces. Mehta and Monterio, 2003, described the various pore sizes along with the solid particles of the hydrated cement paste (Figure 5). Erika (2001) and Koenders (1997) studied the pore size distribution in concrete. The interaction of the pore spaces and internal water is influenced by the surrounding environment. During drying process of fresh concrete, the evaporation rate exceeds the amount of bleed water. Moisture is lost from the free surface exposed to the environment due to the difference in relative humidity and the drying will move into the concrete body as evaporation continues. The loss of water from the internal pores due to diffusion causes the drying shrinkage.

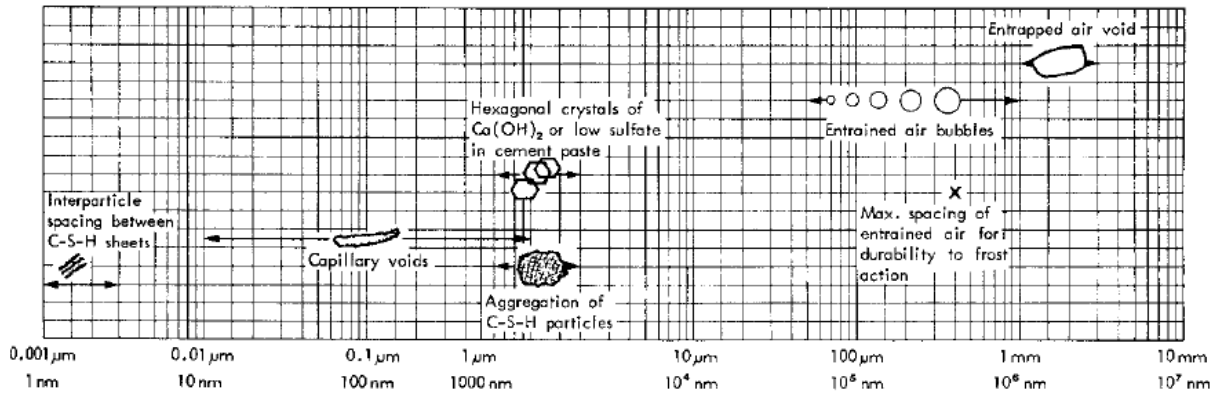


Figure 5 Distribution of solids and pores in hydrated cement paste (Mehta and Monteiro, 2003)

Comparing the types of shrinkage mentioned above, drying shrinkage forms the most significant and critical shrinkage phenomenon. Drying shrinkage is driven by the capillary forces that are induced in cement pores (Figure 6). Cement pore structure is composed of two types of pores: gel pores and capillary pores. Jennings et al. 2007 investigated the movement of water from pores at different levels of relative humidity (RH) and the associated pore type. The removal of water first occurs in capillary pores at RH of 100-85% within which the significant amounts of water escapes from the concrete. This is followed by gel pores at 85-56% RH. Inter particle spaces follows at RH level 54-33% and finally the adsorbed water in the C-S-H gel at RH of 33-7%.

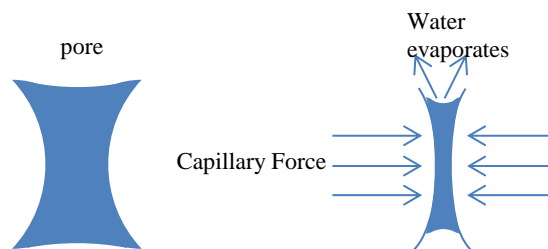


Figure 6 Schematic diagram of drying shrinkage

It is reported that drying shrinkage occurs in a range of pore sizes. Some studies define that the range of 2.5 to 50 nm to be the most significant pore sizes that effect drying shrinkage of concrete (Balogh, 1996). It further states that the pores larger than 50nm are too large for the tensile stresses to be significantly affect drying shrinkage while pores smaller than 2.5 nm are too small to develop a meniscus in them.

2.2 Factors Effecting Shrinkage of Concrete

2.2.1 Effect of cementitious materials

Tazawa and Miyazawa (1997) conducted experiments on the autogenous shrinkage on 10 different cements. The cement types consisted of Normal (N), Moderate heat (M), High early-strength (H), Sulfate resisting (S), Geothermal (G), Oil well (O), Alumina (A) White (W), Blast furnace slag (B) and Low heat (L) cements. High early-strength cement and alumina cement displayed higher early age autogenous shrinkage compared to Portland cement while moderate heat cement, low heat cement and sulfate resisting cement displayed lower early age autogenous shrinkage. Blast furnace slag cement displayed a high shrinkage at the later age. This confirms the effect of alumina compounds to increase the autogenous shrinkage while high C_2S cements like low heat cement display very low autogenous shrinkage (Figure 7).

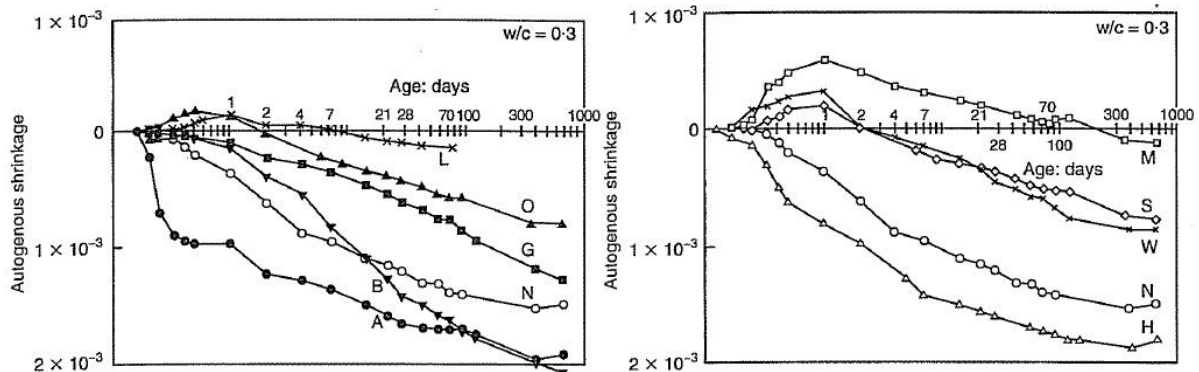


Figure 7 Influence of cement type on autogenous shrinkage (Tazawa, 1997)

Satio (1991) investigated the effect of expansive cements and aggregate type on shrinkage of concrete. The experiments were conducted for both OPC and expansive cement. These results showed that the shrinkage can be reduced significantly by the use of expansive cement. Early age performance for both cements was similar and later age performance of the two cement types was significantly different. MN and ML in Figure 8 refer to natural and light weight aggregate respectively.

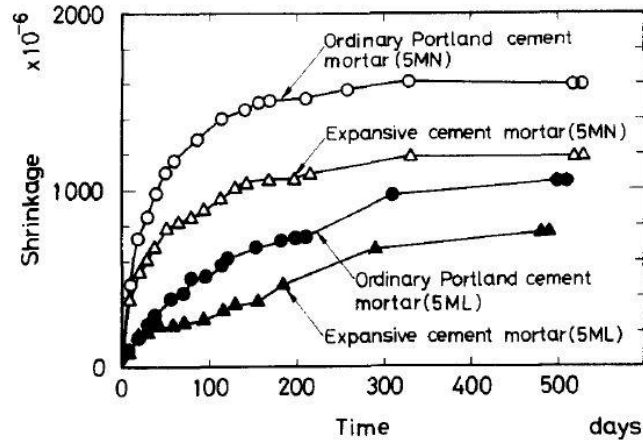


Figure 8 Shrinkage of OPC and Expansive cements concrete (Satio, 1991)

Jianyong (2001) investigated shrinkage and creep of High Performance Concrete (HPC) with OPC, ultrafine (fineness greater than $600\text{m}^2/\text{kg}$) Ground Granulated Blast-Furnace Slag (GGBS) and Silica Fume (SF). Investigations involved 3 HPC mixes: concrete A – pure OPC mixture, concrete B – 70% OPC and 30% GGBS and concrete C – 60% OPC, 30% GGBS and 10% SF. The results revealed that the shrinkage and creep of concrete made with ultrafine supplementary cementitious displayed reduced the shrinkage compared to similar HPC mixes with only OPC (Figure 9).

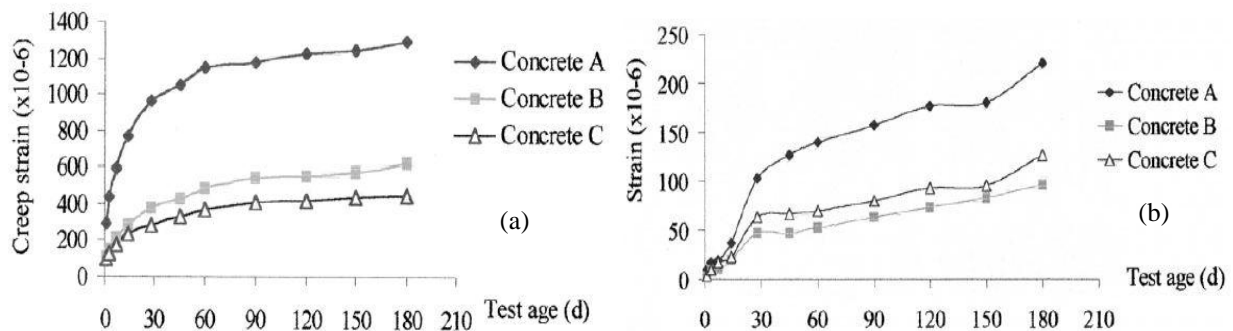


Figure 9 Creep (a) and drying shrinkage strains of HPC (Jianyong, 2001)

Nakarai (2009) conducted experiments on autogenous and drying shrinkage of concrete with Fly Ash (FA) as pozzolanic material. The experiments were conducted for autogenous shrinkage where mixes contained 10%, 30% and 60% fly ash while drying shrinkage was performed on mixes with 30% 50% and 70% replacement levels of OPC. The results yielded that the replacement OPC by FA reduced both drying and autogenous

shrinkage (Figure 10). The amount of reduction in shrinkage increased with increasing replacement of OPC by FA.

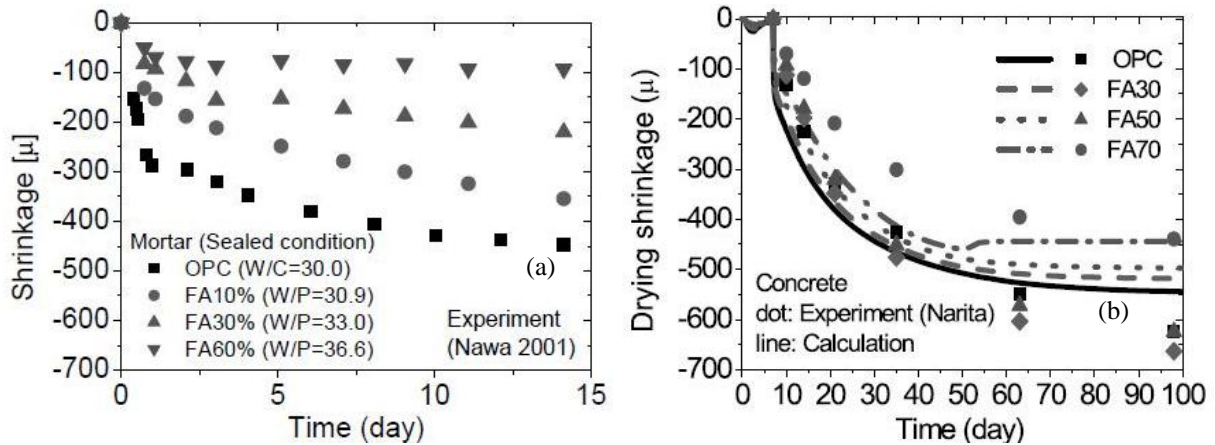


Figure 10 Autogenous shrinkage (a) and drying shrinkage (b) of concrete with fly ash (Nakarai, 2009)

Miyazawa (2009) compared different cement types on their influence on cracking tendency of concretes in the early ages. The tests compared the effects of Ordinary Portland cement (N), Moderate heat (M), and two types of slag cements (BB and LBB). The two slag cements differ in fineness [BB ($4080 \text{ cm}^2/\text{g}$) > LBB ($3380 \text{ cm}^2/\text{g}$)] slag content [BB (40%) < LBB (58%)] and SO_3 % [BB (2.39) < LBB (3.90)]. The findings show that the low heat and slag cement LBB show lesser restrained stress compared to OPC at the early age and continue to show lesser restrained stress (Figure 11).

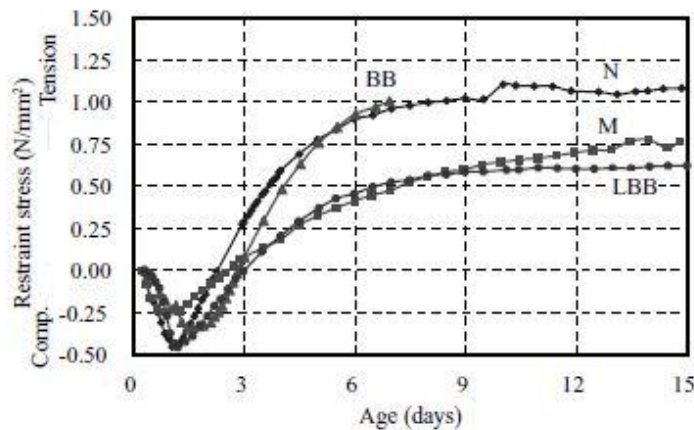


Figure 11 Development of restrained stress (Miyazawa, 2009)

Whiting (2000) studied the effect of silica fume on drying shrinkage and strength of concrete. The experiments were conducted for both base and overlay mixes where base mixes were moist cured for 7 days while the overlay mixes were moist cured for a duration of 3 days. The results revealed that the effects of the replacement of cement by silica fume on shrinkage depend on both the dosage and the duration of curing.

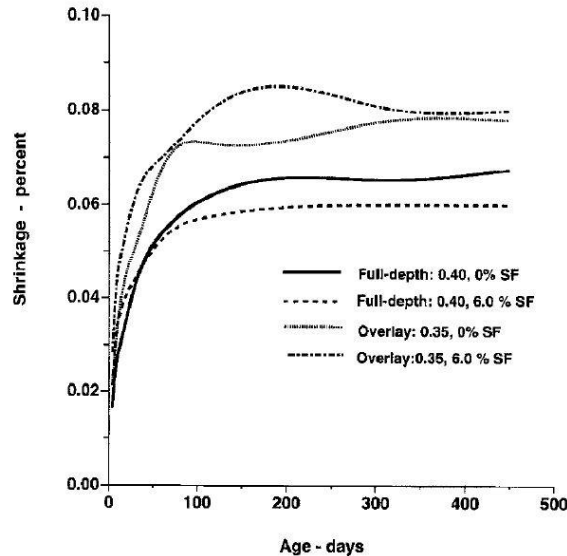


Figure 12 Effect of curing and w/c ratio on drying shrinkage of silica fume concrete (Whiting, 2000)

Brooks (2001) investigated the effect of metakaolin on creep and shrinkage of concrete. The investigations were conducted on concretes with metakaolin replacement levels of up to 15% at 5% intervals. The results revealed that with the increasing amounts of metakaolin the observed amount of autogenous shrinkage reduced (Figure 13a) in the early age stage (<24hrs), but compared to OPC the addition of metakaolin increased the long term autogenous shrinkage measured after 24 hours. However the long term autogenous shrinkage seemed to reduce as the dosage of the metakaolin increased (Figure 13b). This is mainly attributed to the accelerated reaction rate of metakaolin which rapidly increasing the rate of hydration of the concrete. The reaction rate reflects the rate of self-desiccation observed and hence the rate of autogenous shrinkage observed. The inclusion of metakaolin improves the pore structure by making a finer pore structure. The total autogenous shrinkage observations show that there is a reduction in shrinkage at 10 and 15% levels of replacement (Figure 13c).

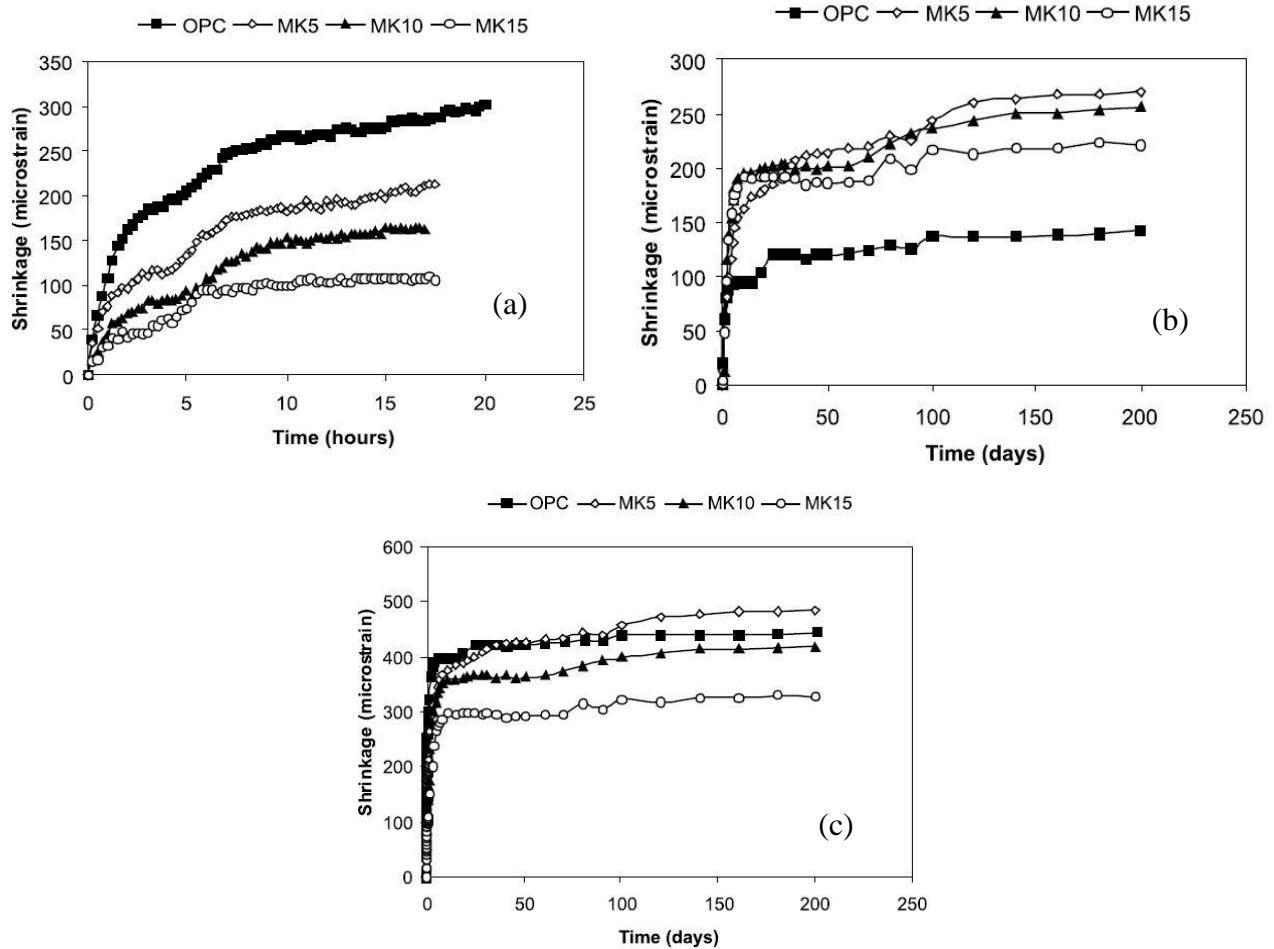


Figure 13 Effect of metakaolin on (a) early age (<24hrs), (b) after 24hrs and (c) total autogenous shrinkage (Brooks, 2001)

The pure drying shrinkage and total shrinkage of concrete with metakaolin displayed an interesting observation. The amount of total shrinkage reduced with increasing amounts of metakaolin (Figure 14a). The dominant portion of shrinkage of concrete with metakaolin was attributed to the autogenous shrinkage since the pure drying shrinkage observed with metakaolin was very low compared to OPC concrete (Figure 14b). This goes to prove that the replacement of cement improves the porosity of the concrete and results in a pore structure that would boost self-desiccation than diffusion of water to the environment.

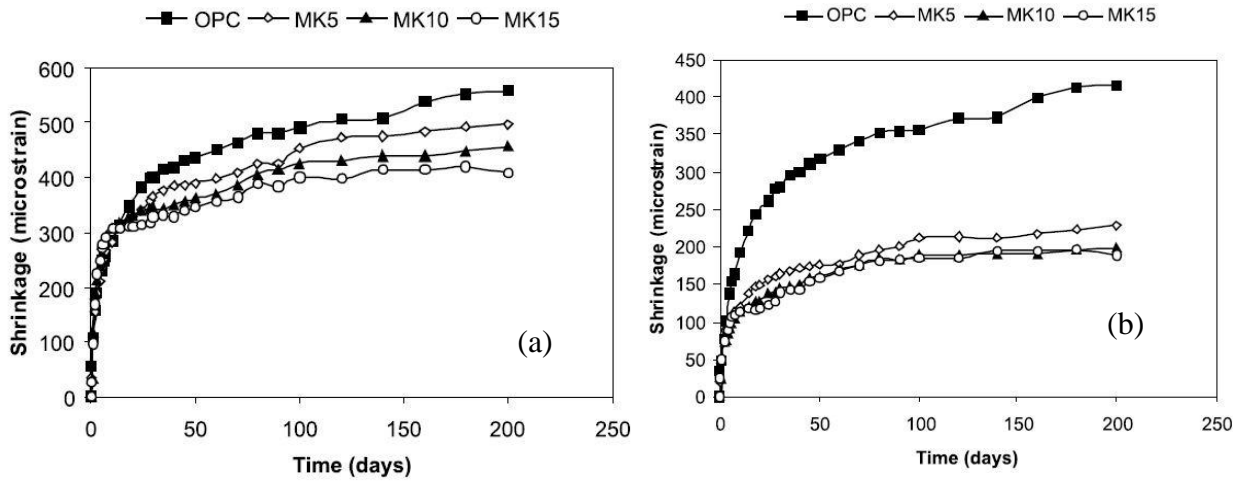


Figure 14 Effect of metakaolin on (a) total shrinkage and (b) pure drying shrinkage of concrete (Brooks, 2001)

Camiletti (2013) investigated the effects of adding nano and micro limestone into Ultra High Performance Concrete (UHPC). The results indicate that the inclusion of micro and nano limestone reduced the drying shrinkage of the concrete at 20 °C. The results indicated below display the drying shrinkage of concrete with 15% micro limestone and varying amounts of nano limestone (Figure 15a). As observed the addition of micro and nano limestone reduces the amount of mass loss.

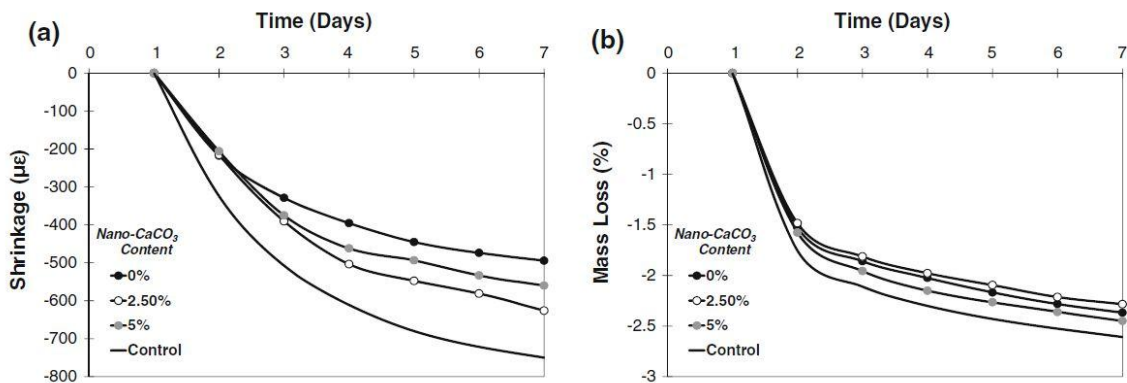


Figure 15 Effect of nano limestone and micro limestone on (a) drying shrinkage and (b) mass loss (Camiletti, 2013)

2.2.2 Effect of aggregates

The presence of aggregates in concrete has two effects towards paste shrinkage, namely they are dilution and restraint (Addis, 1986). The former refers to the effect of reducing shrinkage by the increasing amount of aggregate in the matrix, while the latter refers to the restraint provided by the aggregates to the free shrinkage of the paste of cement by its stiffness. The effect of aggregate content (Figure 16) was shown to reduce the shrinkage of neat cement paste down to approximately 20% at common aggregate concentration levels of 65-70% (Powers, 1971). Almudaiheem (1986) found that shrinkage decreases with increasing aggregate content and the aggregate content has a more profound influence on shrinkage than did the specimen size.

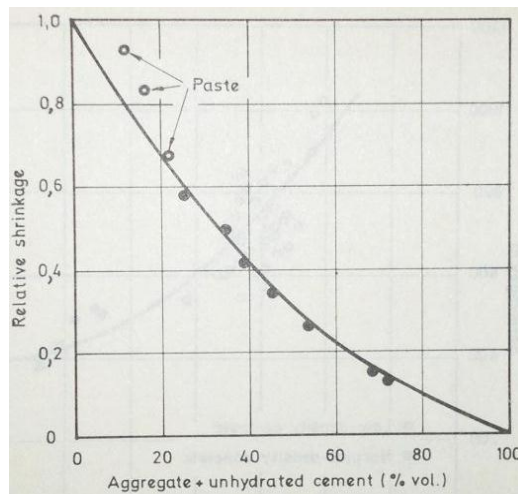


Figure 16 Effect of aggregate concentration on shrinkage of concrete (Powers, 1971)

The effect of the aggregate stiffness can be closely related to the stiffness of the concrete provided the water cement ratio (w/c) and aggregate concentration are kept constant. Therefore the approximation of the effect of aggregate stiffness to the shrinkage also can be made (Figure 17). However the relationship is not that significant in the case of low w/c ratio concretes with high-quality density non-shrinkage aggregates (Hobbs, 1979).

Further the effects of aggregate size are directly related to the water requirement of the concrete for workability. Therefore larger size aggregates perform better in effects of shrinkage resistance. For small size aggregates the shrinkage observed is more uniform indicating no shrinkage cracks have occurred in the paste matrix. However shrinkage effects

can be reduced by cracking in the paste when the concrete employs aggregates larger than $\frac{1}{4}$ in (Troxell, 1968).

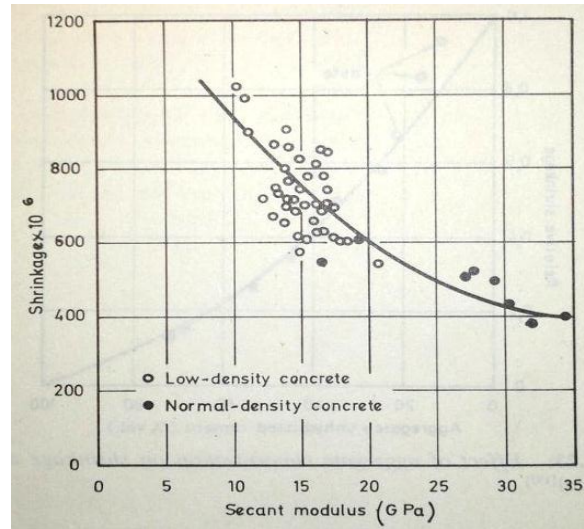


Figure 17 Relationship between shrinkage at 2 years and secant modulus of elasticity of concrete at 28 days (Reichard, 1964)

Absorption of aggregates is of great concern when considering the shrinkage of concrete. High absorption aggregates pose greater shrinkage compared to low absorption aggregates as they are prone to shrink upon drying (e.g., sandstone) and due to their porous structure they are not as rigid as the low absorption aggregates (e.g., limestone) (Troxell, 1968).

Meininger (1966) in his studies of drying shrinkage of concrete quantified the effects that each factor had on the concrete shrinkage. Observations regarding aggregate size indicated that 19mm aggregate displayed 30% more shrinkage than 38mm aggregate, however, the application governs the size of the maximum aggregate size where the aggregate size should be smaller than $\frac{1}{3}$ of the slab thickness. Table 1 summarizes the effects of the individual elements on shrinkage.

Further studies by Meininger investigated the effect of different aggregate sources on drying shrinkage of concrete. The results revealed that depending on the type and source of aggregate the shrinkage observed can vary up to 100%. Table 2 summarizes the different effects the aggregate type has on shrinkage.

Table 1 Effect of various factors on concrete shrinkage (Meininger, 1966)

Factor	Max. Effect (%)
Course aggregate source effect	100
Fine Aggregate source effect	20
Total aggregate source effect	150
Washing out minus No. 200 mesh	15
2 1/2 vs. 3/8 in. max. aggregate size	25
Fine aggregate grading from coarse to fine	0
cement source	15
Cement factor	10
Slump	5
Curing: 7 days vs 3days	5

Table 2 Effect of coarse aggregate on drying shrinkage of concrete (Meininger, 1966)

Coarse aggregate rock type	Shrinkage in millionths Drying period	
	7 days	182 days
Quartz	180	530
Igneous, andesite, sandstone	180	560
Greywacke, quartz, limestone, granite	200	620
Granite, quartzite	220	640
Schist, granite gneiss	210	660
Impure Limestone, Sandstone, igneous	230	640
Igneous, andesite, sandstone	210	700
Sandstone, Limestone	240	700
Granite, granite gneiss	240	750
Sandstone	230	740
Sandstone, greywacke	290	920
Sandstone, greywacke	300	900
Sandstone, greywacke	320	990

2.2.3 Effect of admixtures

Retarders are used to delay the setting time of a concrete mixture. In pavement applications this is useful in constructing large sections such as bridge decks. The slow reaction results in the lowering of the peak temperature during hydration and as a result reduces thermal stresses. The concrete may face problems with plastic shrinkage cracking due to the prolonged setting time. The use of retarders is not recommended in cold weather applications of concrete as the risk of plastic shrinkage is increased and also the risk of the concrete not properly setting. The Minnesota DOT is the only DOT that does not permit the use of retarding admixtures (Krauss, 1996).

Set accelerators are not recommended for bridge decks as the application worsens the early age shrinkage of the mix. Although the accelerator reduces the risk of plastic shrinkage cracking, the temperature rise due to the application and early age modulus of elasticity increase the risk of early age cracking.

The water and paste content are a major concern when considering shrinkage performance of a mixture. Water reducing admixtures provides an advantage in reducing the total volume of water required. Brooks (1989) discussed the effects of the plasticizer and super plasticizer on creep and drying shrinkage. The collected data from various studies yielded that the shrinkage effects increased by in the presence of plasticizers and super plasticizers in which the increase varied for 3 to 120% compared to OPC mixture without admixtures. The effect of plasticizers and super plasticizers depend on the chemical composition and the dosage.

Meininger (1966) also studied the effect of 5 different water reducing admixtures on drying shrinkage performance. The results indicated that the effect mainly depends on the resulting slump of the mixture. For highly flowable (9 inch) slump mixtures the effect of water reducing admixtures was negligible while for stiff mixtures with low water/cement ratios the water reducing admixtures had influenced a slight reduction in shrinkage performance.

Shrinkage reducing admixtures (SRA) have been researched by many as an effective method to reduce the shrinkage of concrete. The mechanism by which the SRA affects shrinkage is by reducing the surface tension of the water used in the mix. This in turn reduces the stress that develops in the capillary pores. Quangphu (2008) studied the influence of SRA

on drying shrinkage of high-performance concrete. Conclusions could be drawn from Figure 18 that the SRA effectively reduces some mechanical properties of HPC. The shrinkage strains of HPC with SRA were only as high as 41% of the average free shrinkage of concrete without SRA after 120 days of drying.

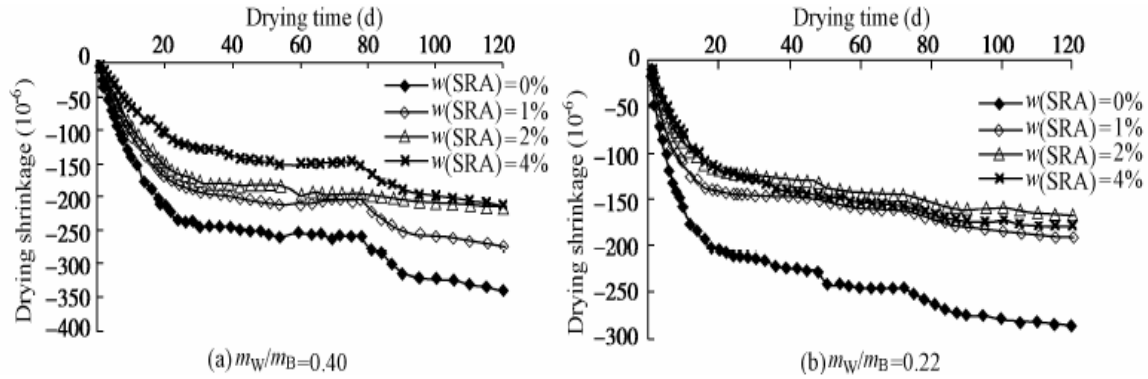


Figure 18 Drying shrinkage of HPC with and without SRA (Quangphu, 2008)

2.2.4 Factors Influencing Drying Shrinkage and Restrained Cracking

Restrained stress development depends on many factors (Table 3) and one of the greatest contributors to restrained stress development is the restraint itself. This comes in many forms such as, reinforcement size, reinforcement density, size and shape of the element. Other major factors that are important in the restrained cracking tendency include curing, construction practice shrinkage, creep, strength and other time dependent material properties of concrete, (Krauss, 1996).

Specimens were exposed to different temperature, humidity and wind conditions to monitor the moisture loss and cracking of specimens in (Almusallam, 1998). It was shown that the relative humidity had a direct effect on the rate of water evaporation when no wind was present. But as the wind became a factor, the relative humidity had less or no impact on the rate of evaporation, and as expected temperature had a direct influence on the rate of water evaporation.

Whiting (2000) investigated the effects of curing duration on cracking of silica fume concrete. The investigation looked at the time to crack for ring specimens cured for 1 and 7 days before being exposed to drying. The two periods were to simulate the effect of bad and good construction practices. The silica fume concrete samples cured for one day displayed cracking at an earlier age compared to that control samples. This is consistent with the field

observations and indicates that the silica fume concrete is sensitive to curing practices. Specimens cured for 7 days displayed longer average time to crack compared to 1 day curing.

Table 3 Factors affecting cracking

Factors	Effects			
	Major	Moderate	Minor	None
Design				
Restraint	✓			
Continuous/simple span		✓		
Deck thickness		✓		
Girder type		✓		
Girder size		✓		
Alignment of top and bottom r/f bars		✓		
Form type			✓	
Concrete cover			✓	
Girder spacing			✓	
Quantity of reinforcement			✓	
Reinforcement bar size			✓	
Dead load deflections during casting			✓	
Stud spacing			✓	
Span length			✓	
Bar type-epoxy coated			✓	
Skew			✓	
Traffic volume				✓
Frequency of traffic induced vibrations				✓
Materials				
Modulus of elasticity	✓			
Creep	✓			
Heat of hydration	✓			
Aggregate type	✓			
Cement content and type	✓			
Coefficient of thermal expansion		✓		
Paste volume-free shrinkage		✓		
Water-cement ratio		✓		
Shrinkage-compensating cement		✓		
Silica fume admixture		✓		
Early age compressive strength			✓	
HRWRAs			✓	
Accelerating admixtures			✓	
Retarding admixtures			✓	
Aggregate size			✓	
Diffusivity			✓	
Poisson's ratio			✓	
Fly ash				✓
Air content				✓
Slump				✓
Water content				✓
Construction				
Weather	✓			
Time of casting	✓			
Curing period and method		✓		
Finishing procedures		✓		
Vibration of fresh concrete			✓	
Pour length and sequence			✓	
Reinforcement ties				✓
Construction loads				✓
Traffic induced vibrations				✓
Revolutions in concrete truck				✓

Min, et.al. (2009) investigated the effect of different curing environments on the early age shrinkage and creep behavior of concrete. The experimental procedure employed 4 different curing environments to investigate the effect of the curing environment. Two of the conditions were similar field conditions (air dried and sealed) that a fresh concrete could face while the other two were artificial methods (chloride solution and tap water) to evaluate the effect of the conditions provided.

2.3 Prediction Models for Creep

2.3.1 B3 model

The use of creep prediction models defer according to the sensitivity of their applications (Bazant, 2000). For structures that are highly sensitive to input values it is recommended to use laboratory tested values. The classifications divides the structures in to 5 classes that vary from reinforced concrete beams of less that 20m span to large span bridges and other special structures. The B3 model is necessary for class 4 and 5 (highly sensitive to input values) but not necessarily for class 3.

The B3 model has limitations to its application in the concrete mix proportions. The use of the model is limited to a Portland cement concrete mixture with the following parameter ranges:

$$0.35 \leq w/c \leq 0.85, \quad 2.5 \leq a/c \leq 13.5 \quad (1)$$

$$2,500 \text{ psi} \leq f_c \leq 10,000 \text{ psi}, \quad 10 \text{ lb/ft}^3 \leq c \leq 45 \text{ lb/ft}^3 \quad (2)$$

where w is water content in lb/ft^3 , c is cement content in lb/ft^3 , a is total aggregate content in lb/ft^3 , and f_c is the 28 day compressive strength of concrete in psi or MPa.

Compliance function for strain (creep and elastic strain) at time t due to a unit uniaxial constant stress applied at the age of t' :

$$J(t, t') = q_i + C_0(t, t') + C_d(t, t', t_0) \quad (3)$$

where q_i is the instantaneous strain due to the stress, $C_0(t, t')$ is the compliance function for basic creep (no moisture movement) and $C_d(t, t', t_0)$ is the additional compliance function for simultaneous drying.

Creep coefficient $\phi(t, t')$ is calculated from the compliance function:

$$\phi(t, t') = E(t') J(t, t') - 1 \quad (4)$$

where $E(t')$ is the static modulus of elasticity at load age of t' .

The calculation of the basic creep is derived from the time rate of basic creep. The derived equation for normal concrete is as follows.

$$C_0 = q_2 Q(t, t') + q_3 \ln[1 + (t - t')^n] + q_4 \ln(t/t') \quad (5)$$

Where $Q(t, t')$ is a given in Table 4, q_2 , q_3 and q_4 are empirical constitutive parameters. The parameters q_2 , q_3 and q_4 represent aging viscoelastic compliance, non-aging viscoelastic compliance and flow compliance respectively.

Table 4 Values of function $Q(t, t')$ for $m = 0.5$ and $n = 0.1$

log (t-t')	log t'								
	0.0	0.5	1.0	1.5	2.0	2.5	3.0	3.5	4.0
-2.0	0.4890	0.2750	0.1547	0.08677	0.04892	0.02751	0.01547	0.008699	0.004892
-1.5	0.5347	0.3009	0.1693	0.09519	0.05353	0.03010	0.01693	0.009519	0.005353
-1.0	0.5586	0.3284	0.1848	0.1040	0.05846	0.03288	0.01849	0.01040	0.005846
-0.5	0.6309	0.3571	0.2013	0.1133	0.06372	0.03583	0.02015	0.01133	0.006372
0.0	0.6754	0.3860	0.2185	0.1231	0.06929	0.03897	0.02192	0.01233	0.006931
0.5	0.7108	0.4125	0.2357	0.1334	0.07516	0.04229	0.02379	0.01338	0.007524
1.0	0.7352	0.4335	0.2514	0.1436	0.08123	0.04578	0.02576	0.01449	0.008149
1.5	0.7505	0.4480	0.2638	0.1529	0.08727	0.04397	0.02782	0.01566	0.008806
2.0	0.7597	0.4570	0.2724	0.1602	0.09276	0.05239	0.02994	0.01687	0.009494
2.5	0.7652	0.4624	0.2777	0.1652	0.09708	0.05616	0.03284	0.01812	0.01021
3.0	0.7684	0.4656	0.2808	0.1683	0.1000	0.05869	0.03393	0.01935	0.01094
3.5	0.7703	0.4675	0.2827	0.1702	0.1018	0.06041	0.03541	0.02045	0.01166
4.0	0.7714	0.4686	0.2838	0.1713	0.1029	0.06147	0.03641	0.02131	0.01230
4.5	0.7720	0.4692	0.2844	0.1719	0.1036	0.06210	0.03702	0.02190	0.01280
5.0	0.7724	0.4696	0.2848	0.1723	0.1038	0.06247	0.03739	0.02225	0.01314

$$q_1 = 0.6 \times 10^6 / E_{28}, \quad E_{28} = 57000 \sqrt{f_c} \quad (\text{fc psi}) \quad (6)$$

$$q_2 = 451.1 c^{0.5} f_c^{-0.9}, \quad q_3 = 0.29 (w/c)^4 q_2, \quad q_4 = 0.14 (a/c)^{-0.7} \quad (7)$$

Shrinkage,

$$\varepsilon_{s\infty} = -\alpha_1 \alpha_2 [26w^{2.1} f_c^{-0.28} = 270] \quad (\text{in } 10^{-6}) \quad (8)$$

$$k_t = 190.8 t_0^{-0.08} f_c^{-1/4} \text{ days/in}^2 \quad (9)$$

where, α_1 is 1.0 for Type I cement, 0.85 for Type II cement and 1.1 for Type III cement, α_2 is 0.75 for steam curing, 1.2 for sealed or normal curing in air with protection against drying 1.0 for curing in water or at 100% relative humidity.

$$q_5 = 7.57 \times 10^5 f_c^{-1} |\varepsilon_{sh\infty}|^{-0.6} \quad (10)$$

Humidity dependence,

$$k_h = (1 - h^3) \quad \text{for} \quad h \leq 0.98$$

$$k_h = -0.2 \quad \text{for} \quad h = 1, \text{ interpolate for } 0.98 \leq h \leq 1 \quad (11)$$

Size dependence,

$$\tau_{sh} = k_t (k_s D)^2, \quad D = 2v/s \quad (12)$$

$$\begin{aligned} k_s &= 1.00 \text{ for and infinite slab} \\ &= 1.15 \text{ for an infinite cylinder} \\ &= 1.25 \text{ for an infinite square prism} \\ &= 1.30 \text{ for a sphere} \\ &= 1.55 \text{ for a cube} \end{aligned}$$

2.3.2 Modified NCHRP 496 model

The NCHRP model from report 496 (Al-Omaishi, 2009) has been modified for high strength concrete. These equations were developed because the existing LRDF provisions for estimation of creep did not provide a reliable estimate for high strength concrete.

$$\varphi(t, t_i) = 1.9 k_{td} k_{vs} k_f k_{hc} t_i^{-0.118} \quad (13)$$

Ambient Relative humidity correction factor k_{hc} ,

$$k_{hc} = 1.56 - 0.008RH \quad (14)$$

Size Correction factor k_{vs} ,

$$k_{vs} = 1.45 - 0.13\left(\frac{v}{s}\right) \quad (15)$$

Strength correction factor k_f ,

$$k_f = \frac{5}{(1 + f'_{ci})}, \text{ where } f'_{ci} = 0.8f'_c \quad (16)$$

Time development factor k_{td} ,

$$k_{td} = \frac{t}{(61 - 4f'_{ci} + t)}, \text{ where } t \text{ is the time for loading} \quad (17)$$

2. 4 Restrained Shrinkage

ASTM C157/C illustrates the prism molds in detail and the measurement for drying shrinkage of mortar that commonly used. Restrained ring samples are prepared according to ASTM C 1581. Photos of circular mold and ring test are presented in Figure19 and Figure 20 provides an example of test result. The sudden release of the steel ring strain is indicative of cracking on the concrete annulus.

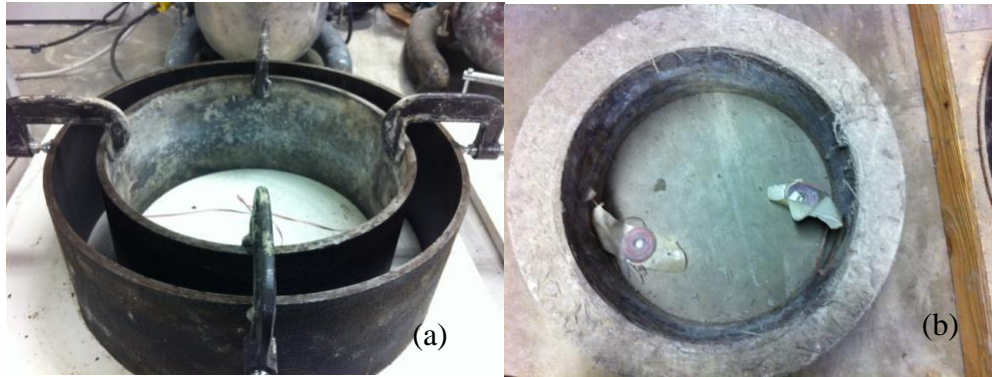


Figure 19 Ring tests mold (a) cast specimen (b)

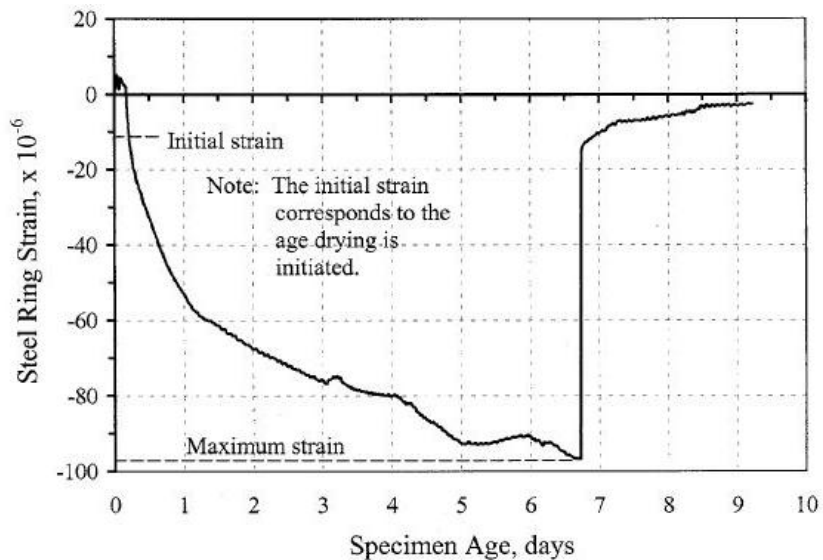


Figure 20 An example of measuring ring strain vs. specimen age

The restrained ring test was developed as an economical method of obtaining the cracking potential of a concrete mix. The concrete forms an annulus cast around the steel ring, where the ring provides restraint to the shrinkage of the concrete that occurs as a consequence of the drying that occurs from the outer surface. When the stresses are of sufficient magnitude the concrete may crack. Geometry of the specimens vary from researcher to researcher and from standard to standard. The AASHTO PP34-99 employs a 75mm thick concrete annulus cast around a 12.5mm steel ring the ASTM 1581-04 employs a 37.5mm thick concrete annulus around a 12.5mm thick steel ring. The different geometries result in different times for the concrete to crack. This is directly influenced by the restraint provided to the specimen. Although the cracking can be observed at an earlier age in the

ASTM standard, limitations in maximum aggregate size and fiber reinforced concrete hinder its range of applications.

Since drying shrinkage is greatest at the surface exposed to the environment it causes nonlinear shrinkage profile to develop through the thickness. The resulting differential strain causes axial and bending stresses. The restrained ring is used to evaluate cracking sensitivity or time to cracking due to restrained drying shrinkage. The cracking resistance of concrete primarily depends on the combined effects of shrinkage potential, shrinkage rate, tensile creep, tensile strength (See, 2003) and fracture toughness (Weiss, 2000).

In the restrained shrinkage observed through the steel annulus the observed shrinkage is the composite effect of several components of strain (See, 2003).

$$\varepsilon_{sh}(t) = \varepsilon_e(t) + \varepsilon_{cp}(t) + \varepsilon_{st}(t) \quad (18)$$

where $\varepsilon_{sh}(t)$ is the free shrinkage strain, ε_e is the elastic concrete strain, ε_{cp} is the tensile creep strain and $\varepsilon_{st}(t)$ is the elastic steel strain at time t. Therefore the observed shrinkage through the concrete annulus is the equivalent of elastic, shrinkage and creep effects.

The degree of restraint provided by the steel ring is calculated by the following equation

$$R = \frac{A_{st}E_{st}}{A_{st}E_{st} + A_cE_c} \quad (19)$$

where A_{st} and A_c are the cross section area of the steel and concrete respectively and E_{st} and E_c are the modulus of elasticity of the steel and concrete respectively (Moon, 2006).

Further studies of See (2003) observed that the cracking time calculated from theoretical equations yielded a smaller time to crack than actual when the creep effect of the concrete was neglected. Stress-strength ratio has widely been used as a measure of cracking potential. The cracking was observed at stress strength ratio of 0.35 to 0.51. This level falls in the range at which micro cracks initiate under tensile or compressive strength (See, 2003).

Table 5 Theoretical analysis of effects of elastic strain rate and tensile creep on time to cracking (See, 2003)

Concrete mixture	Elastic strain at cracking, μ -strain	Theoretical time to cracking (neglecting creep) t_{ncp} , days	Actual time to cracking t_{cp} , days	Magnitude of creep effect t_{cp}/t_{ncp}	Theoretical rate of elastic strain buildup, μ -strain/day
NSC	153	2.4	17	7.1	63.8
NSC-SRA	170	6.3	32	5.1	26.9
HPC	140	1.5	5	3.3	92.1
HPC-SRA	213	7.7	19	2.5	27.7

CHAPTER 3. MATERIALS AND EXPERIMENTS

3.1 Materials

The materials used in this research and their sources are listed in Table 6.

Table 6 Materials used and their sources

Materials	Resource
Cement	Type IP Cement (Ash Grove)
	Type I/II Cement (Lafarge)
	Type I Cement (Lehigh)
Coarse aggregates	Limestone (Ft. Dodge Mine)
	Quartzite (Dell Rapids, SD)
Sand	Ames
Fly ash	Headwaters Resources
GGBFS	Holcim
Metakaolin	Davison Catalysts
Standard WR /WRDA 82	WR Grace
Mid-range WR /Mira 62	WR Grace
Retarder /Daratarad 17	WR Grace
AEA /Daravair 1000	WR Grace

Three types of cement: Type I, Type I/II and Type IP cement, together with three types of supplementary cementitious materials: fly ash (FA), ground granulated blast-furnace slag (GGBFS) and metakaolin (MK) were used, and their chemical and physical properties are listed in Table 7.

Table 7 Chemical and physical properties of cementitious materials

	Chemical composition (%)									Mineral composition (%)				Fineness (m ² /kg)
	CaO	Al ₂ O ₃	SiO ₂	Fe ₂ O ₃	SO ₃	MgO	Na ₂ O	K ₂ O	LOI	C ₃ S	C ₂ S	C ₃ A	C ₄ AF	
Type I	63.0	5.2	20.0	2.6	3.0	3.0	0.07	0.54	2.5	60	14	6	9	398
Type I/II	63.1	4.6	20.2	3.2	3.4	2.4	0.09	0.67	1.2	57	15	7	10	397
Type IP	48.3	8.9	29.3	4.1	3.1	3.1	0.3	0.7	1.7	-	-	-	-	490

Limestone and quartzite were used as coarse aggregates. Original coarse aggregates were sieved and combined to the designated gradations as indicated in Table 8. Coarse aggregates were used in saturated surface dry (SSD) condition and fine aggregates were in oven-dried condition. The gradation curves of aggregates are shown as Figure 21. The calculated fineness modulus of sand is 3.13.

Table 8 Gradations of coarse aggregates used

Sieve Size	O type mixes	S type mixes
	% passing	% passing
1"	-	100.0
3/4"	100.0	99.0
1/2"	100.0	60.0
3/8"	80.0	29.0
#4	13.5	4.5
#8	1.0	1.0

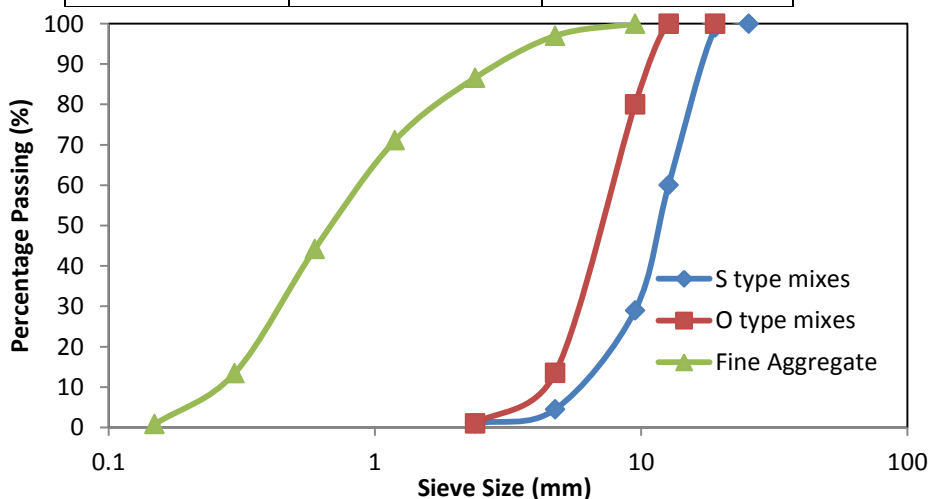
**Figure 21 Particle size distribution of coarse and fine aggregate**

Table 9 Dosage of chemical admixtures

Type	Name	Dosage (fl.oz/100lbs)
Standard WR	WRDA-82	3.5
Mid-range WR	Mira-62	6.0
Retarder	Daratard 17	2.0
AEA	Daravair 1000	1.8

3.2 Mix Proportions

The present study focuses on the chemical, autogenous, and drying shrinkages of the HPC used for Iowa bridge decks and bridge deck overlays. In this study, 11 HPC mixes, selected by Iowa Department of Transportation (Iowa DOT), were investigated (Table 10). The main difference in HPC-O and HPC-S mixtures are their aggregate gradation and chemical admixture. HPC-O mixes have MRWR while HPC-S has NRWR. The coarse aggregate gradation of HPC-O mixes is finer than that of HPC-S mixes.

Table 10 HPC mixes to be used in this study

ID	Mix	Cement	Fly Ash	GGBFS	Metakaolin
1	HPC-O	Ash Grove IP	0	-	-
2	HPC-O	Ash Grove IP	20%	-	-
3	HPC-S	Ash Grove IP	20%	-	-
4	HPC-O (control)	Lafarge I/II	0	-	-
5	HPC-S (control)	Lafarge I/II	0	-	-
6	O-4WR	Lafarge I/II	0	-	-
7	HPC-O	Lafarge I/II	0	25%	-
8	HPC-O (quartzite coarse aggregate)	Lafarge I/II	20%	25%	-
9	HPC-S	Lafarge I/II	20%	25%	-
10	HPC-O	Lafarge I/II	20%	-	5.6%
11	HPC-S	Lehigh I	20%	25%	-

These mixes are divided into 4 groups for comparison:

- Group 1: Mixes 1, 2 and 3 for the same Ash Grove IP cement used; the same w/cm 0.40 and the replacement of 20% of cement by fly ash. Shrinkage test results for this group may show the effects of 20% fly ash replacement.
- Group 2: Mixes 4, 6, 7 and 10 for HPC-O mixtures, using the same Lafarge I/II cement and different replacements of cement by fly ash, GGBFS and MK. Shrinkage test results for this group may show the effects of different supplementary cementitious materials.
- Group 3: Mixes 8 and 9 for the same Lafarge I/II cement used and the same fly ash and GGBFS replacing percentages, but for different HPC types and various coarse aggregates adopted. Shrinkage test results for this group may show the effects of different coarse aggregates.
- Group 4: Mixes 5 and 11, both for HPC-S mixtures with the same w/cm 0.42, but with different type of cement and cementitious materials constituents used. Shrinkage test results for this group may show the effects of ternary cementitious materials.

The shrinkage behavior of cement paste, mortar and concrete of the 4 groups of HPC mixes were studied. The mix proportion used for paste is different from those for mortar and concrete. For paste, water to cementitious materials ratio is kept constant at 0.40; and no air entraining agent is used. The mix proportions of mortar are basically the same as those of concrete, except that no coarse aggregate is added.

The mix proportions for concrete are presented in Table 11. In the tables, FA denotes fly ash; GGBFS, ground granulated blast-furnace slag; MK, metakaolin; w/c, water-to-cementitious material ratio; AEA, air entraining agent; MRWR, mid-range water reducer; and NRWR, normal range water reducer.

Table 11 Mix proportions for concrete

ID	Cement lbs/yd ³	FA lbs/yd ³	GGBFS lbs/yd ³	MK lbs/yd ³	Limestone (Quartzite) lbs/yd ³	Sand lbs/yd ³	W/C	Water lbs/yd ³	NRWR ml/yd ³	MRWR ml/yd ³	Retarder ml/yd ³	AEA ml/yd ³
1	666.3	-	-	-	1431.7	1383.9	0.40	288.5	-	1182.3	394.1	354.7
2	521.2	130.3	-	-	1439.6	1391.6	0.40	282.7	-	1156.1	385.4	346.8
3	459.0	114.8	-	-	1513.4	1463.1	0.40	264.2	593.9	-	339.4	305.4
4	709.2	-	-	-	1429.7	1382.0	0.40	305.7	-	1258.4	419.5	377.5
5	624.5	-	-	-	1483.9	1434.5	0.42	285.1	646.4	-	369.4	332.5
6	825.7	-	-	-	1386.8	1344.7	0.33	291.4	854.6	-	-	439.5
7	519.7	-	173.2	-	1417.4	1370.1	0.40	299.0	-	1229.5	409.8	368.9
8	367.8	133.8	167.2	-	(1430.4)	1382.6	0.39	289.5	-	1186.6	395.5	356.0
9	323.9	117.8	147.2	-	1504.8	1454.8	0.42	270.5	609.6	-	348.3	313.5
10	502.2	135.0	0.0	37.8	1427.1	1379.4	0.40	291.9	-	1197.6	399.2	359.3
11	323.9	117.8	147.2	-	1504.8	1454.8	0.42	270.5	609.6	-	348.3	313.5

3.3 Experiments

3.3.1 Autogenous shrinkage test

All mixes are cast in accordance with ASTM C192 (standard practice for making and curing concrete test specimens in the laboratory). In the mixing, oven dried sand is used while coarse aggregates used are in saturated surface dry (SSD) condition. Three specimens for a mixture are cast in molds (3" × 3" × 11.25"), which are oiled in advance and into the ends of which the studs are inserted. Freshly mixed concrete is loaded in one layer and then compacted on a vibrating table. Excess is removed and leveled off. Concrete specimens are covered by a polythene sheet and wet towels to avoid moisture loss during the first 24 hours, demolded at the age of 1d and then immediately wrapped by a self-sealing polythene film and an aluminum foil sealed with tape to avoid any moisture loss. After being sealed, the specimens were stored in an environment chamber at constant 73°F and the initial length and weight are measured.

Shown in Figure 23, length is measured using a length comparator, which is kept in the same temperature chamber to avoid any variations due to temperature change according to ASTM C157 (standard test method for length change of hardened hydraulic-cement mortar and concrete). The lengths of concrete specimens at 4, 7, 14, 21, 28, 35, 42, 49 and 56 days are measured relative to the standard bar, and their weights are also tested to monitor the moisture loss.



Figure 22 Mold, length comparator, and concrete specimens stored in the environment chamber

3.3.2 Free drying shrinkage test

The specimen preparation for free drying shrinkage is the same as that for autogenous shrinkage, with all fresh mixture cast in the same batch of concrete. The specimens are cured for 7 days in a 100% relative humidity room and are measured for the initial length; then are cured in environment room at 73°F and 50% relative humidity.

Length and weight measurements are taken at the ages of 3, 7, 14, 21, 28, 35, 42, 49 and 56 days seen as in Figure 24, following the same procures as previously-mentioned for autogenous shrinkage test of concrete.



Figure 23 Length measurements of concrete specimens

3.3.3 Restrained ring shrinkage test

Restrained ring test is performed for concrete specimens according to ASTM C 1581: standard test method for determining age at cracking and induced tensile stress characteristics of mortar and concrete under restrained shrinkage (Figure 24). The ring molds are oiled and held in place using four 3" C-clamps (Figure 25(a)). Fresh mixture is poured and compacted in two layers on a vibrating table. Leads of the strain gage are attached to the module to collect the data every minute. The clamps are released immediately after the modules are connected. The specimens are then covered with polythene and stored at $73.5 \pm 3.5^\circ\text{F}$. At the age of 1day the outer steel ring is removed as shown in Figure 25 (b). The ring specimens are then placed in a 50% relative humidity and $73.5 \pm 3.5^\circ\text{F}$ environment room. The top surface is coated with a thin layer of wax.

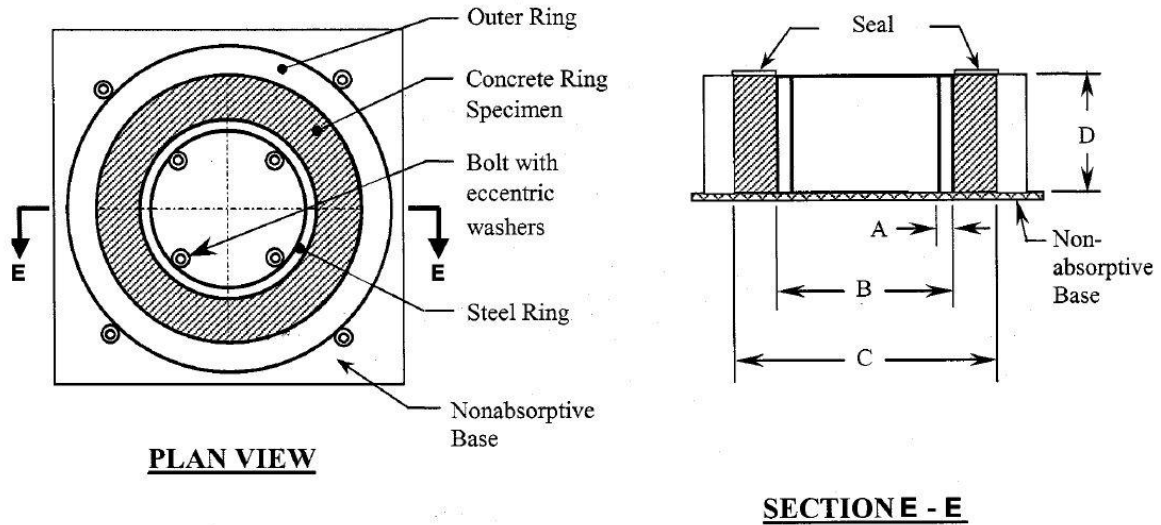


Figure Dimensions	Inch-Pound Units	SI Units
A	0.50 ± 0.12 in.	12.5 ± 0.13 mm
B	13.0 ± 0.12 in.	330 ± 3 mm
C	16.0 ± 0.12 in.	406 ± 3 mm
D	6.0 ± 0.25 in.	150 ± 6 mm

Figure 24 Standard dimensions of the ring test setup (ASTM Standard C1581, 2008)

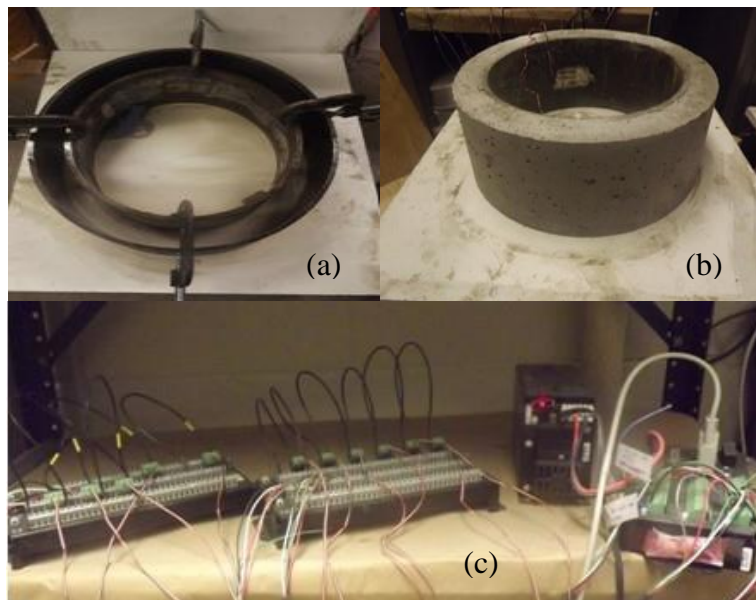


Figure 25 Ring steel mold (a) concrete ring specimen (b) and data logger setup (c)

Figure 25(c) illustrates the setup of the strain gauges where two strain gauges on the interior surface of the inner steel ring were mounted at mid-height locations on diametrically opposite locations. The gages were placed to measure strain along the circumferential

direction. The manufacturer's specifications were used for mounting and waterproofing the gauges on the steel ring and connecting lead-wires to the strain gauge modules.

Test strain gage response data were automatically recorded by the data logger. The data recorded were transferred into MS Excel then converted to the shrinkage of concrete specimens with time. The record includes the time, ambient temperature of the testing environment every day. The data logger program monitors the strains in the steel rings at intervals of 1 minute, recording the output of each strain gauge separately with the data acquisition system. A sudden decrease in compressive strain in one or both strain gauges indicates cracking of the ring. The specimens were checked every 3 days for cracks. The strain in the steel rings were recorded for 28 days after initiation of drying, unless cracking occurs prior to 28 days.

3.3.4 Strength and elastic modulus test

Compressive strength was performed according to ASTM C39 (standard test method for compressive strength of cylindrical concrete specimens). Specimens of 100mm (4") diameter and 200mm (8") height are molded in two equal layers, applying 25 strokes of a 10mm (3/8") rod for each cast. Specimens were demolded at the age of 24hrs and cured in a 100% humidity curing room. The same batches of fresh mixture were also used to cast the specimens for elastic modulus test, which follows ASTM C469 (standard test method for static modulus of elasticity and Poisson's ratio of concrete in compression).

Tensile strength of concrete specimens was tested according to ASTM C496 (standard test method for splitting tensile strength of cylindrical concrete specimens). Specimens of 150mm diameter and 300mm height are cast in 3 equal layers, compacted with 25 strokes. The specimens were demolded at 24hrs after cast and stored in 100% humidity curing room for 28days.

Specimens were tested for their strength and elastic modulus at the age of 1, 3, 7, 14, 28 and 56 days. Tensile strength of specimens was measured after 28days curing.

CHAPTER 4. RESULTS AND ANALYSIS

4.1 Autogenous Shrinkage

Autogenous shrinkage test results of the 11 concrete mixes studied are summarized in Figure 26 through Figure 30.

Figure 26 shows the test results of Group1, which includes mix 1, 2 and 3. The same cement source is used in all three mixes. But, mix 1 has no cement replacement while mix 2 and mix 3 consists of 20% of fly ash. When comparing mix 1 to mix 2, mix 1 has 665 lb/yd³ while mix 2 has 650 lb/yd³ and 573 lb/yd³. By comparing mixes 1 and 2 the results indicate that of fly ash replacement in the concrete reduces the autogenous shrinkage of concrete. Mixes 2 and 3 differ in having two types of water reducers and also having different coarse aggregate gradation. Mix 2 being an O-type mix has mid-range water reducer while mix 3 an S-type mix has a standard water reducer. Aggregate gradation of mix 3 has a coarser gradation than that of mix 2. The cement content of mix 3 (575 lb/yd³) is significantly less than that of mix 2. Regardless the differences, mixes 2 and 3 have similar autogenous shrinkage values, all significantly lesser than that of mix 1. This suggests that 20% fly ash replacement plays a significant role in reducing autogenous shrinkage of concrete.

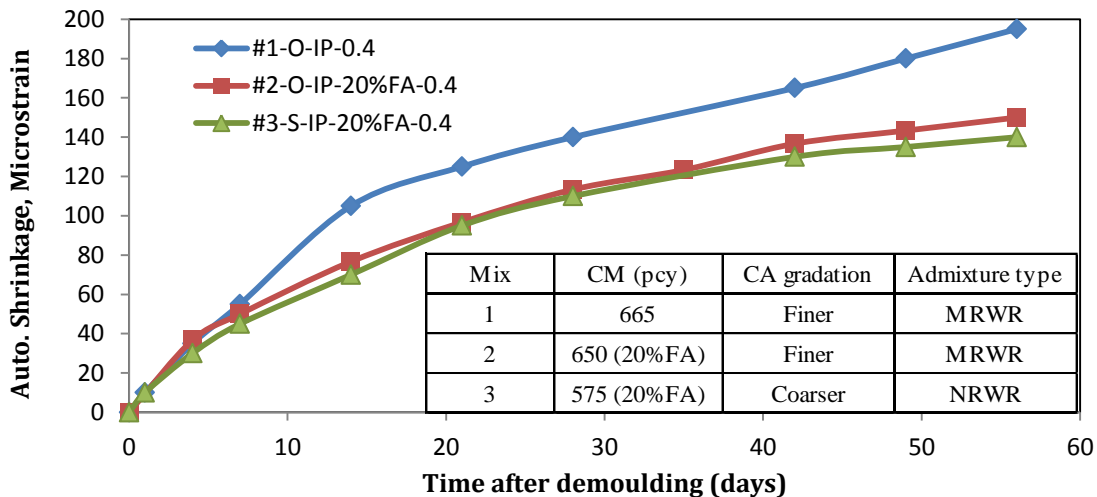


Figure 26 Autogenous Shrinkage of Concrete (Group1)

The autogenous shrinkage test result of concrete group 2 is shown in Figure 27. The mixes in Group 2 have the same cement (Lafarge I/II) and all mixes are O-type mixes. That

is the water reducer and aggregate gradations of all 4 mixes are the same except for mix proportion of mix 6 being different from others. Mix 4 doesn't consist of any SCM's and mix 7 consists of 25% GGBFS. Mix 4 consists of 710 lb/yd³ of cementitious material while mix 7 has 690 lb/yd³. The GGBFS replacement causes the autogenous shrinkage of a mix to increase. Mix 10 contrasts in a greater autogenous shrinkage than Mix 7 even though the cementitious material content is 675lb/yd³, lesser than mix 7. This implies that MK significantly increases the autogenous shrinkage. Comparison of mix 4 and mix 6 shows that high cement content and low w/cm (mix 6) greatly increased in the autogenous shrinkage of the concrete.

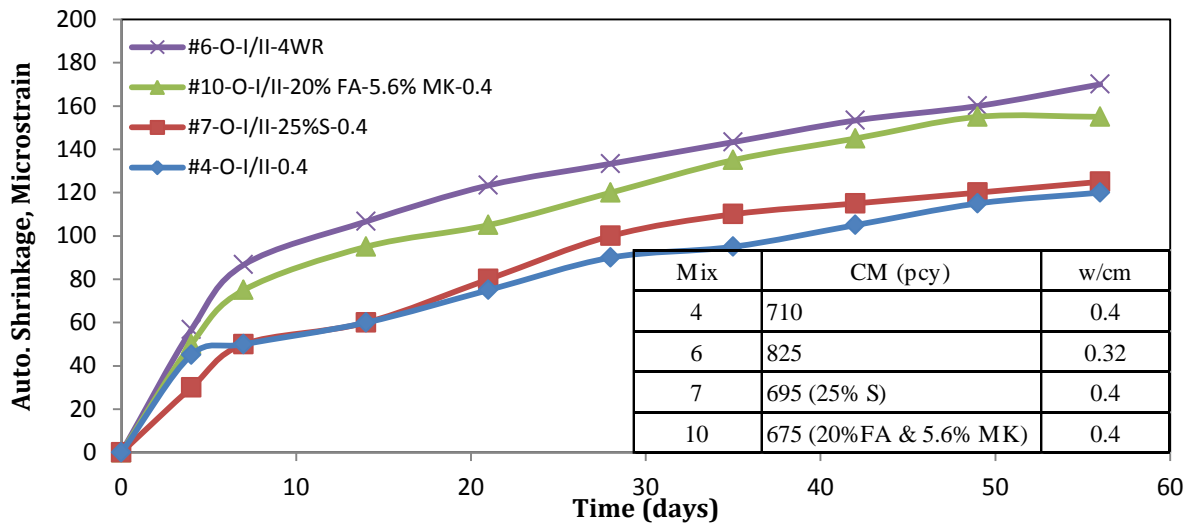


Figure 27 Autogenous Shrinkage of Concrete (Group 2)

Figure 28 illustrates the autogenous shrinkage of concrete of Group 3, which consists of Mixes 8 and 9. Both mixes contain 20% fly ash and 25% GGBFS replacement but different w/cm, cementitious content, water reducer type, coarse aggregate type and coarse aggregate gradation. Mix 8 contains 670lb/yd³ while mix 9 contains 590 lb/yd³. This by far is of huge significance and is displayed in the autogenous shrinkage of mix 8 being significantly larger than mix 9. Mix 8 contains high shrinkage resistant aggregate quartzite while mix 9 has limestone.

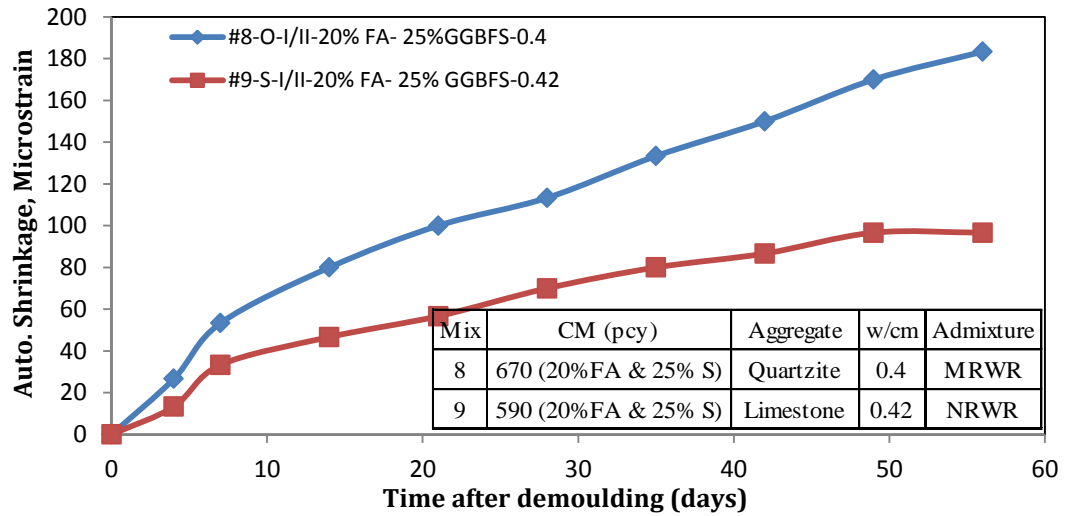


Figure 28 Autogenous Shrinkage of Concrete (Group 3)

Autogenous shrinkage test results of group 4 is shown in Figure 29. Both mixes 5 and 11 have the same water cementitious material ratio, water reducer and coarse aggregate gradation. Replacement of cement by fly ash and slag has affected the Mix 11 to have lesser shrinkage than that of Mix 5. Therefore the mix of 20% Fly ash and 25% GGBFS is also an option in reducing the autogenous shrinkage of concrete than the case of using GGBFS alone (see mix 7 in Group 2). Mix 9 and mix 11 are identical mixes in all aspects other than the cement type used. Mix 9 composes of Type I/II cement while mix 11 has Type I cement. Type I cement is a typically displays higher shrinkage. Figure 29 shows mix 11 displays consistently higher shrinkage than mix 9.

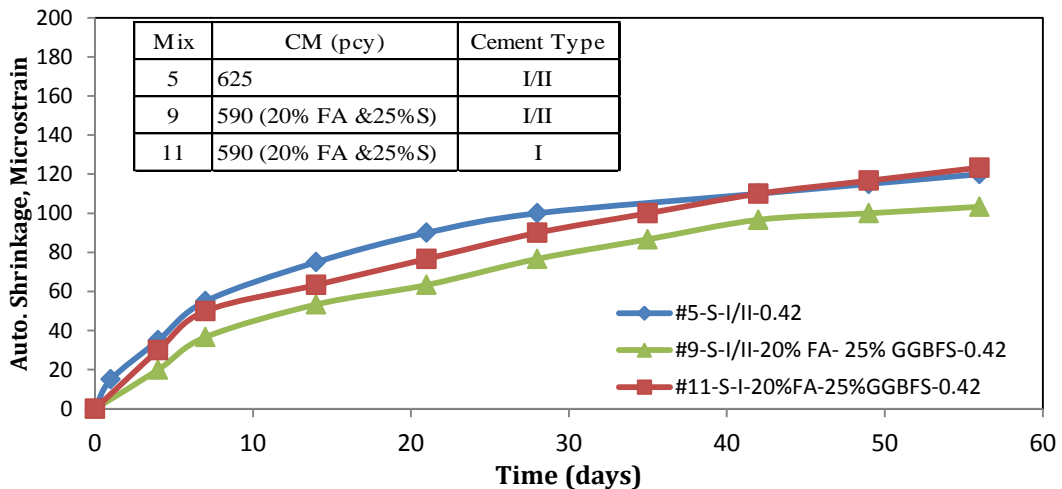


Figure 29 Autogenous Shrinkage of Concrete (Group 4)

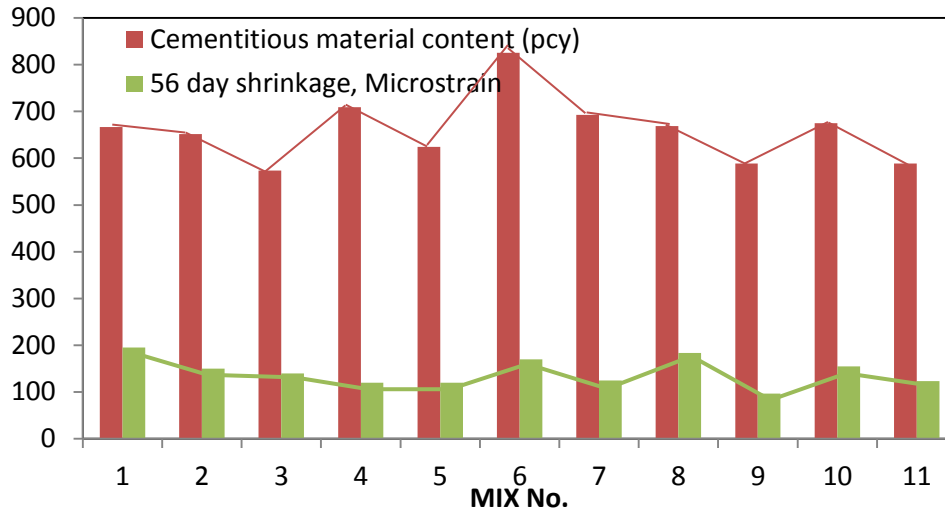


Figure 30 Autogenous Shrinkage of Concrete at 56 day for all mixes

Figures 26 to 29 shows that the rate of shrinkage slowed down with time. Generally, greater amount of the shrinkage was observed in the first 28 days but it decreased significantly thereafter. Use of 20% fly ash replacement alone showed a reduction of shrinkage from 100% cement mixtures. Use of GGBFS at 25% replacement alone increased autogenous shrinkage combination 20% fly ash and 25% GGBFS showed little effect on concrete autogenous shrinkage.

Autogenous shrinkage is closely related to the amount of cementitious material (Figure 30) Autogenous shrinkage is closely related to the amount of cementitious material content (Figure 30) Type I cement also provides concrete higher autogenous shrinkage than other types of cement (Type I/II and Type IP) used.

4.2 Free Drying Shrinkage

4.2.1 Mass loss of the specimens for free drying shrinkage test

The results of mass loss of concrete specimens for all 11 mixes are presented in Figure 31 to Figure 34. Figure 31 shows the mass loss test results of concretes for Group 1. It can be seen from the figure that the major portion of mass loss occurs during the first 14 days. Mix 1 displays the least amount of mass loss and mix 3 shows the greatest amount of mass loss. The trend of mass loss is consistent with the free shrinkage development as the majority of shrinkage occurs in the first 14 days.

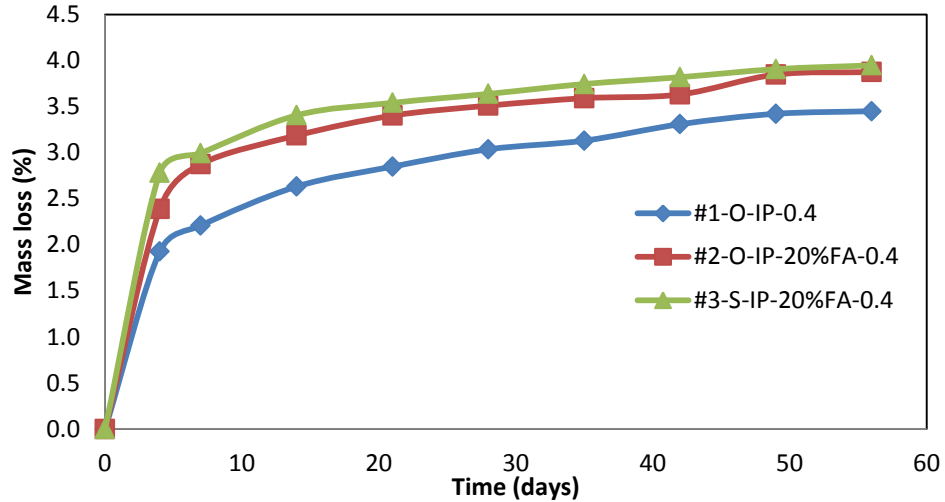


Figure 31 Mass loss of Concrete (Group 1)

Figure 32 illustrates the results of mass loss of mortar specimens in Group 2. The mass loss is similar to that of group 1 but smaller in magnitude. Mix 6 displays the least amount of mass loss while mix 10 shows the greatest amount of mass loss.

Figure 33 illustrates the results of mass loss of mortar specimens in Group 3. The mixes 8 and 9 have no significant differences in mass loss. Mass loss is rapid in the first 7 days and rapidly slows down at the age of 14 days for both mix 8 and 9.

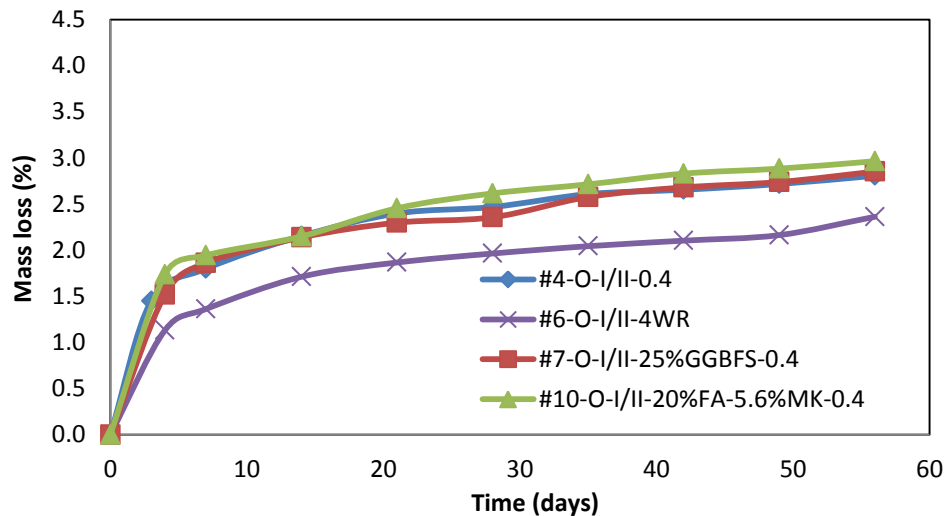


Figure 32 Mass loss of Concrete (Group 2)

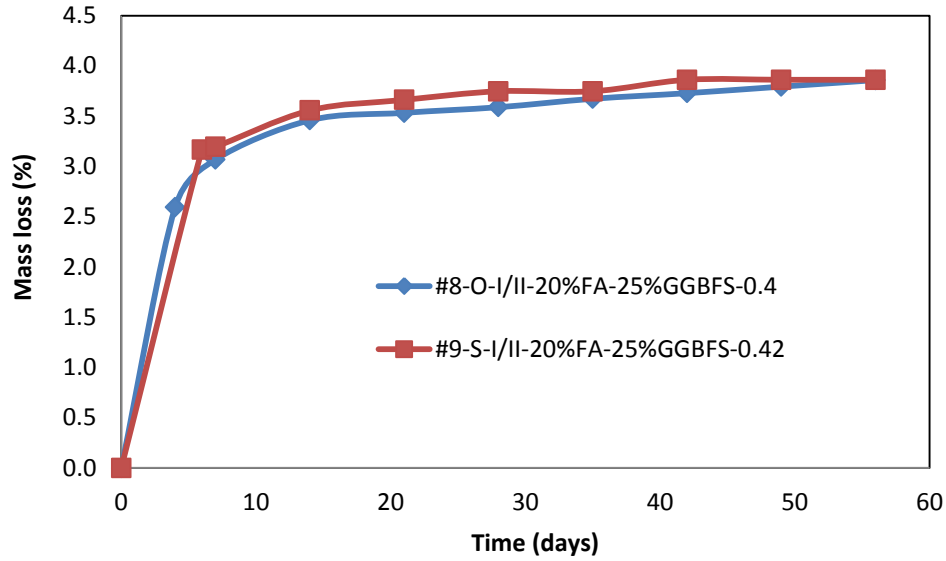


Figure 33 Mass loss of Concrete (Group 3)

Figure 34 presents the results of mass loss for concrete in Group 4. Mix 5 the control mix displays the least amount of mass loss while mixes 9 and 11 show significantly large amount of mass loss.

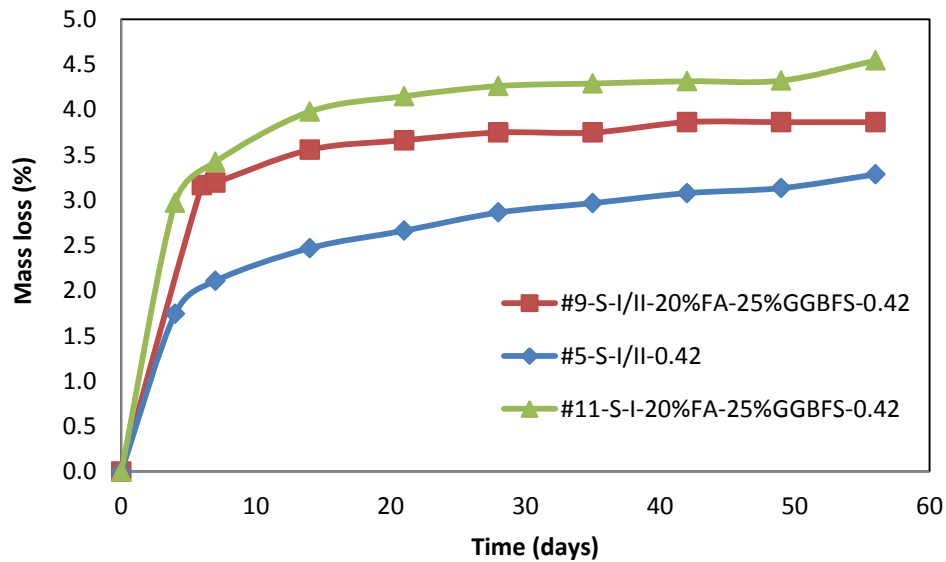


Figure 34 Mass loss of Concrete (Group 4)

4.2.2 Free drying shrinkage

Typical Measurements

Typical free drying shrinkage measurements are shown in Figures 35 and Figure 36. Both plots indicate a very small variation among the 3 samples tested for each mix. Therefore the average of the 3 samples have been taken as representative for each mix.

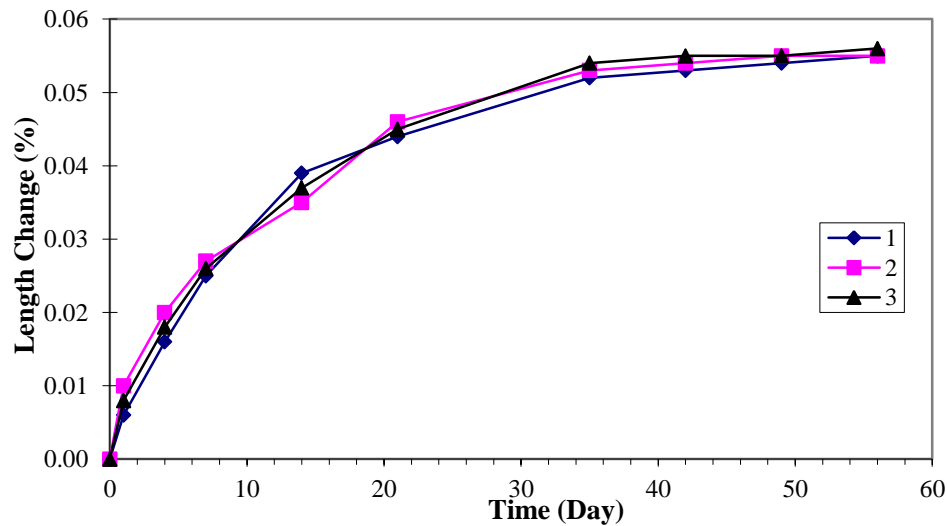


Figure 35 Typical free drying shrinkage measurement of mix 5

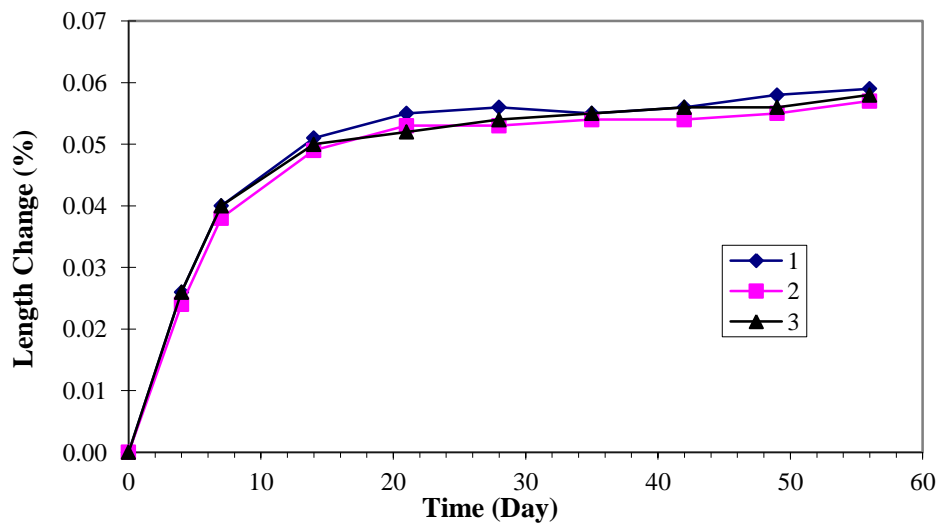


Figure 36 Typical free drying shrinkage measurement of mix 11

Free drying shrinkage of the 11 mixes is discussed in the following section. The behavior of the 11 test mixes will be illustrated by Figure 37 to Figure 41.

Figure 37 illustrates the free drying shrinkage test results of concrete in Group 1. The shrinkage development of the 3 mixes is similar in the first 7 days of drying. The performance of the Mixes 1 and 2 do not show a significant difference in its performances. The addition of fly ash in a mix generally reduces free drying shrinkage. It is not clear why such reduction has not occurred as observed for mortar. Pore structure of mortar needs to be investigated to help explain this behavior. Mix 3 displays a lesser free shrinkage to that of mix 1 and 2. Mix 3 is composed of a coarser coarse aggregate portion and has lesser cementitious material content compared to that of Mix 1 and 2.

Comparing the mass loss (Figure 31) and shrinkage observed (Figure 37) the mass loss in mix 2 and 3 are greater than that of mix 1. This forms a partial explanation to why mix 2 displays greater shrinkage than mix 1 with only type IP cement.

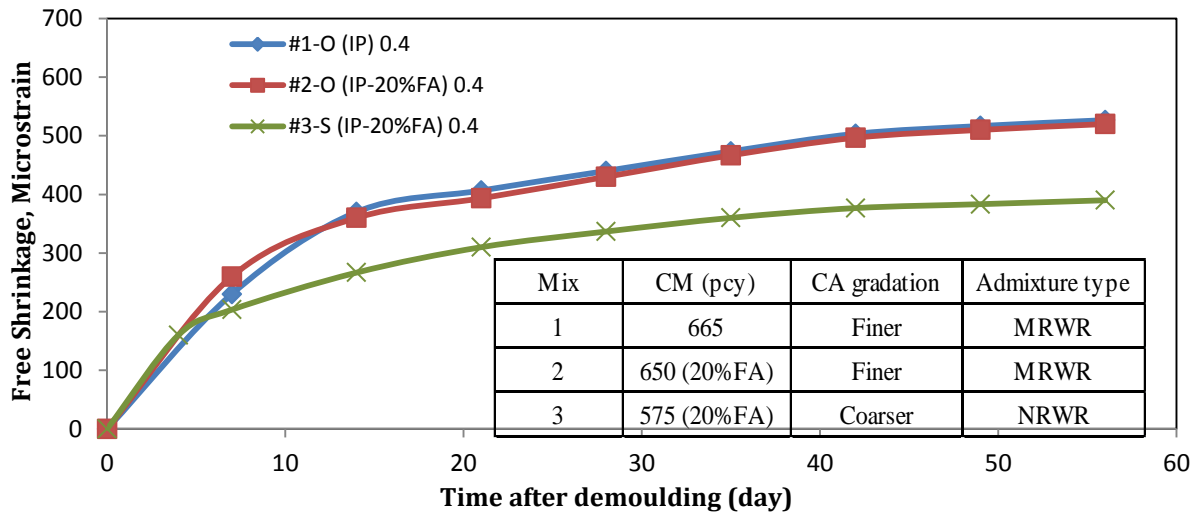


Figure 37 Free Drying Shrinkage of Concrete (Group 1)

Mix 4 and Mix 6 have no SCM's in them. Mix 7 with the addition of 25% GGBFS shows the greatest free drying Shrinkage. Mix 6 shows higher shrinkage than mix 4 due to the high cement factor. In mix 10 addition of 20% fly ash and 5.6% metakaolin has reduced the amount of free drying shrinkage of concrete than mix 4. But the reduction is not as a large reduction and the behaviour is almost similar in the first 28 days. This may be a result of the metakaolin having an shrinkage increasing effect while the shrinkage reducing effect of fly ash is countering this effect. Therefore the combined effect of 20% fly ash and 5.6% metakaolin reduces the free drying by a small amount.

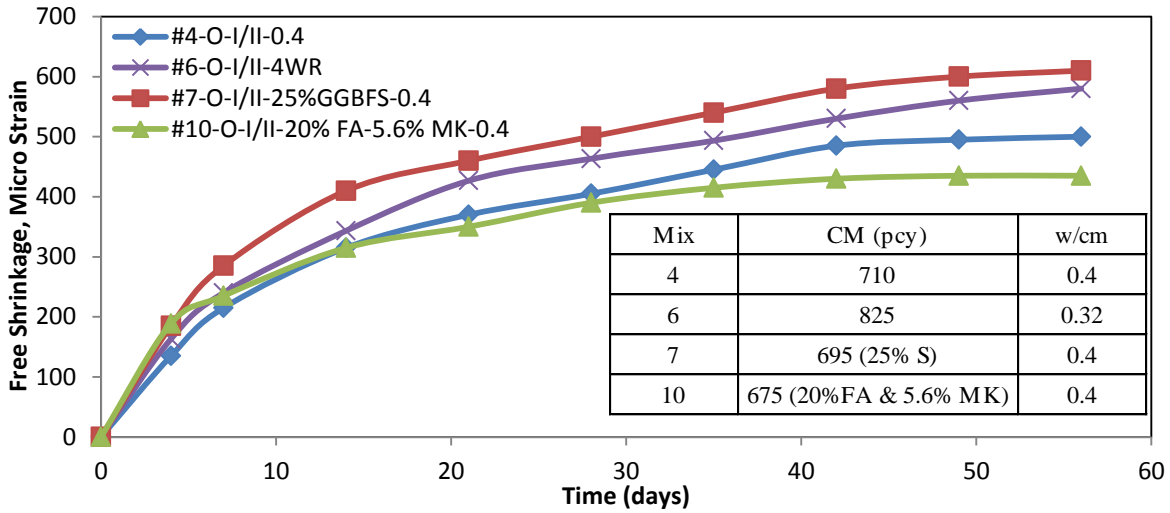


Figure 38 Free Drying Shrinkage of Concrete (Group 2)

The results related to free drying shrinkage of concrete in Group 3 is shown in Figure 39. In Group 3 mix 8 and mix 9 differ by many factors. Among these factors are the two mixes employing two coarse aggregate types and two gradations. Mix 8 contains a coarser graded quartzite while mix 9 employs a finer graded limestone. Other than that mix 8 has higher paste content (0.302) to that of mix 9 (0.274) leading to a greater amount of anticipated drying shrinkage in mix 8 than mix 9. Moreover mix 8 has a mid-range water reducer while mix 9 has a standard water reducer. Although there are so many factors that differ mix 8 from mix 9 there is no significant difference in performance in the two mixes.

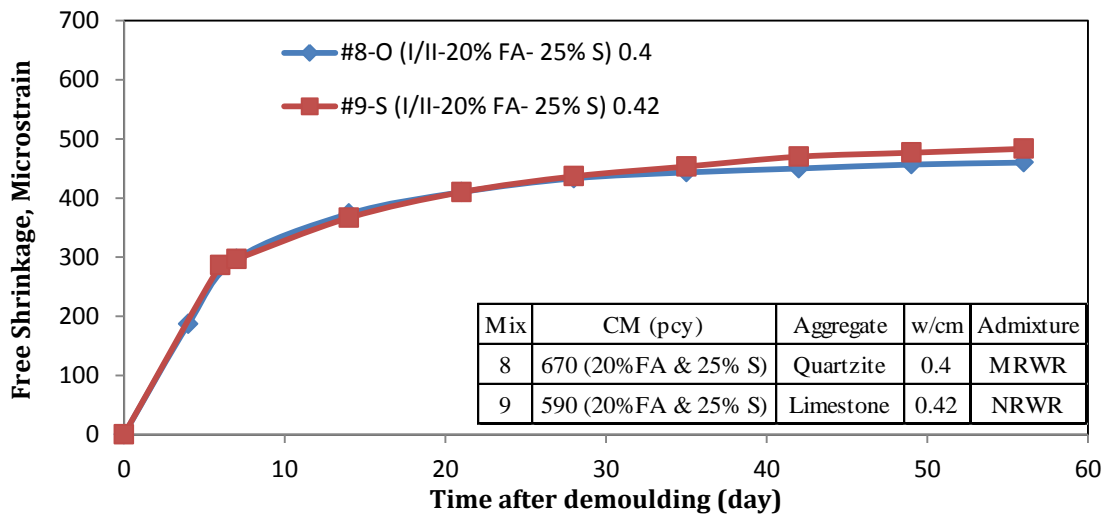


Figure 39 Free Drying Shrinkage of Concrete (Group 3)

Figure 40 illustrates the results of group 4. Here the results indicate that the addition of 20% fly ash and 25% GGBFS has had a positive effect on the mix and reduced the free drying shrinkage. Initially mix 5 and mix 9 have similar shrinkage behavior, but due to the high levels of cement replacement the rate of shrinkage reduces. It is also important to note that mix 11 employs Type I cement that Type I/II in mix 9. With all other being the same the mix 11 displays higher shrinkage than mix 9. The behavior is typical of Type 1 cements.

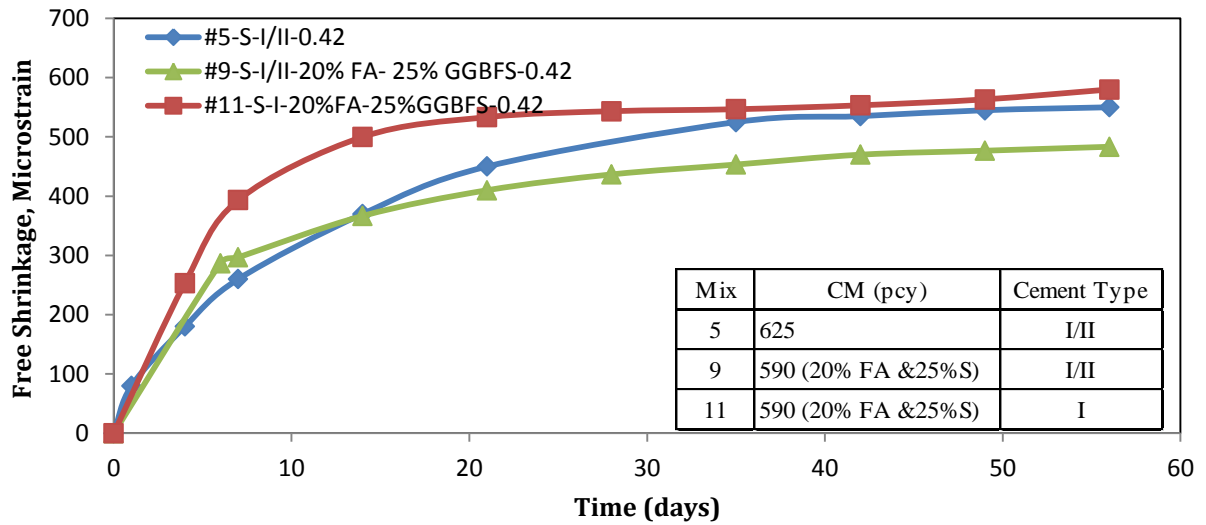


Figure 40 Free Drying Shrinkage of Concrete, Group 4

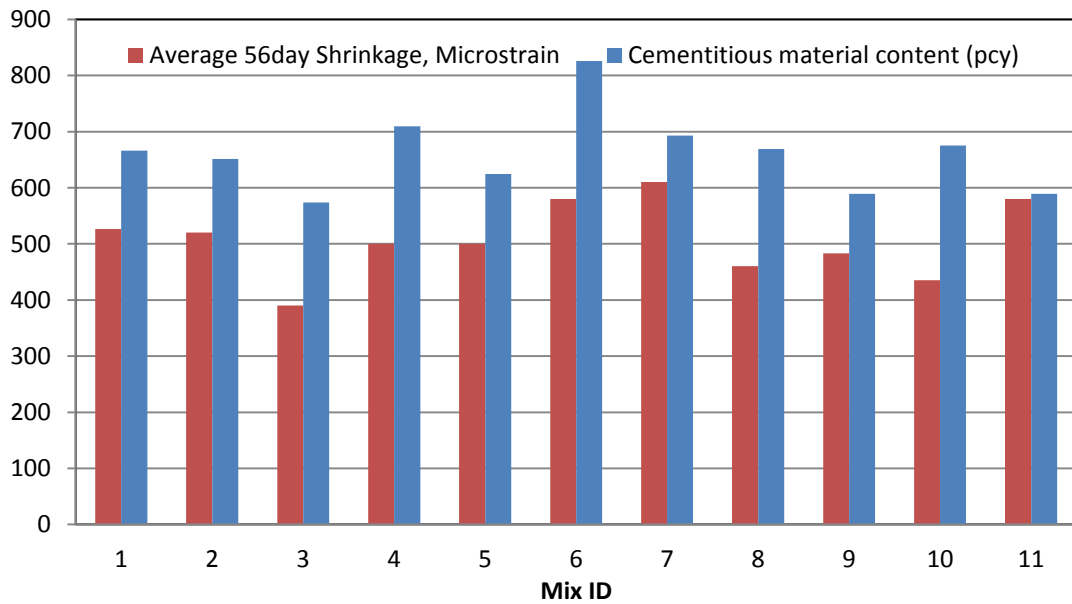


Figure 41 Free Drying Shrinkage of Concrete at 56 days

Shrinkage of these mixes studied significantly slowed down after 28 days. Measurements were made for duration of 56 days and upon approaching 56 days the rate of shrinkage slowed down significantly. The cementitious material content has a direct influence on the amount of free drying shrinkage of concrete (Figure 41).

Figure 42 illustrates the comparison of individual mixes, where the shrinkage of each mix is individually correlated to its moisture loss. The R^2 values range from 0.82 to 0.99 improving the argument that comparison of free drying shrinkage of each mix with the moisture loss is a good measure of quality control for measurements.

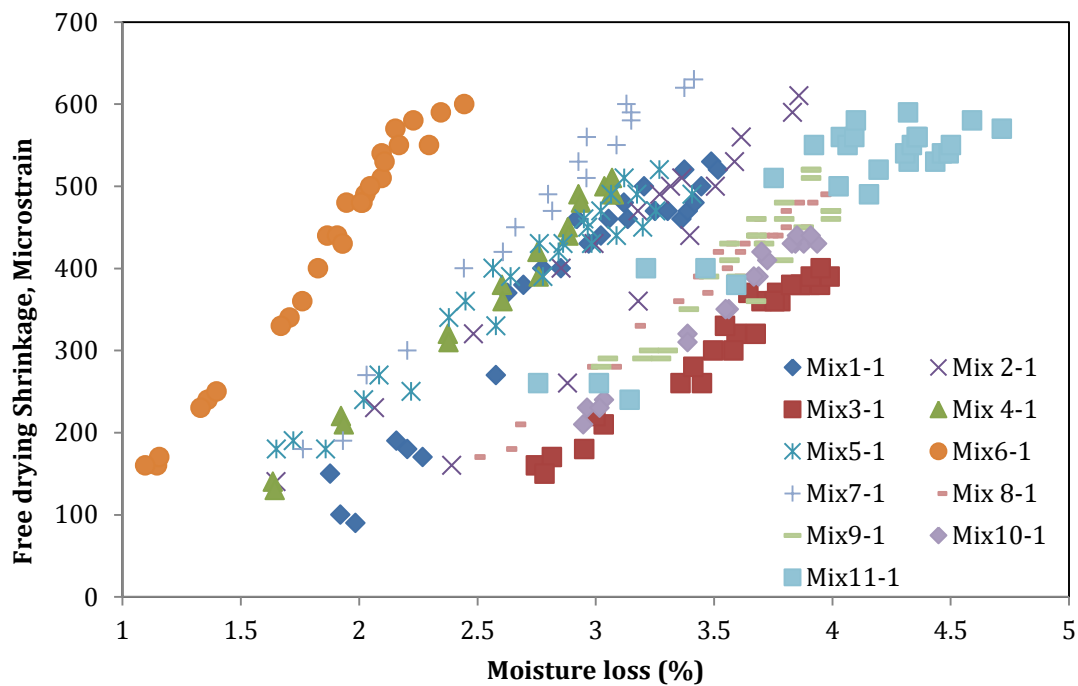


Figure 42 Free Drying Shrinkage vs. Mass loss (%)

4.3 Restrained Ring Shrinkage

Restrained ring shrinkage test evaluates the cracking tendency of a concrete mix in addition to restrained shrinkage behavior. Typical results if 3 rings made from one batch are close (Figure 43) and the average shrinkage can be used as a representative result.

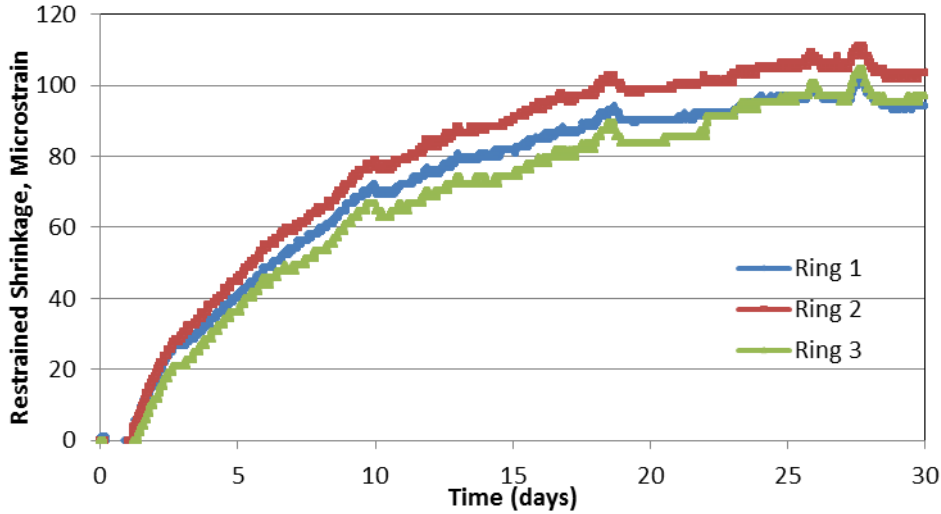


Figure 43 Typical result of restrained shrinkage Mix 10

Figure 44 illustrates the restrained ring shrinkage results of Group 1. Mix 1 displays the greatest amount of shrinkage having only Type IP cement in the mixture. Both mix 2 and 3 having 20% fly ash and display lesser shrinkage than Mix 1. Mix 2 and Mix 3 display similar behavior at early age but, mix 3 shows less shrinkage at the later age. The difference is small compared to that of mix 1.

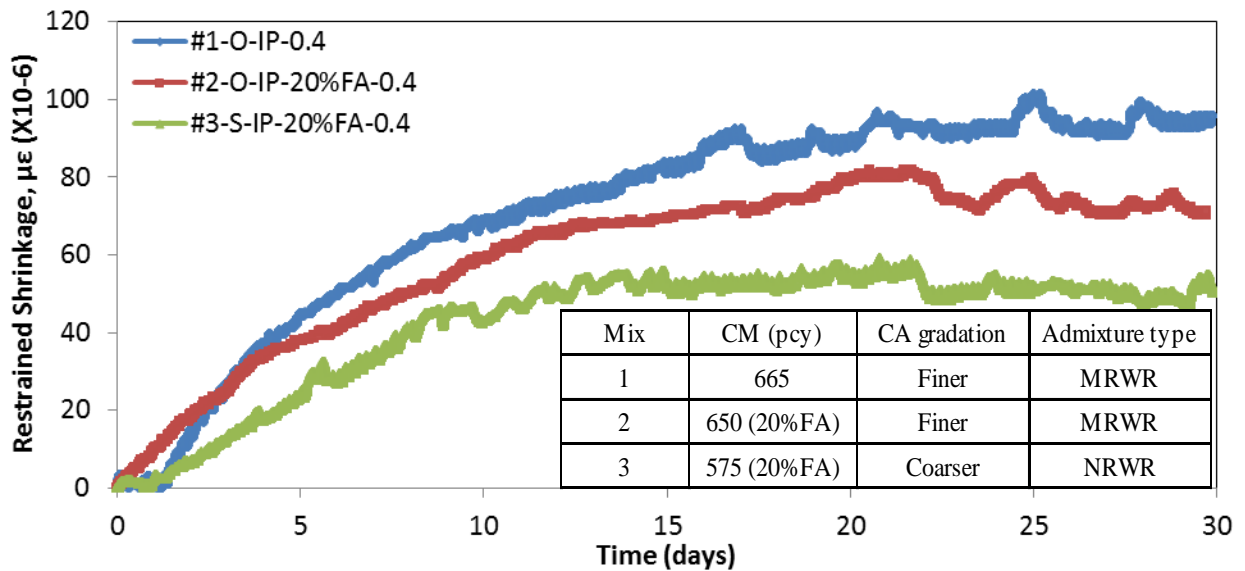


Figure 44 Restrained Shrinkage of Group 1

Restrained ring shrinkage of concrete in Group 2 is illustrated by Figure 45. The group of mixes do not show a significant variation among the early or late age restrained ring

shrinkage. Mix 7 shows the greatest rate of early age strain development while mix 10 is the slowest. All 3 rings cast for mix 6 cracked at 16, 16.5 and 18 days respectively (Figure 87). Two rings out of 3 cast for mix 4 cracked at ages 13 and 18 days (Figure 85). Both mix 4 and mix 6 are only composed of Type I/II cement and mix 6 has a greater content of Type I/II cement ($w/c = 0.32$). The replacement of cement by 25% slag had an influence towards increasing the rate at which the strain developed initially. But the strain development slowed down significantly after 7 days. The replacement of cement by 20% fly ash and 5.6% metakaolin had an influence towards reducing the initial rate of shrinkage but the steady growth of shrinkage resulted in similar shrinkage observed at 28 days to that of Mix 4 which had no cement replacement.

The early age shrinkage in Group 2 is similar to that observed in free drying shrinkage of concrete. Mix 4 & 6 cracked although the mixes were not the mix with the highest restrained shrinkage. This indicates that these mixes had lower cracking resistance.

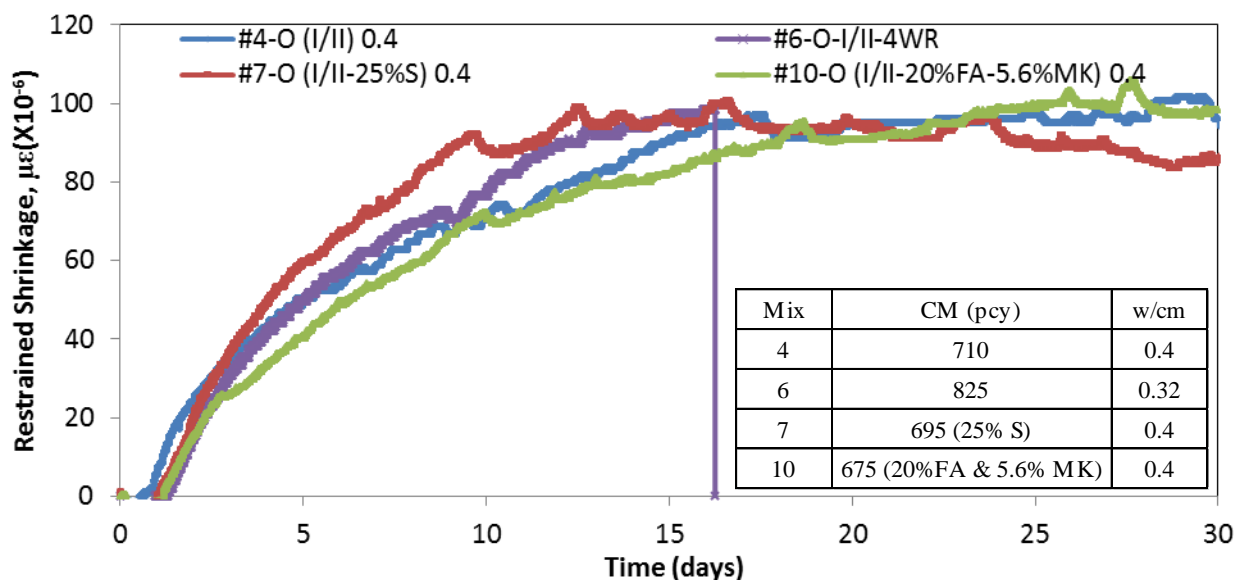


Figure 45 Restrained Shrinkage of Group 2

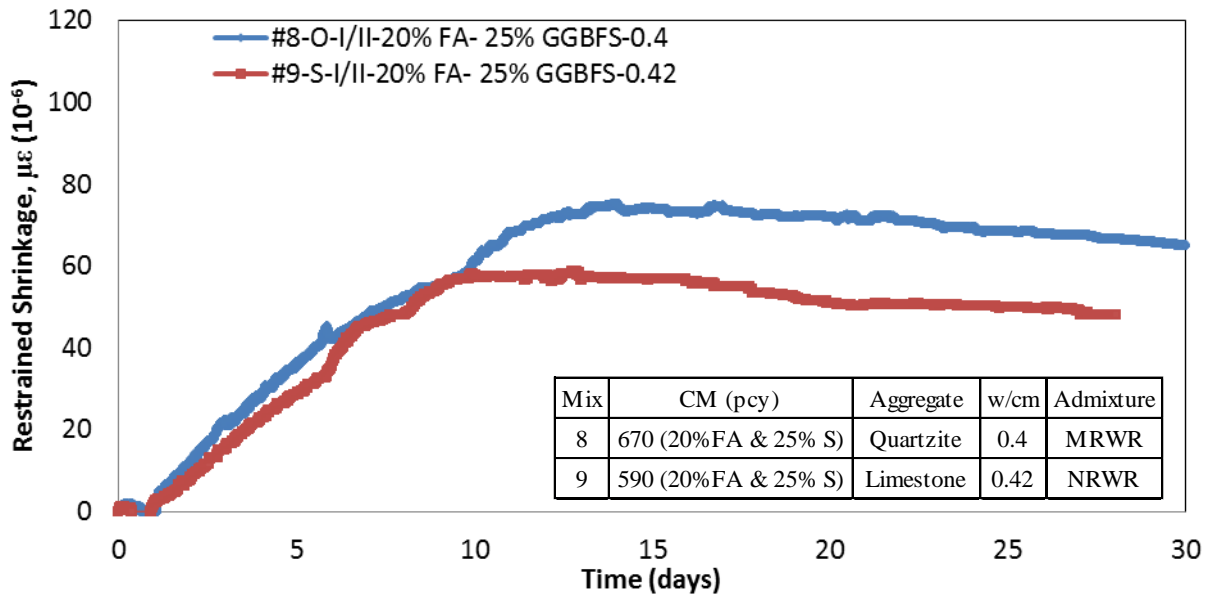


Figure 46 Restrained Shrinkage of Group 3

Figure 46 illustrates the restrained ring shrinkage of Group 3. The early age performances of the mixes are identical. The inclusion of Quartzite in mix 8 is the most significant difference between the two mixes. The trend of the early age shrinkage is similar to that of free drying shrinkage concrete.

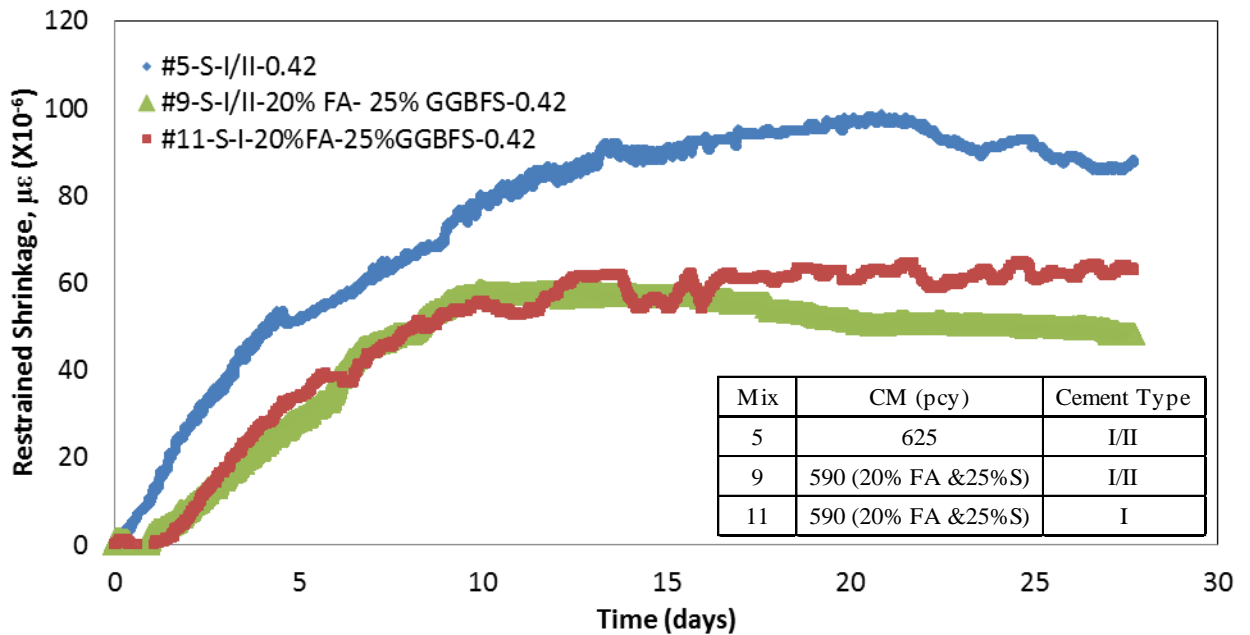


Figure 47 Restrained Shrinkage of Group 4

Figure 47 illustrates the restrained shrinkage of group 4. All three mixes have the same water cement ratio, water reducers and coarse aggregate gradation. Mix 5 is a control mix composed of Type I/II cement, mix 9 is composed of type I/II cement 20% fly ash and 25% slag while mix 11 is composed of Type I cement, 20% Class C fly ash and 25% GGBFS. Mix 5 is the only mix to display cracking, where one ring cracked at the age of 11 days (Figure 86). The cement replacement by 20 % fly ash and 25% slag has reduced both the rate and the shrinkage. This is clearly visible when comparing mix 5 and mix 9. When comparing mix 9 and mix 11 the two mixes show similar behavior in the early age while in the later age mix 11 displays greater shrinkage.

Table 12 summarizes the results of restrained shrinkage of concrete ring test. ASTM 1581 provides equations for estimation of the strain rate in samples and rankings of cracking potential. The strain development (ε_{net} , μstrain) is plotted against the square root of time (t , days) and the slope of the graph is defined as the strain rate factor (α , $\mu\text{strain}/\sqrt{\text{day}}$).

$$\varepsilon_{net} = \alpha\sqrt{t} + k \quad (20)$$

- Where k is the regression constant.

The average of the strain rate factor for the rings (α_{avg} , $\mu\text{strain}/\sqrt{\text{day}}$) can be used to find the stress rate factor (q , psi/day) and the average time to cracking (t_r , days) the cracking potential can be found. Where the rings did not crack the t_r was taken as the time of termination of the test (28 days).

$$q = \frac{G |\alpha_{avg}|}{2 \sqrt{t_r}} \quad (21)$$

- Where G is a constant based on the ring dimension $10.5 \times 10^6 \text{psi}$ (72.2GPa)

Table 12 Summary of restrained shrinkage

Mix	Total cementitious material content/pcy	Average Strain Rate, (in/in)/day	Cracking time(days)			Average Stress Rate, psi/day	Rank	ASTM Cracing Potential Rating
			S1	S2	S3			
1	665	23.8	-	-	-	23.6	9	Moderate-Low
2	650	17.0	-	-	-	16.8	10	Moderate-Low
3	575	16.8	-	-	-	16.6	11	Moderate-Low
4	710	25.1	-	13	17	31.9	3	Moderate-High
5	625	24.7	11	-	-	28.9	4	Moderate-High
6	825	29.3	16	16	18	37.3	1	Moderate-High
7	695	36.0	-	-	-	35.6	2	Moderate-High
8	670	24.8	-	-	-	24.5	7	Moderate-High
9	590	27.4	-	-	-	27.1	6	Moderate-High
10	675	28.0	-	-	-	27.7	5	Moderate-High
11	590	24.5	-	-	-	24.2	8	Moderate-Low

Mix 2 and 3 shows the lowest cracking potential. 20% class C fly ash has the greatest effect towards reducing the restrained shrinkage. All mixes with Type I/II cement display moderate-high shrinkage potential rank. Addition of GGBFS in mix 7 has caused mix 7 to display a greater strain rate factor and as a result moderate-high cracking potential. Mix 6 with the greatest amount of cement (lowest w/c) displays the greatest shrinkage potential. Mixes 4, 5 and 6 consisting of only Type I/II cement were the only mixes that had at least one ring that cracked during its drying period.

4.4 Mechanical Strength Parameters

The following chapter discusses about the mechanical strength parameters of the 11 mixes. Parameters measured include compressive strength, Elastic modulus and split tensile strength. All measurements were made using 4"X8" cylinders.

4.4.1 Compressive strength

Figure 48 illustrates the compressive strength of the 11 mixes. Addition of fly ash has induced an increase in compressive strength. Comparing mix 1 and 2 this becomes clear. The two mixes have the same w/cm ratio and approximately the same amount of cementitious

material. Mix 2 has 20% of its cement replaced by class C fly ash and shows greater compressive strength than mix 1 with type 1 cement.

The compressive strength of concrete Group 2, Mix 6 with the greatest amount of cementitious materials and lowest w/c ratio displays the greatest compressive strength. Mix 7 has similar (690 pcy) total cementitious material content to that of mix 4 (710 pcy). Mix 4 is the control mix, mix 7 composed of type I/II cement and 25% GGBFS displays similar strength development. Introduction of GGBFS has no effect on the strength of concrete. Mix 10 with 675pcy total cementitious material content, is composed of type I/II cement, 20% fly ash and 5.6% MK, displays higher strength compared to the control mix 10. This can be partially attributed to the fly ash in the mix. It is also important to note that the rate of strength development is higher in mix 10 compared to mix 4. This can be attributed to the MK and its high reactivity.

The compressive strength development of Group 3 mixes, Mix 8 and mix 9 consist of a similar composition of cementitious material but, vary in aggregate type and aggregate gradation. The principal deciding factor for strength of w/cm ratio makes the greatest impact towards the strength. Due to the high levels of replacement the concrete displays a lower rate of strength development compared to the mixes in concrete group 2.

The concrete strength development of Group 4, comparing mix 5 and mix 9, mix 9 displays the slow strength development which is influenced by the high replacement level of cementitious materials. Mix 11 compared to mix 9 yields the effect of Type I cement compared to that of Type I/II cement. It's clear that the Type I cement develops strength at a greater rate compared to that of Type I/II.

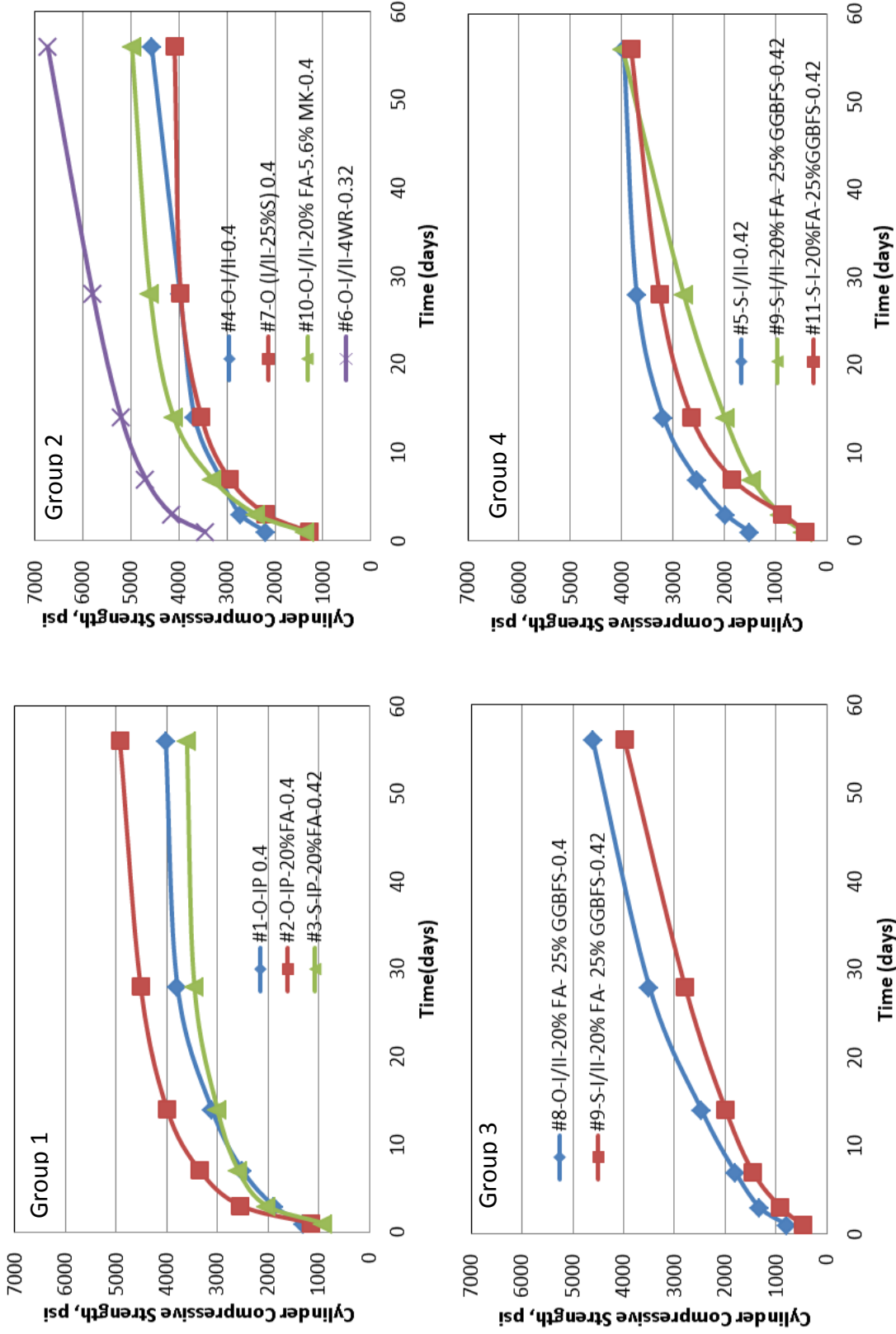


Figure 48 Compressive strength of concrete Group 1-4

4.4.2 Elastic modulus

Figure 49 displays the elastic modulus of the 11 mixes. Elastic modulus was calculated for the loading of 40% of the crushing load of the specimens.

The elastic modulus development of concrete in Group 1 is illustrated in Figure 49. The three mixes do not display a significant difference. The higher w/cm ratio of mix 3 has slowed down the development of the elastic modulus but it reaches the value obtained in mixes 1 and 2.

When comparing the elastic modulus of concrete in Group 2, Mix 4 the control mix compared to mix 6, the difference of the w/c ratio has driven mix 6 to have a much greater elastic modulus. The replacement of cement by SCM's has influenced the concrete mixes 7 and 10 to display lesser modulus to that of mix 4.

When considering the elastic modulus development of concrete in Group 3, The influence of quartzite and lower water cement ratio aided mix 8 to display a greater elastic modulus than mix 9.

When comparing mix 5 to mix 9 the replacement of cement by 20% fly ash and 25% GGBFS has influenced the concrete to display lesser elastic modulus. The effect of type I cement to Type I/II cement. Type I cement displays a greater elastic modulus (mix 11) to that observed by type I/II cement (mix9).

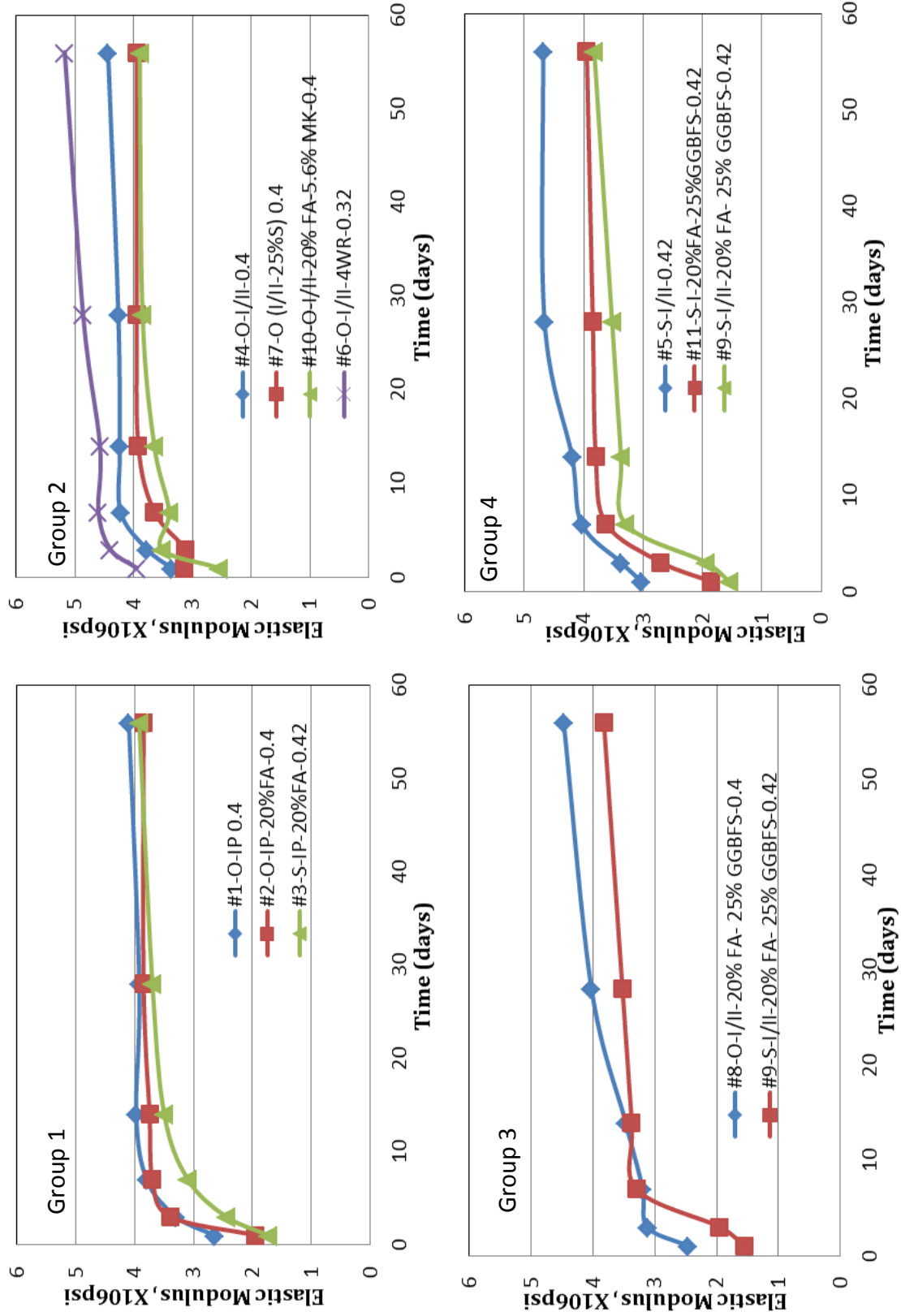


Figure 49 Elastic modulus of concrete Group 1-4

4.4.3 Split tensile strength

Split tensile test were performed on 4"x8" cylindrical samples. The set up laid the sample axis on horizontal and applied the load on its cylindrical surface. The results of the split tensile tests are illustrated in the figures below.

In concrete Group 1 (Figure 50) there is no significant difference among the 3 mixes till the 28 day strength is obtained. Mix 2 with 20 % fly ash displays a continuing growth of strength. The lowest strength is shown by mix 3 which has a w/cm ratio of 0.42 compared to mix 1 and 2 which have 0.4.

Strength development in mix 10 is continuous and can be attributed to the SCM's in the mix. MK due to its high reactivity displays high strength development in the early age and fly ash activated by the calcium hydroxide developed in the hydration of cement continues its action thereafter. Mix 6 with the greatest amount of cement displays a great increase of split tensile strength compared to mix 4(control) throughout its life. Addition of slag has an influence on increasing the split tensile strength as shown in mix 7 compared to the control mix.

Mix 8 consisting of quartzite displays lower split tensile strength than mix 9. This is shown even with a greater w/cm ratio in mix 9 compared to mix 8. Mix 8 having a finer aggregate gradation may have influenced this. Also the siliceous aggregate material (quartzite) having a potentially weaker interfacial transition zone compared to calcareous aggregate (limestone) may also affects the result.

The replacement of cement by 20% fly ash and 25% GGBFS has influenced the initial strength development to be slow but as time progresses the additions have brought about a similarly strong mix to that of mix 5. Type I cement shows high early age strength development compared to Type I/II cement (mix 9 and mix 11).

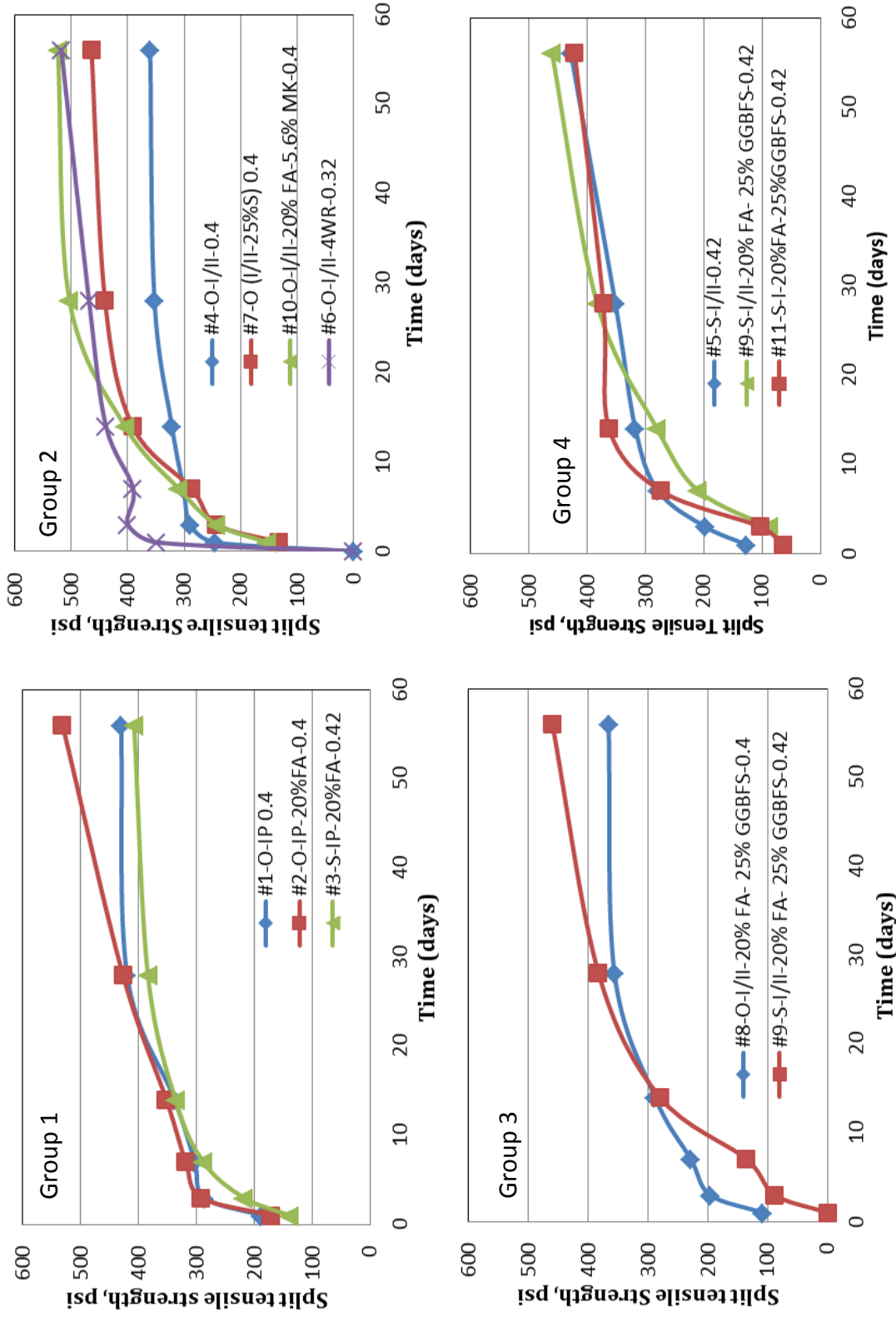


Figure 50 Split tensile strength of concrete Group 1-4

4.5 Relationships among Test Results

This section discusses the relationships that were observed among the test results. Relationships among results are useful tools in reassuring the accuracy of data and also can be used as an alternative tool in estimating performance of a mix in one test. The relationships among shrinkage parameters discussed include moisture loss vs. free drying shrinkage (Figure 51,52) and concrete ring shrinkage vs. free drying shrinkage of concrete (Figure 53). Further elastic modulus of concrete vs. compressive strength of concrete vs. split tensile strength of concrete are relationships investigated for strength parameters.

4.5.1 Free drying shrinkage and mass loss of concrete

Figure 51 and Figure 52 show that moisture loss of the concrete prism is linearly correlated to the free drying shrinkage of concrete within the 56 day period of measurement. Therefore measurement of mass loss can be a good indicator of the free drying shrinkage of concrete with R^2 values greater than 0.95 (Table 13).

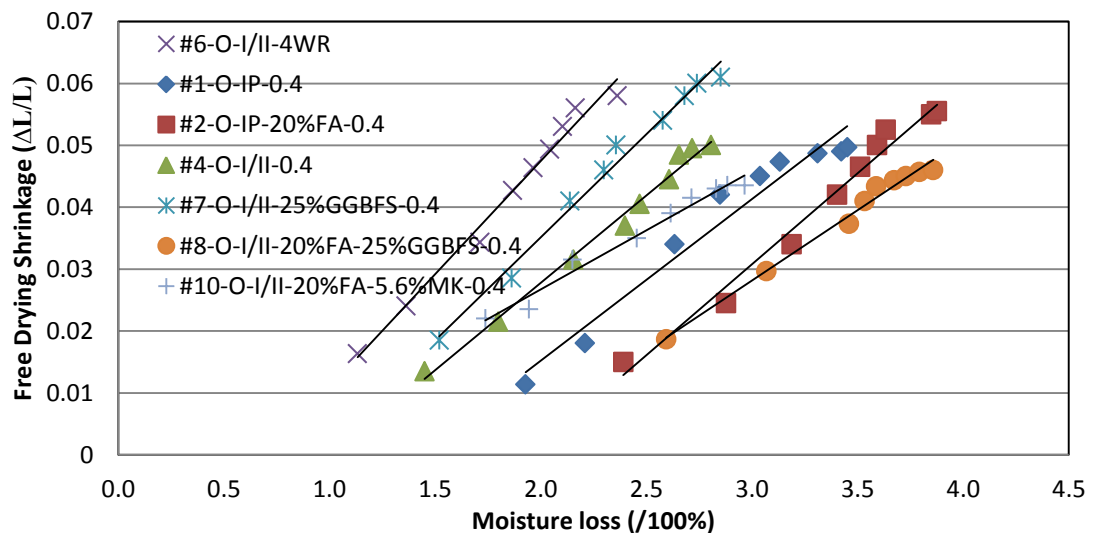


Figure 51 Free drying shrinkage vs. mass loss of concrete (a)

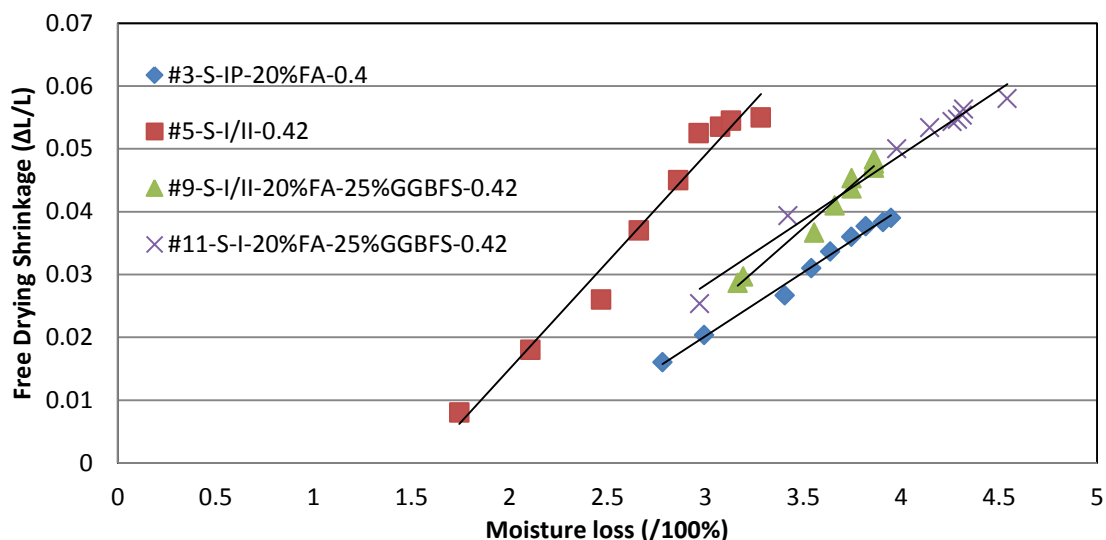


Figure 52 Free drying shrinkage vs. mass loss of concrete (b)

Table 13 Relationship between free drying shrinkage and moisture loss

Free Drying Shrinkage Vs. Moisture Loss		
Mix no.	Eqn.	R ²
1	$y = 0.0261x - 0.037$	0.95
2	$y = 0.0294x - 0.0575$	0.98
3	$y = 0.0203x - 0.0409$	0.99
4	$y = 0.0282x - 0.0287$	0.99
5	$y = 0.0341x - 0.0533$	0.97
6	$y = 0.0365x - 0.0256$	0.99
7	$y = 0.0333x - 0.0316$	0.99
8	$y = 0.0227x - 0.0399$	0.99
9	$y = 0.0274x - 0.0584$	0.98
10	$y = 0.0191x - 0.0114$	0.98
11	$y = 0.02808x - 0.034$	0.98

4.5.3 Restrained drying and free drying shrinkage stress of concrete

Performing the ring shrinkage test poses several difficulties in casting and maintaining the environment for the proper evaluation of strain. Casting the ring, the control of compaction effort is hard as vibrating the setup can cause the clamps to lose its tension and as a result the spacing of the rings is affected. Strain gauges attached to the surface of the ring may produce erroneous readings resulting in bad or unreliable test results. These reasons are important factors in using alternative measures to estimate the ring stress induced.

Table 14 Rating range for concrete shrinkage

Shrinkage type	Low Rating	Medium Rating	High Rating
Autogenous	< 90	90 to 110	≥ 110
Free Drying	< 450	450 to 500	≥ 500
Ring	< 75	75 to 100	≥ 100

Table 15 Shrinkage Rating

Mix No.	Concrete Shrinkage at 28 days					
	Autogenous Shrinkage (microstrain)		Free Drying Shrinkage (microstrain)		Ring Shrinkage	
	Shrinkage	Rating	Shrinkage	Rating	Shrinkage	Rating
1	140	high	440	med.	103	high
2	115	high	430	med.	75	med.
3	110	high	335	low	67	low
4	90	med.	405	low	107	high
5	100	med.	450	med.	98	med.
6	115	high	465	med.	115	high
7	100	med.	500	high	116	high
8	115	high	435	med.	80	med.
9	75	low	435	med.	76	med.
10	120	high	390	low	110	high
11	90	low	545	high	72	low

The ring stress is calculated by the measured strain in the ring (ε_{si}) by the strain gauge. The calculation converts the measured strain from the inside of the ring to a pressure (p) on the outer most fibre facing the concrete (20) (Lomboy G., 2011). The pressure calculated on the outer surface of the steel ring is used to calculate the stress (σ_c) induced in the inner wall of the concrete (21). Free drying stress was calculated on the Hooke's law (22), where the concrete prism was assumed to be fully restrained while the shrinkage occurred (ε_{free}). The resulting stress was defined as the free drying stress (σ_{free}).

$$p = \varepsilon_{si} E_s \frac{R_{so}^2 - R_{si}^2}{2R_{so}^2} \quad (22)$$

Where, E_s is the elastic modulus of steel, R_{so} and R_{si} are the internal and external radii of the steel ring.

$$\sigma_c = p \left[\frac{R_{co}^2 + R_{ci}^2}{R_{co}^2 - R_{ci}^2} + \nu \right] \quad (23)$$

Where, R_{co} , R_{ci} are the external and internal radii of the concrete ring and ν is the Poisson's ratio of concrete (0.2).

$$\sigma_{free}(t) = E_c(t) * \varepsilon_{free}(t) \quad (24)$$

Where, E_c is the elastic modulus of concrete.

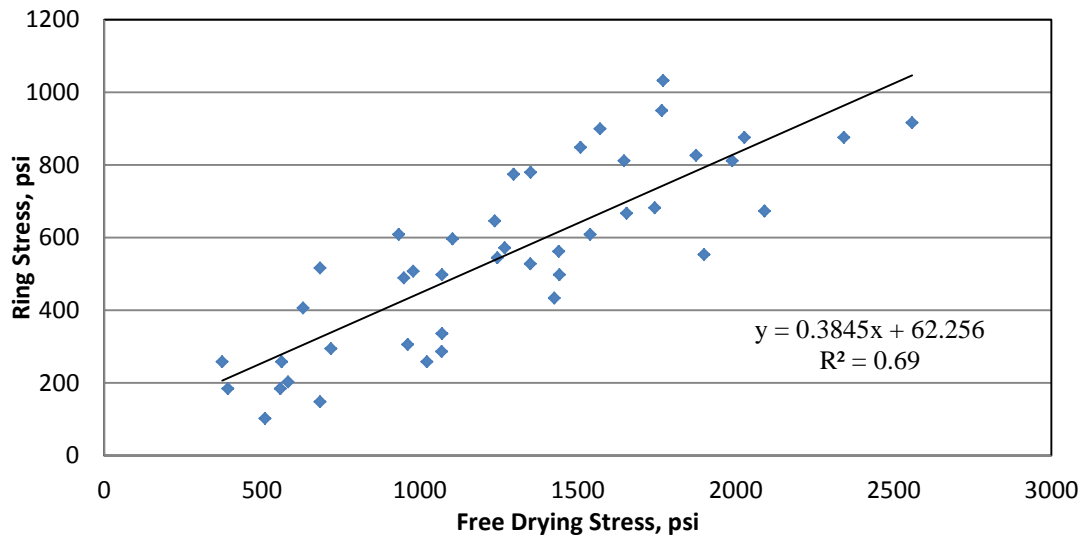


Figure 53 Ring stress vs. free drying shrinkage of c

Figure 53 illustrates the relationship between restrained stress in the ring concrete and free drying stress of concrete prisms. The R^2 of 0.69 is indicative of a positive correlation between the two parameters.

4.5.4 Relationships among strength parameters

The compressive strength displayed a strong relationship to the split tensile strength of the concrete. The regression coefficients were 0.78 and 0.91 for compressive strength vs. elastic modulus and split tensile strength respectively (Figure 56 & 57).

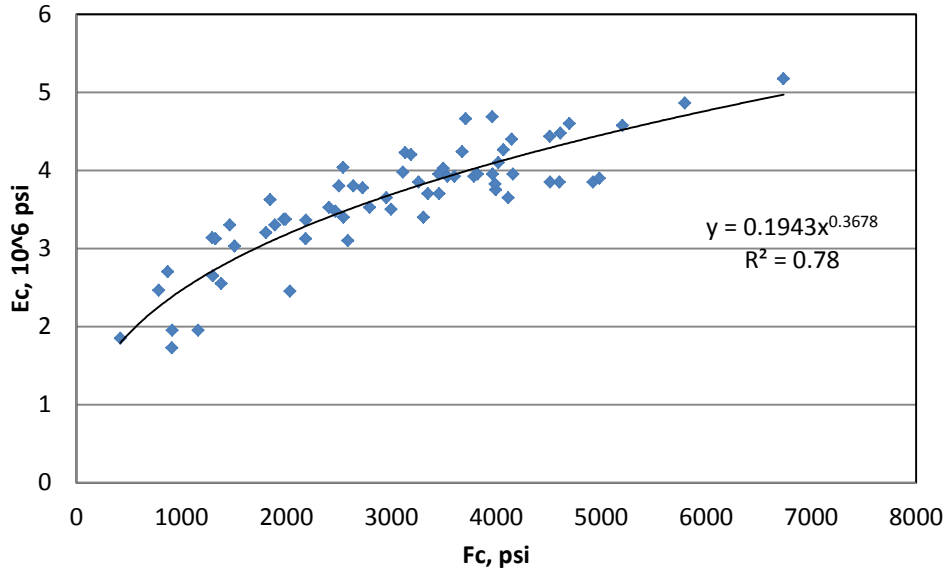


Figure 54 Elastic modulus of concrete vs. compressive strength of concrete

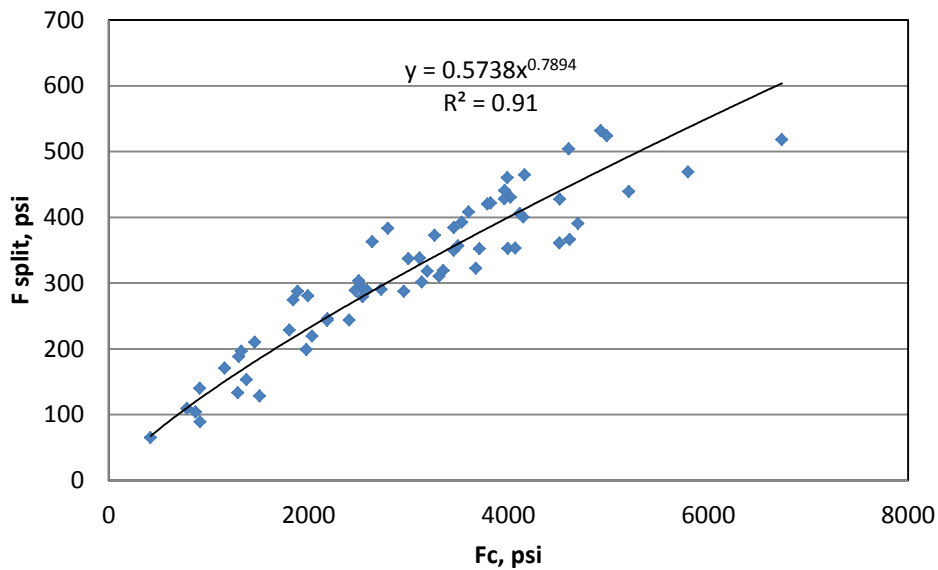


Figure 55 Split tensile strength vs. compressive strength of concrete

4.6 Concrete Cracking Potential

Table 16 summarizes the concrete mix cracking potential calculated according to ASTM C 1581, ring stress and free drying concrete stress. ASTM 1581 provides a rating ranging from low, moderate-low, moderate-high to high based on the average stress rate calculated for the restrained ring specimens.

The free shrinkage measured is free of the creep effects. In order to simulate the conditions of the restrained shrinkage the stress calculated using Hooke's law was factored by the average creep coefficient ($\phi_{avg.}$) calculated by the B3 and NCHRP report 496 model to find the equivalent stress in the restrained conditions (equation 25). The ratio between the stress and the split tensile strength was used to evaluate the cracking potential. When the stress ratio greater than 1.7 cracking was observed in the restrained concrete (ASTM C 1581). Therefore concrete which has a stress ratio of 1.7 was given a high cracking potential. Concretes that displayed stress ratio of 1.7 to 1.2 did not display cracking but did have appreciably high shrinkage and elastic modulus development were given a medium cracking potential and concrete mixes that displayed low shrinkage and a stress ratio lesser than 1.2 were given a low cracking potential.

$$\sigma_{effective} = \frac{\sigma_{free}}{(1+\phi_{avg.})} \quad (25)$$

$$Stress\ ratio = \frac{(\sigma_{free}/(1+\phi))}{F_{sp}} \quad (26)$$

In the calculation of cracking potential using restrained stress data for the stress ratio, the stress induced in the concrete ring (σ_{ring} , psi) calculated from equations 22 and 23 was divided by the splitting tensile strength of concrete. Where stress ratio exceeding 2.7 the concrete annulus cast displayed cracking within the 28 day span of measurement and therefore the cracking potential high for those mixes. The concretes with stress ratio less than 2.7 and greater than 2.0 were given a medium cracking potential because they displayed high cracking potential and did not

The rating obtained was different from that given by the ASTM C1581, where the samples made with Type I/II displayed moderate-high potential and Type IP and Type I cements used showed moderate-low cracking potential.

Table 16 Concrete Shrinkage Potential

Mix No.	Based on Free Shrinkage							Based on Ring Shrinkage			Stress rate method	
	$\sigma_{free} = E * \epsilon_{free}$ (psi)		$\sigma_{free}/(1+\phi)$, psi		$(\sigma_{free}/1+\phi)/F_{sp}$		Rank	Cracking Potential	Peak σ_{ring}/F_{sp} , (psi/psi)	Cracking Potential	Average Stress Rate, S (psi/day)	ASTM Cracking Potential Rating
	14 day	28day	14 day	28day	14 day	28day						
1	1351	1766	363	513	1.07	1.22	7	Medium	2.66	Medium	23.6	Moderate-Low
2	1350	1656	395	508	1.12	1.19	8	Low	1.84	Low	19.68	Moderate-Low
3	933	1246	243	343	0.71	0.89	11	Low	1.87	Low	16.6	Moderate-Low
4	1441	1876	414	560	1.37	1.74	3	High	3.05	High	31.9	Moderate-High
5	1989	2344	542	678	1.71	1.93	1	High	3.18	High	24.9	Moderate-High
6	1571	2253	516	766	1.32	1.74	2	High	2.76	High	37.3	Moderate-High
7	1647	2028	466	600	1.19	1.36	6	Medium	2.34	Medium	35.6	Moderate-High
8	1297	1744	315	490	1.09	1.37	4	Medium	2.54	Medium	24.5	Moderate-High
9	1238	1539	277	396	0.99	1.03	10	Low	1.98	Medium	27.1	Moderate-High
10	1509	1771	457	558	1.13	1.11	9	Low	2.41	Medium	27.7	Moderate-High
11	1900	2092	479	575	1.29	1.36	5	Medium	2.13	Low	24.2	Moderate-Low

Based on Table 16,

- Mixes 4, 5 and 6 have high cracking potential,
- Mixes 1, 7, 8, 9 and 10 have medium cracking potential and
- Mixes 2, 3 and 11 have low cracking potential.

It is noted that the mixes having high cracking potential (Table 16) also have high elastic modulus at the early age (7-days). This may cause high stress development in the concrete. Those mixes also have appreciably high shrinkage strain. As pointed out previously the mixes that display the greatest shrinkage are not the mixes that crack first. But, the ASTM method for the comparison of concrete mixes on its restrained cracking potential considers only the rate at which the stress develops in the concrete. Therefore a mix that has a high shrinkage development is deemed to have high cracking potential. Yet the cracking potential depends not only on the shrinkage development but also the development of other mechanical properties such as modulus of elasticity and strength. Another consideration in the concrete mixture cracking potential is the creep.

The cracking potential analysis performed here using the free shrinkage stress (Table 16) takes in to account the elastic modulus to evaluate the stress level in the concrete (Hooke's law), split tensile strength of the mix as a measure of capacity of the concrete to crack and creep which is an important factor on concrete that is loaded. The loading on the overlay concrete considered here is by way of shrinkage strain.

In the restrained shrinkage observed through the steel annulus the observed shrinkage is the composite effect of several components of strain (See, 2003).

$$\varepsilon_{sh}(t) = \varepsilon_e(t) + \varepsilon_{cp}(t) + \varepsilon_{st}(t) \quad (18)$$

where $\varepsilon_{sh}(t)$ is the free shrinkage strain, ε_e is the elastic concrete strain, ε_{cp} is the tensile creep strain and $\varepsilon_{st}(t)$ is the elastic steel strain at time t . Therefore the observed shrinkage through the concrete annulus is the equivalent of elastic, shrinkage and creep effects. Therefore the stress calculated for the restrained shrinkage already has consideration for effects of restraint and creep.

The use of the stress ratio for restrained and unrestrained shrinkage data, the evaluation for cracking potential displays a good indication of a concrete cracking potential. Unlike the ASTM method for evaluating concrete cracking potential where the only consideration is the average strain rate which in turn is converted to stress rate, the calculated cracking potential looks into strength and creep aspects that affect the concrete performance. Therefore the calculated stress ratio gives a good indication of overall performance of the mix in a restrained condition over the ASTM method.

4.7 Finite Element Analysis

To model the effect of creep and shrinkage of the concrete overlay in a typical structure in the field a finite element analysis was conducted. The software selected was midas Civil 2013. The software primarily analyses bridge engineering problems in which the construction stage analysis can be performed. A construction stage analysis allows the structure to be analyzed as both a completed structure and as interim stages in its construction. Complex structure constantly change and evolve in the period of construction and varying material properties of materials like concrete where strength and elastic modulus development has a significant effect on adjacent members due to the varying maturity of the material. The software allows the input of shrinkage and creep parameters along with the strength parameters of concrete to analyze the effects on the structure in different time steps and stages of the structure.

The design and analysis of the structure in the construction stage analysis can be summarized as follows.

1. Create a structural model. Assign elements, loads and boundary conditions to be activated or deactivated to each construction stage together as a group.
2. Define time dependent material properties such as creep and shrinkage. The time dependent material properties can be defined using the standards such as ACI or CEB-FIP, or you may directly define them.
3. Link the defined time dependent material properties to the general material properties. By doing this, the changes in material properties of the relevant concrete members are automatically calculated.
4. Considering the sequence of the real construction, generate construction stages and time steps.
5. Define construction stages using the element groups, boundary condition groups and load groups previously defined.
6. Carry out a structural analysis after defining the desired analysis condition.
7. Combine the results of the construction stage analysis and the completed structure analysis.

Details on the design and inputs are attached in the appendix.

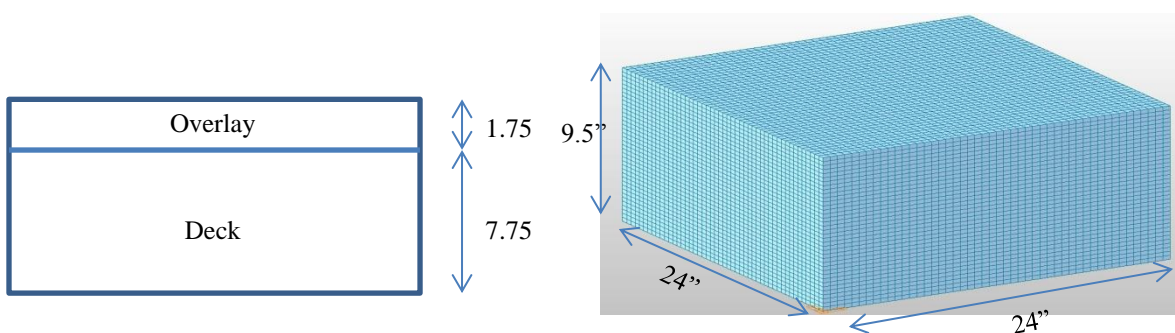


Figure 56 Section of the deck and overlay in a slab and the finite element model of the slab

The element used in the design meets the dimensional specifications set by the Iowa Department of Transportation for a bridge deck and overlay. The original deck is 8 inches in thickness. Before the overlay is being constructed $\frac{1}{4}$ inches of the existing deck is ground off. This forms a good contact surface for the overlay to be bonded to. The overlay constructed is of $1\frac{3}{4}$ inches thickness giving a net raise of the deck by $1\frac{1}{2}$ inches. The

element modeled is a part of the slab panel 24 inch by 24 inch square section. The element is broken down to smaller elements of $\frac{1}{2} \times \frac{1}{2} \times \frac{1}{4}$ inch³.

Table 17 Summary of input data for developing the model

Parameter	Details of input used in the model
Slab size	24"x24"x9.5"
Boundary condition	Fully restrained in displacement and rotation on the outer edge of the panel
Type of element	Solid Element
Element size	0.5"x0.5"x0.25"
Material input data	Measured strength, modulus and tensile strength
	Measured free shrinkage
	Calculated average creep coefficient
Duration of analysis	56 days
Intermediate steps	1, 3, 7, 14 and 28 days
Type of analysis	Construction stage analysis

The interaction between the deck and overlay is defined as a fully bonded composite section.

4.7.1 Modeling stress due to creep in midas Civil

The point of interest for the analysis undertaken was the creep and shrinkage of the overlay concrete. Analyzing creep effects in midas Civil, the concrete can be done by both using creep coefficient or by integrating the stress history of the structure. The following description outlines the method adopted by midas Civil.

$$\begin{aligned} \text{Creep strain:} & \quad \varepsilon_c(t, t_0) = \varphi(t, t_0)\varepsilon(t_0) \\ \text{Loading due to creep strain:} & \quad P = \int_A E(t) \varepsilon_c(t, t_0) dA \\ \text{Strain due to stress at time } t_0: & \quad \varepsilon_o(t) \\ \text{Creep coefficient from } t_0 \text{ to } t: & \quad \varphi(t, t_0) \end{aligned}$$

The following outlines the method in which specific functions of creep are numerically expressed, and stresses are integrated over time.

$$\varepsilon_c(t) = \int_0^t C(t_0, t - t_0) \frac{\partial \sigma(t_0)}{\partial t_0} dt_0$$

where,

Creep strain at time t:	$\epsilon_c(t)$
Specific creep:	$C(t_0, t - t_0)$
Time of load application:	t_0

If the stress at each stage is assumed to be constant the above equation can be simplified in this manner

$$\epsilon_{c,n} = \sum_{j=1}^{n-1} \Delta\sigma_j C(t_j, t_{n-j})$$

Using the above expression, the incremental creep strain $\Delta\epsilon_{c,n}$ between the stages can be calculated.

4.7.2 Results and observations

The stress pattern in the deck and overlay composite section remains the same throughout the period of the 56day duration of the analysis whiles increasing the magnitude of the stress observed in the structure with time. The maximum axial tensile stress occurs at the interface between the deck and overlay concrete on the y axis.

Figure 57 displays the plane in which the maximum tensile stress is observed. The tensile stress reaches the peak value at the mid-point of the 2 foot long interface between the two concrete layers (deck and overlay). Figure 58 displays the time dependent development of the stress in the deck and overlay interface. The orange dots on Figure 57 correspond to the locations at which these values were extracted. The stress levels increase throughout the section as the concrete ages and the concrete matures in strength and the level of shrinkage and creep increase with time.

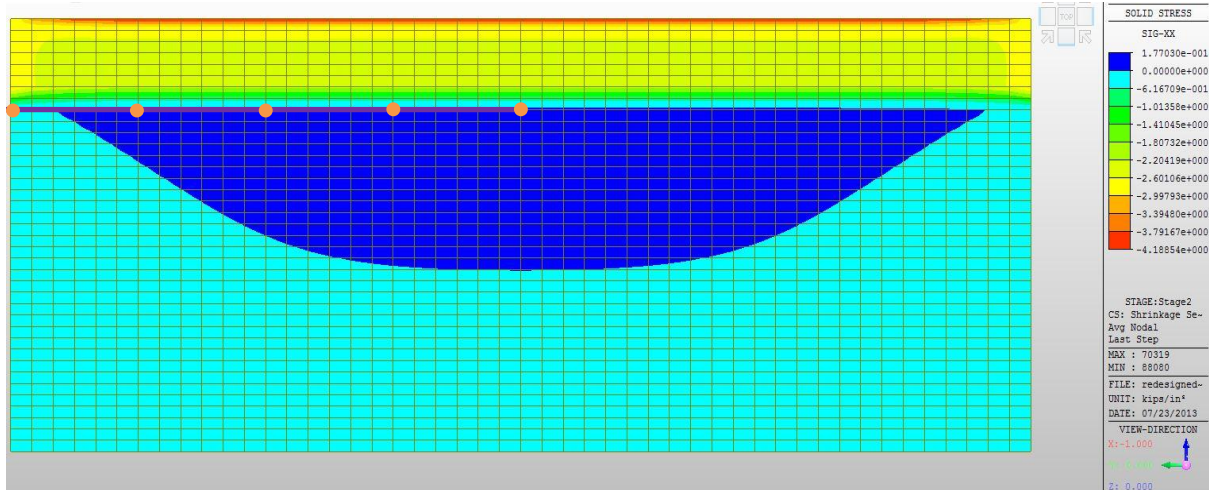


Figure 57 Typical axial tensile stress (σ_{xx}) pattern on the y axis

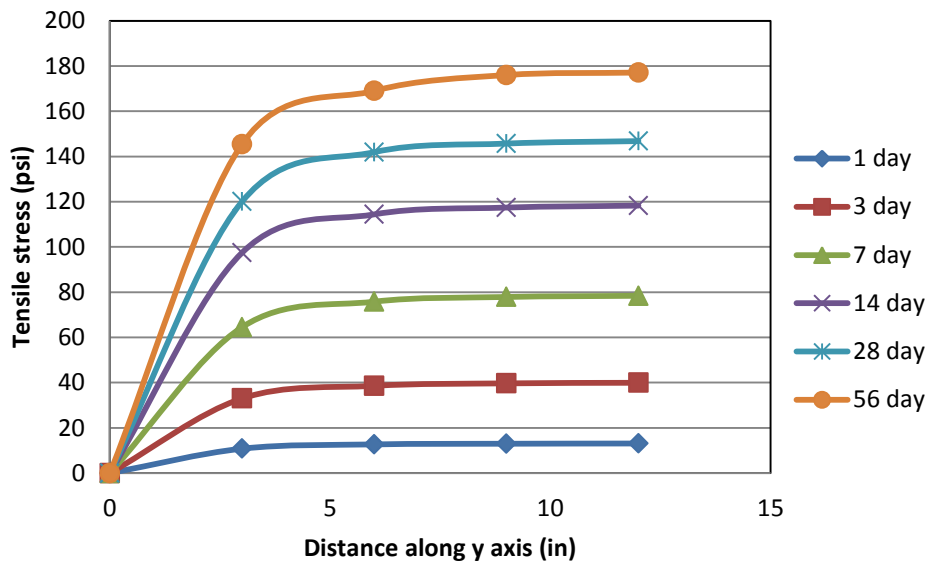


Figure 58 Axial stress (σ_{xx}) development with time in mix 1

Figure 59 illustrates the tensile stress development in all 11 mixes at 56 days. The pattern is similar in all 11 mixes and the peak axial tensile stress occurs at the mid-point of the interface between the deck and overlay on the y axis. Table 18 summarizes the maximum axial tensile stress of the structure for the 11 mixes in the 56 day duration.

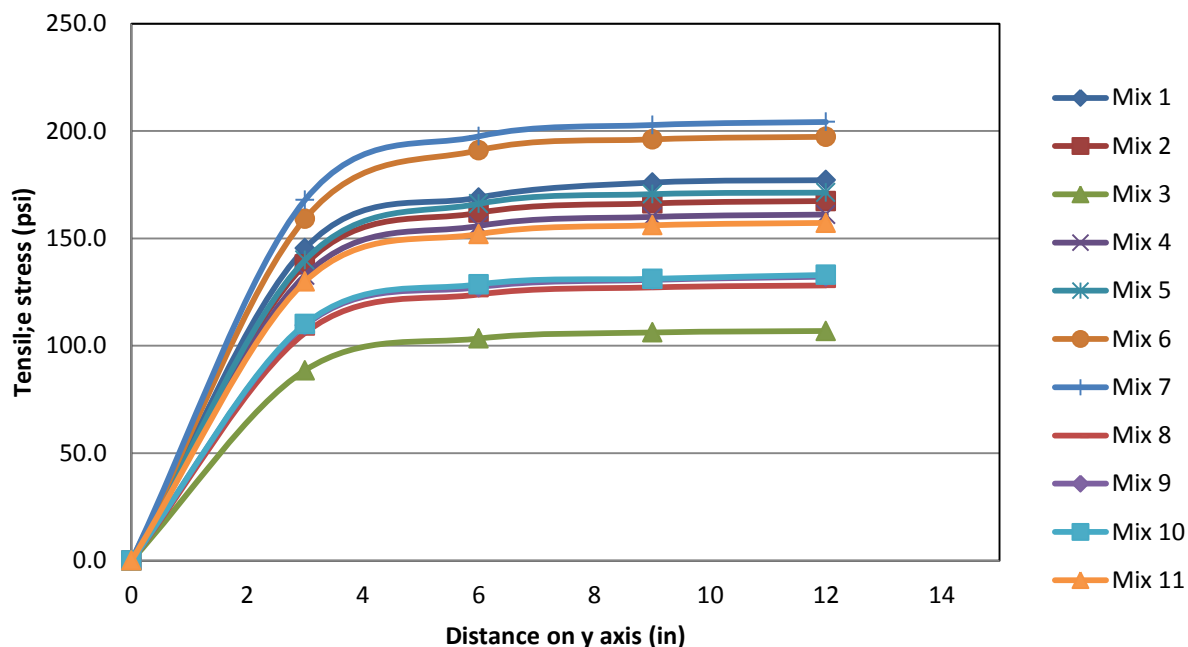


Figure 59 Axial stress (σ_{xx}) development in the critical section for the 11 overlay mixes at 56 days

Table 18 Max tensile stress (σ_{xx}) in the overlay concrete

Age of concrete (days)	Maximum tensile stress in restrained condition (psi)										
	Mix 1	Mix 2	Mix 3	Mix 4	Mix 5	Mix 6	Mix 7	Mix 8	Mix 9	Mix 10	Mix 11
1	13.1	14.9	14.9	13.0	13.5	17.4	15.8	18.3	17.0	14.7	24.4
3	39.9	39.8	26.0	34.8	35.5	39.3	46.2	47.0	53.9	44.1	61.4
7	78.4	77.9	42.4	62.2	65.5	69.3	84.0	74.5	69.7	63.3	99.0
14	118.2	107.2	64.3	93.7	107.7	110.1	123.6	98.4	93.0	88.4	130.0
28	146.7	136.7	89.0	129.4	151.8	152.1	159.2	118.6	116.3	116.8	142.6
56	177.1	167.4	106.9	161.1	171.7	197.3	204.2	128.1	132.2	133.0	157.2

The maximum axial tensile stresses being displayed by the model was compared to the maximum split tensile strength of the concrete as previously investigated in the free and restrained shrinkage analysis. The results indicate that the shrinkage induced would not generate a stress exceeding the split tensile strength. However there are no experimental findings to prove that the stress levels displayed here in the model are accurate or that it simulates the actual deck-overlay composite action. Therefore it is strongly recommended that the parameters observed in the concrete through the midas model be validated using

laboratory measurements made on a slab of similar construction. Table 3 summarizes the rank given to mixes using the method of analysis used here to evaluate cracking potential. The midas model does show similarities to those obtained by other methods but the order had no direct correlation to any of the methods used previously.

Table 19 Stress ratio of concrete overlay

midas finite element model			Rank		
Mix ID	Stress ratio	Rank	Free shrinkage method	Restrained shrinkage method	ASTM C1581 method
1	0.412	3	7	4	9
2	0.315	8	8	11	10
3	0.262	10	11	10	11
4	0.447	1	3	2	3
5	0.401	4	1	1	4
6	0.381	5	2	3	1
7	0.440	2	4	7	2
8	0.350	7	6	5	7
9	0.287	9	10	9	6
10	0.254	11	9	6	5
11	0.373	6	5	8	8

The midas Civil software is a good tool that can be used to estimate the stress that would occur in the concrete or even be used as a tool to identify the critical locations of interest where the concrete would display peak stresses. There by it would provide useful information for an initial study of concrete shrinkage induced stress for field studies.

4.8 Summary of Results

All the test results of the 11 mixes are summarized as follows in Tables 17 and 18.

Table 17 summarizes the concrete shrinkage parameters measured. The ranks given are ordered from high shrinkage to low shrinkage where the replacement of cement by slag displays the greatest shrinkage observed for free and restrained shrinkage while autogenous shrinkage shows a reduction. Addition of fly ash has reduced concrete shrinkage. Metakaolin has had an effect towards reducing autogenous and free drying shrinkage but the restrained shrinkage performance shows increase in observed strain.

The compressive strength and split tensile strength of concrete show development with time although the rate at which the development occurs deters with time (Table 18). On the other hand elastic modulus values tend to become constant after 28 days. The presence of cementitious materials makes the growth of strength continue in a greater rate than with only cement in the mix.

Table 20 Summary of Concrete Shrinkage

Mix No.	Concrete Shrinkage									
	Autogenous Shrinkage (microstrain)			Free Drying Shrinkage (microstrain)				Ring Shrinkage (microstrain)		
	7	28 day	56 day	7 day	28 day	56 day	Rank	7 day	28 day	Rank
1	55	140	190	230	440	526	5	62	103	5
2	50	113	150	260	430	520	6	45	75	9
3	45	110	140	203	336	390	11	41	67	11
4	50	90	120	215	405	500	7	59	107 (15)	4
5	55	100	120	180	450	550	4	60	98	6
6	86	113	170	240	463	580	3	62	114 (17)	2
7	50	100	125	285	500	610	1	72	116	1
8	53	113	183	296	433	460	9	48	80	7
9	36	76	103	296	436	483	8	46	76	8
10	75	120	155	235	390	435	10	53	110	3
11	50	90	123	393	543	580	2	43	72	10

Note: The values indicated in brackets are the age at which peak strains were recorded prior to 28 days

Table 21 Summary of Mechanical Properties

Mix no	Elastic Modulus X10 ⁶ psi			Compressive Strength, psi			Split Tensile Strength, psi		
	7 day	28 day	56 day	7 day	28 day	56 day	7 day	28 day	56 day
1	3.80	3.93	4.10	2500	3790	4020	300	420	430
2	3.70	3.85	3.85	3450	4515	4925	320	430	530
3	3.10	3.70	3.90	2590	3450	3600	290	385	410
4	4.20	4.25	4.45	3130	4070	4510	300	350	360
5	4.00	4.65	4.70	2540	3710	3960	280	350	430
6	4.60	4.85	5.20	4700	5800	6740	390	470	520
7	3.65	3.95	3.95	2950	3970	4160	290	440	465
8	3.20	4.00	4.45	1800	3500	4610	230	360	370
9	3.30	3.50	3.80	1460	2795	3990	210	380	460
10	3.40	3.85	3.90	3300	4600	4985	310	500	525
11	3.60	3.85	3.95	1850	3260	3820	275	370	420

CHAPTER 5. CONCLUSIONS AND RECOMMENDATIONS

Through an experimental investigation the shrinkage behavior of 11 high performance concrete mixes commonly used for Iowa bridges were studied. Autogenous shrinkage, free shrinkage and restrained shrinkage of concrete were monitored. Compressive strength, elastic modulus and split tensile strength were tested for different ages. The following conclusions and recommendations are drawn from these tests results:

1. Concrete shrinkage and cracking behavior

- Among 11 mixes studied, cracking were observed in the restrained concrete (ring specimens) of mixes 4, 5 and 6. Cracking was observed for 2 of the 3 specimens of Mix 4 at 13 and 18 days; for one of the 3 specimens of Mix 5 at 11 days; and for all 3 specimens of Mix 6 at 16, 16.5 and 18 days. These were the only rings that cracked during the monitoring period.
- Mixes 4 to 10 were ranked as having moderate-high shrinkage cracking potential based on ASTM C 1581. Mixes 4 to 10 all contain Lafarge Type I/II cement.
- Mixes 4, 5 and 6 displayed high shrinkage cracking potential while Mixes 2, 3 and 9 displayed low cracking potential based on the calculated shrinkage stress to strength with consideration of creep.
- Not all mixes having high shrinkage cracked. Cracking is associated mainly with restrained shrinkage strain ϵ_{sh} , modulus of elasticity E_c and creep coefficient ϕ . This behavior can be observed in mixes 7 and 10 where they have comparable shrinkage to mix 4 and 6 but do not display cracking.

2. Effect of concrete materials and proportions

- The replacement of 20% Class C Fly ash for cement reduced all types of shrinkage in concrete.
- The replacement of cement by 25% GGBFS had little effect on autogenous shrinkage but significantly increased free shrinkage and restrained shrinkage.
- The combination of 20% class C fly ash and 25% GGBFS reduced shrinkage.
- Replacing cement by 20% fly ash and 5.6% metakaolin increased autogenous shrinkage. However, free and restrained shrinkage of concrete was similar to that of the mixes without the fly ash and metakaolin.

- Mixes with cement contents greater than 700 pcy (mixes 4, 5 and 6) showed high potential for cracking.
 - Mixes made with Type I cement yielded greater shrinkage than Type I/II cement.
 - Mixes made with finer graded quartzite displayed similar shrinkage behavior to the mixes made with coarse graded limestone as coarse aggregate.
3. Relationships among test results
 1. Mass loss shows a strong linear relation with free drying shrinkage for a given mix.
 2. The stress resulting from restrained drying shrinkage has an acceptable linear relationship with the stress from free drying shrinkage of concrete.
 3. There is a good relationship between concrete compressive strength and elastic modulus (Figure 4-64) and excellent relationship between the compressive strength and tensile strength (Figure 4-65).

5.1 Recommendations

1. Materials selection and mix design improvement
 - 20% fly ash which reduces shrinkage and 25% GGBFS which has little effect on the shrinkage and are recommended to be used in bridge deck overlay concrete.
 - Type I/II Cement may be preferred over Type I cement and Type IP is preferred over Type I/II cement for the consideration of the shrinkage cracking resistance.
 - Controlling the paste volume in concrete to maintain minimum paste volume is highly recommended. Cautions shall be taken when total cementitious material content in concrete of over 700lb/ft³ is used for bridge decks.
2. Test methods
 - Since free drying shrinkage and mass loss have a strong correlation, Mass loss can be used as a good indicator for free drying shrinkage.
 - Compressive strength is a good indicator to evaluate elastic modulus and split tensile strength.
3. Future research
 - Creep behavior of these concrete mixes was estimated based on the existing models used in this project and it should be investigated experimentally.

- Internal curing and shrinkage-reducing agents may be considered to be used in Mixes 4, 5, and 6 to control concrete cracking.
- Effects of aggregate characteristics (type, size, and bond with cement) on concrete shrinkage should be studied further.
- A study should be conducted to evaluate stress development in concrete pavement deck-overlay composite section as there is no current data to validate the stress pattern or the stress level observed.

BIBLIOGRAPHY

Addis B. J., e. a., 1986. *Fulton's Concrete Technology*. 6th ed. Mirand, South Africa: Portland Cement Institute.

Almudaiheem J.A., H. W., 1986. Effect of specimen size and shape on drying shrinkage of concrete. *ACI Materials Journal*, Issue 16, pp. 130-135.

Almusallam A.A., M. M. A.-W. M. K. M., 1998. Effects of proportions on plastic shrinkage cracking of concrete in hot environments. *Construction and Building Materials* , 12(6-7), pp. 353-358.

Al-Omaishi N., T. M. a. S. S., 2009. Elasticity modulus, shrinkage, and creep of high-strength concrete as adopted by AASHTO. *PCI Journal*, pp. 44-63.

ASTM Standard C157/C , 2008. Standard test method for length change of hardened hydraulic cement mortar and concrete. In: *Annual book of standards*. WestConshohocken,PA: ASTM International.

ASTM Standard C1581, 2008. Determining age at cracking and induced tensile stress characteristics for mortar and concrete under restrained shrinkage. In: *Annual Book of Standards*. Westconshohoken,PA: ASTM International.

Balogh A., 1996. New Admixture Combats Concrete Shrinkage. *Concrete Construction*, pp. 546-551.

Bazant Z.P., B. S., 2000. Creep and Shrinkage Prediction for Model Analysis and Design of Concrete Structures: Model B3. In: *Adam Neville Symposium: creep and Shrinkage—Structural Design Effects*. Farmington Hills, Michigan: American Concrete Institute, pp. 1-83.

Brooks J. J., J. M. A. M., 2001. Effect of metakaolin on creep and shrinkage of concrete. *Cement and Concrete Composites*, Issue 23, pp. 495-502.

Camiletti J., S. A. M. N. M. L., 2013. Effects of nano- and micro-limestone addition on early age properties of ultra-high-performance concrete. *Maerials and Structures*, Issue 46, pp. 881-898.

Davis H.E, 1940. Autogenous volume changes of concrete. *Procedings, American Society of Testing and Materials*, 32(40), pp. 1103-1112.

dos Santos S.B., F. L. C. J., 2012. Early-age creep of mass concrete: effect of chemical and mineral admixtures. *ACI Materials Journal*, 109(5), pp. 537-544.

Hobbs D.W., P. L., 1979. Prediction of drying shrinkage. *Concrete*, 13(2), pp. 19-24.

Jennings H.M., T. J. G. j. C. G. U. F., 2007. A multi-technique investigation of the nanoporosity of cement paste. *Cement and Concrete Research*, Volume 37, pp. 329-336.

Jensen O.M., H. P., 2001. Autogenous Deformation and RH-change in Perspective. *Cement and Concrete Research*, Volume 31, pp. 1859-1865.

Jianyong L., Y. Y., 2001. A study on creep and shrinkage of high performance concrete. *Cement and Concrete Research*, Issue 31, pp. 1203-1206.

Krauss E.A., R. P., 1996. *Report 380: Transverse Cracking in Newly Constructed Bridge Decks*, Washington D.C.: National Academy Press.

Lomboy G., W. K. O. C., 2011. Shrinkage and Fracture of Semiflowable Self-consolidating Concrete. *Journal of Materials in Civil Engineering*, 23(11), pp. 1514-1524.

Mehta P.K. & Monteiro P.J.M., 2003. *Concrete, Microstructure, Properties and Materials*. 3rd ed. New York: McGraw-Hill.

Meininger R.C., 1966. *Drying Shrinkage of Concrete*, Silver Spring: National Ready Mixed Concrete Association.

Miyazawa S., H. A. K. K. O. T., 2009. Influence of cement type on restraint stress in concrete in early ages. In: T. e. al, ed. *Creep, Shrinkage and Durability Mechanics of Concrete Structures*. London: Taylor & Francis Group, pp. 373-379.

Mokarem D.W., L. D. O. H. S. M., 2008. *Measurement of early age shrinkage of Virginia concrete mixtures*, Charlottesville, VA: Virginia Transportation Research Council.

Moon J.H., e. a., 2006. Quantifying the influence of Specimen Geometry on the Results of the Restrained Ring Test. *Journal of ASTM International*, 3(8), pp. 1-14.

Nakarai K., I. T., 2009. Numerical evaluation of influence of pozzolanic materials on shrinkage base on moisture state and pore structure. In: T. e. al., ed. *Creep, Shrinkage and Durability Mechanics of Concrete and Concrete Structures*. London: Taylor & Francis Group, pp. 153-159.

Powers T.C., 1947. A discussion of cement hydration in relation to the curing of concrete. *Proceedings Highway Research Board*, Volume 27, pp. 178-188.

Powers T.C., 1971. Fundamental aspects of concrete shrinkage. *Rev. Matériaux et Constructions*, Issue 545, pp. 79-85.

Quangphu N., e. a., 2008. Influence of shrinkage reducing admixture on drying shrinkage and mechanical properties of high-performance concrete. *Water Science and Engineering*, 1(4), pp. 67-74.

Reichardt T.W., 1964. *Creep and drying shrinkage of lightweight and normal weight concrete*, Washington DC: National Bureau of Standards.

Satio M, K. M. a. A. S., 1991. Role of aggregate in the shrinkage of ordinary Portland and expansive cement concrete. *Cement and Concrete Composites*, Issue 13, pp. 115-121.

See H.T., A. E. M. M., 2003. Shrinkage characteristics of concrete using ring specimens. *ACI Materials Journal*, 100(3), pp. 239-245.

Soroushian P., R. S., 1998. Control of Plastic Shrinkage Cracking with Specialty Cellulose Fibers. *ACI Materials Journal*, pp. 429-435.

Tazawa E., 1999. *Autogenous Shrinkage of Concrete*, New York: Routledge.

Tazawa E., M. S., 1995. Influence of Cement and Admixture on Autogenous Shrinkage of Cement Paste. *Cement and Concrete Research*, pp. 281-287.

Tazawa E., M. S., 1997. Influence of constituents and composition on autogenous shrinkage of cementitious materials. *Magazine of Concrete Research*, Issue 49, pp. 15-22.

Troxell G.E., D. H. K. J., 1968. *Composition and properties of concrete*. 2nd ed. New York: McGraw-Hill.

Wang K., S. S. P. P., 2001. Plastic Shrinkage Cracking in concrete Materials-Influence of Fly Ash and Fibers. *ACI Materials Journal*, pp. 458-464.

Weiss W.J., Y. W. S. S., 2000. Influence of specimen size and geometry on shrinkage cracking. *Journal of Engineering Mechanics*, 126(1), pp. 93-101.

Whiting D. A., D. R. L. E. S., 2000. Cracking tendency and drying shrinkage of silica fume concrete for bridge applications. *ACI Materials Journal*, 97(1), pp. 71-77.

Appendix

Test Measurements

Autogenous shrinkage measurements

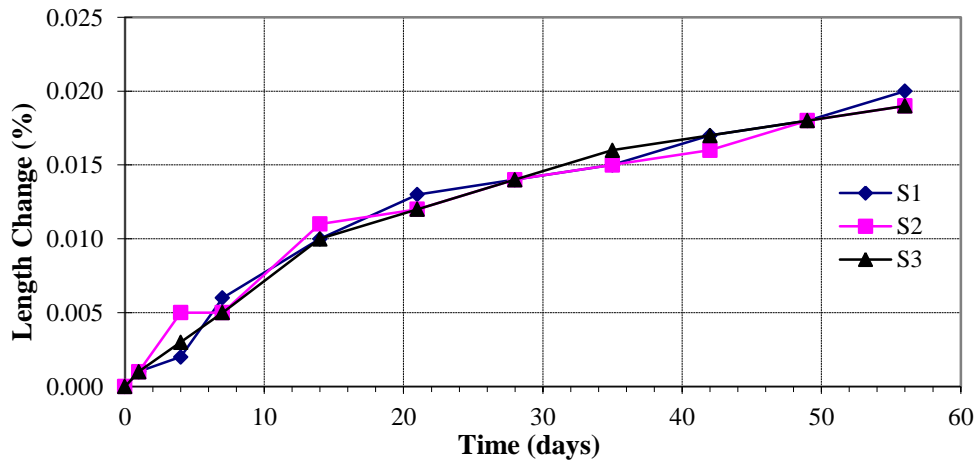


Figure 60 Mix 1 autogenous shrinkage results

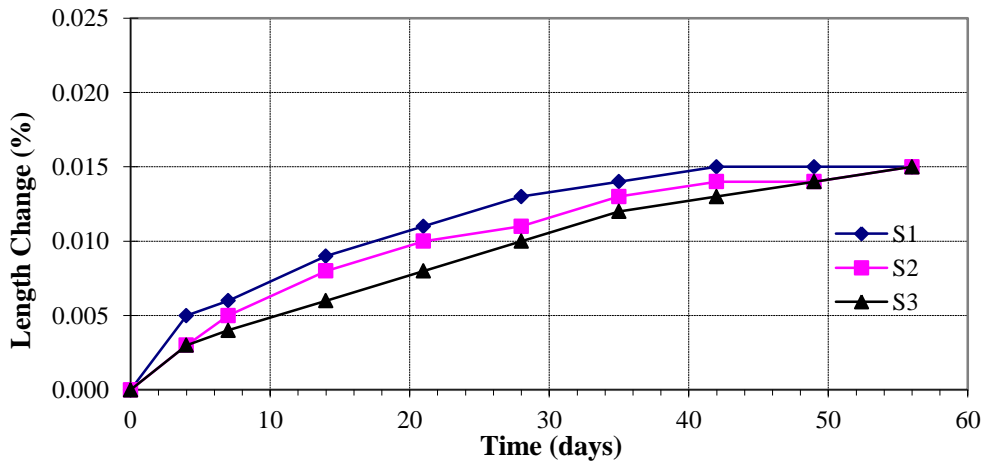


Figure 61 Mix 2 autogenous shrinkage results

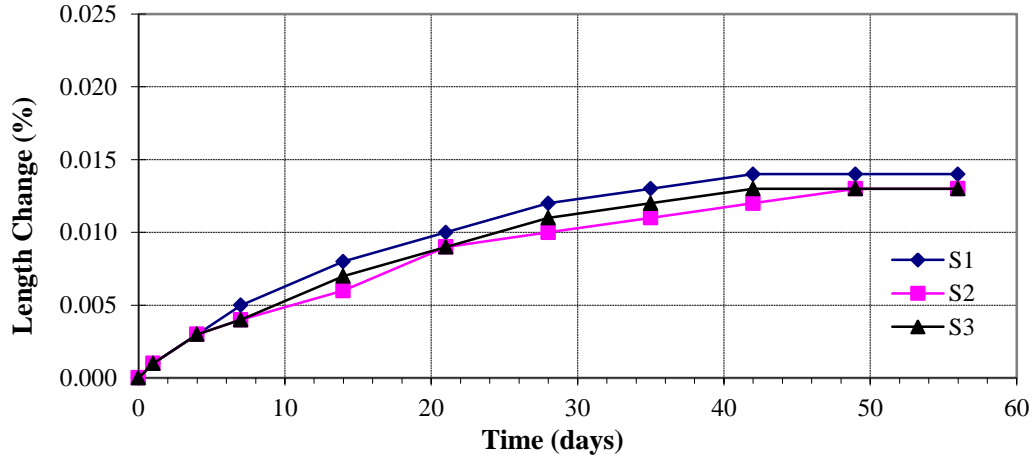


Figure 62 Mix 3 autogenous shrinkage results

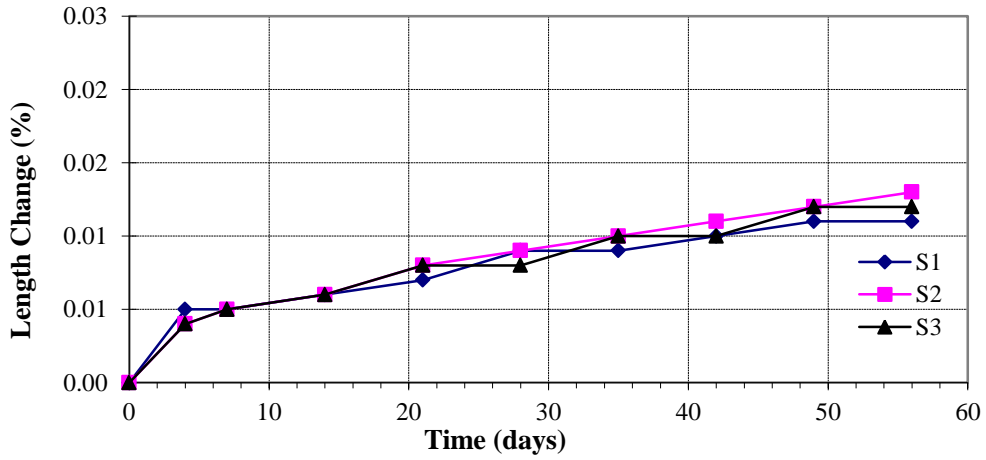


Figure 63 Mix 4 autogenous shrinkage results

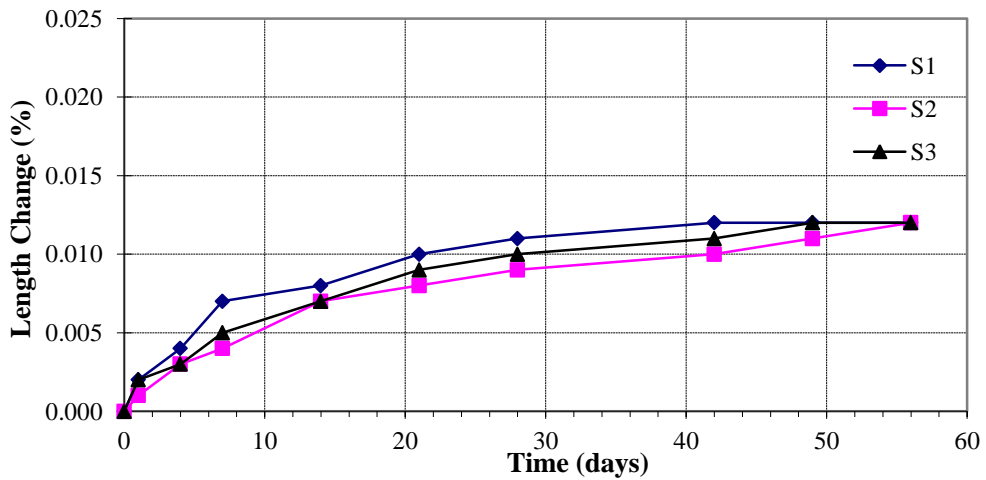


Figure 64 Mix 5 autogenous shrinkage results

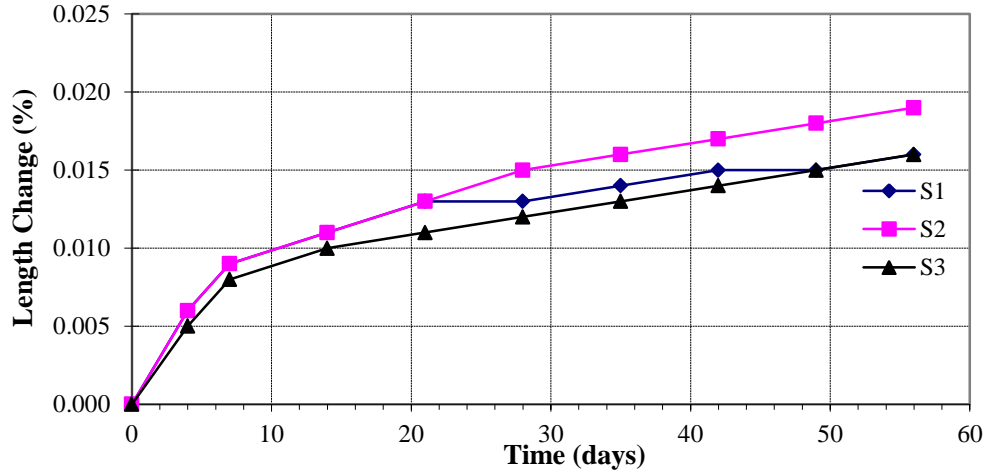


Figure 65 Mix 6 autogenous shrinkage results

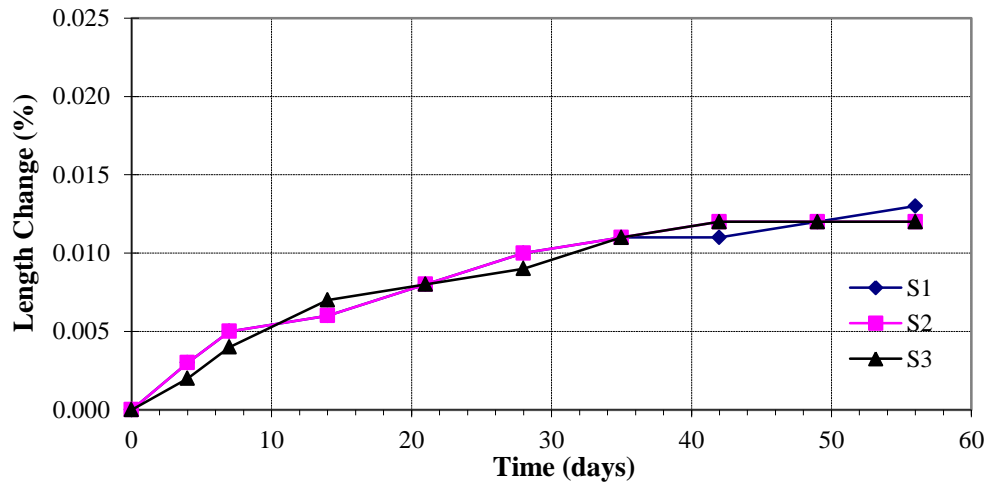


Figure 66 Mix 7 autogenous shrinkage results

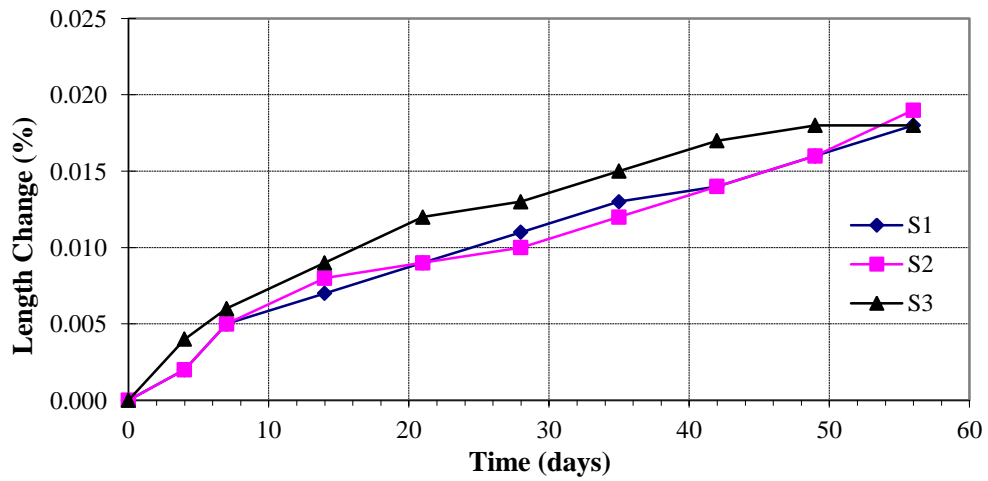


Figure 67 Mix 8 autogenous shrinkage results

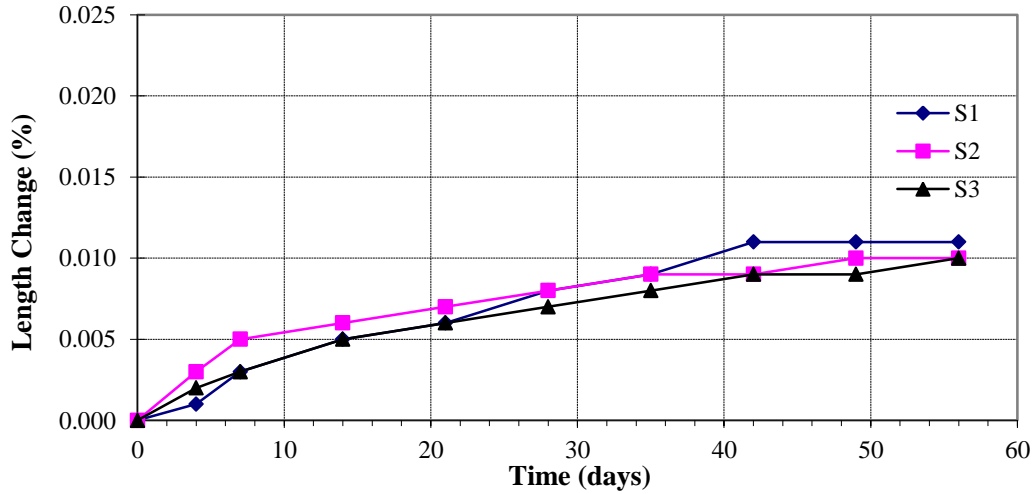


Figure 68 Mix 9 autogenous shrinkage results

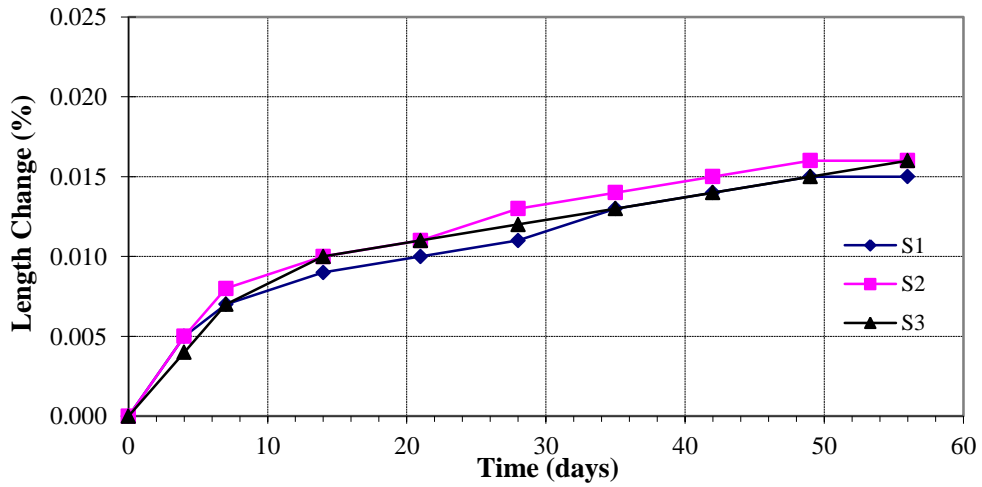


Figure 69 Mix 10 autogenous shrinkage results

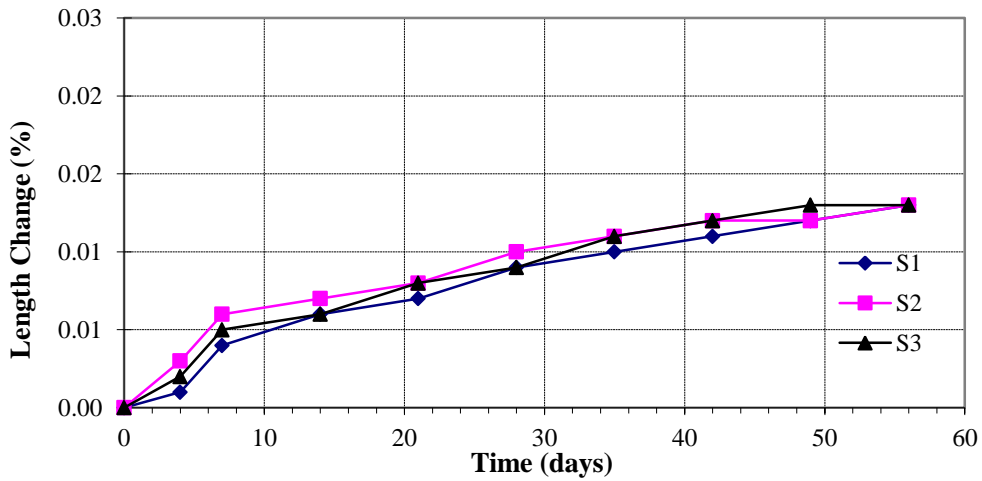


Figure 70 Mix 11 autogenous shrinkage results

Free shrinkage measurements

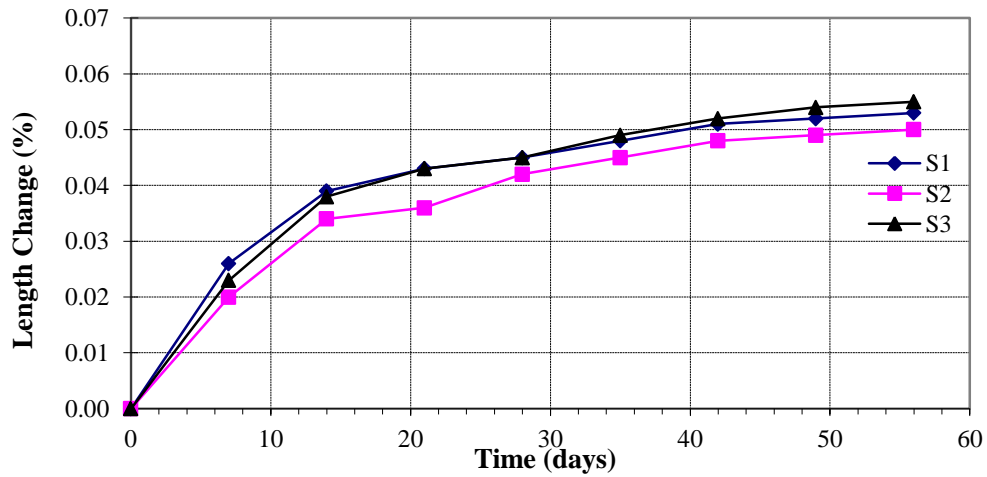


Figure 71 Mix 1 free drying shrinkage results

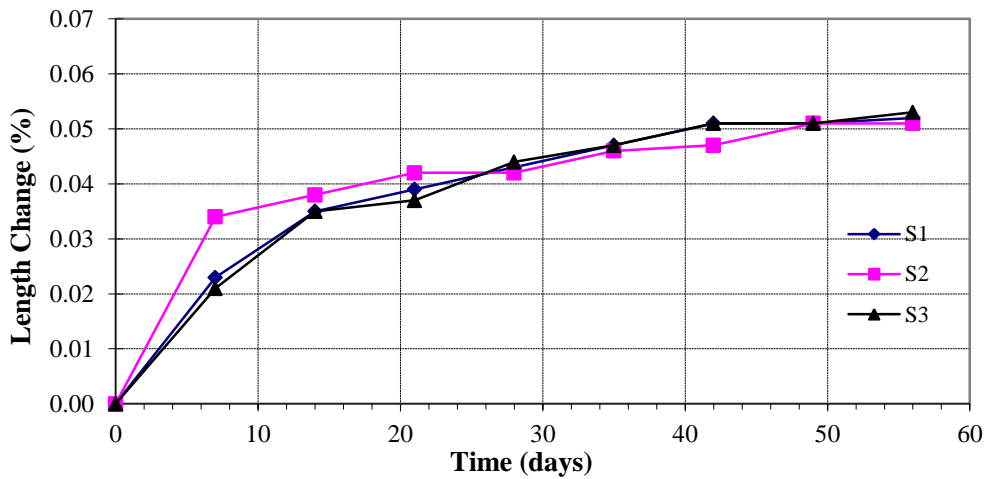


Figure 72 Mix 2 free drying shrinkage results

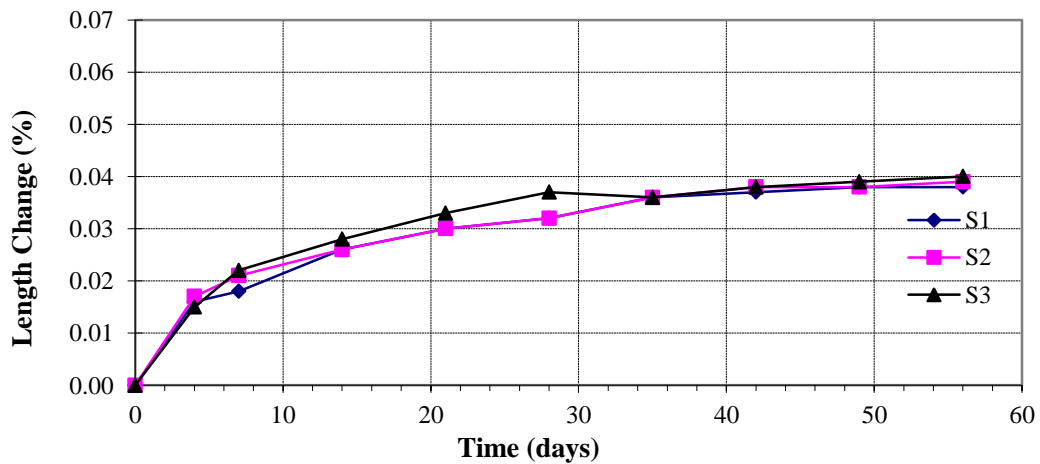


Figure 73 Mix 3 free drying shrinkage results

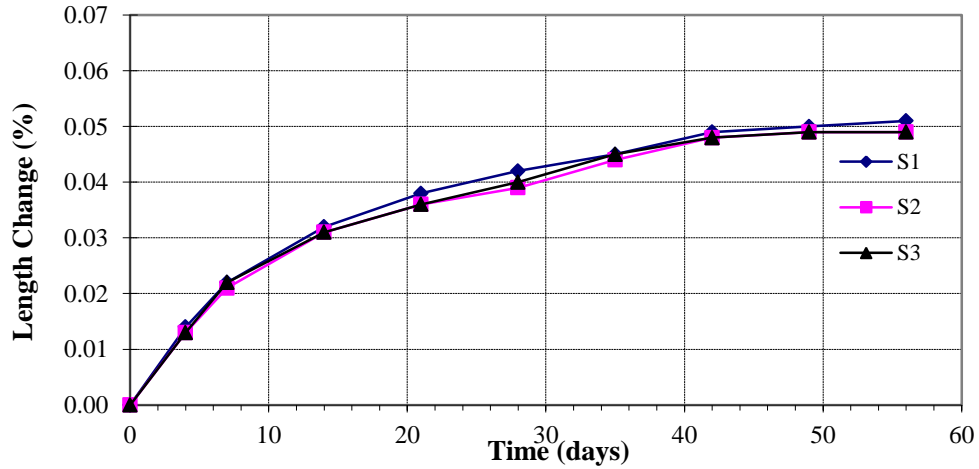


Figure 74 Mix 4 free drying shrinkage results

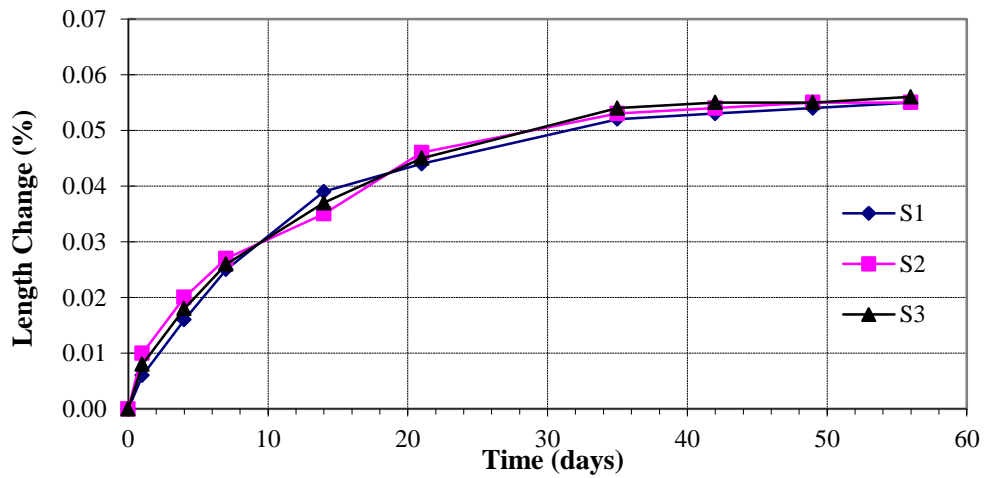


Figure 75 Mix 5 free drying shrinkage results

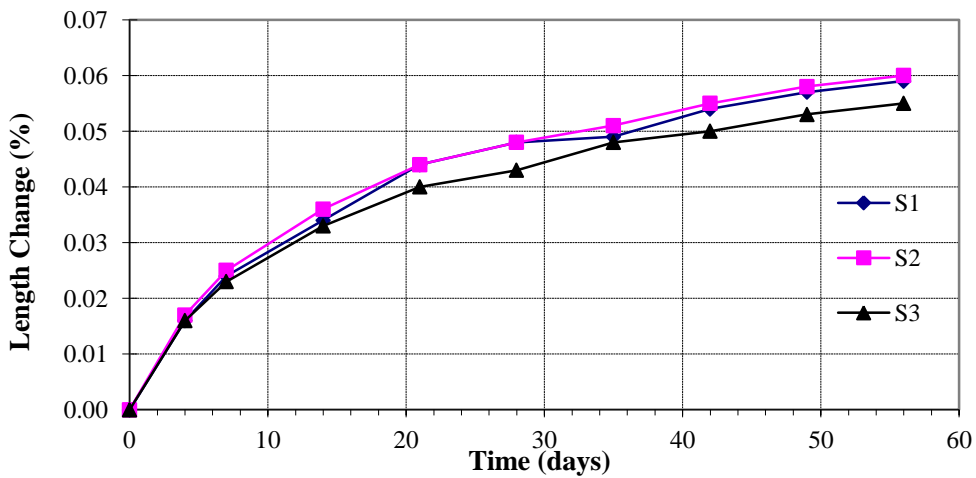


Figure 76 Mix 6 free drying shrinkage results

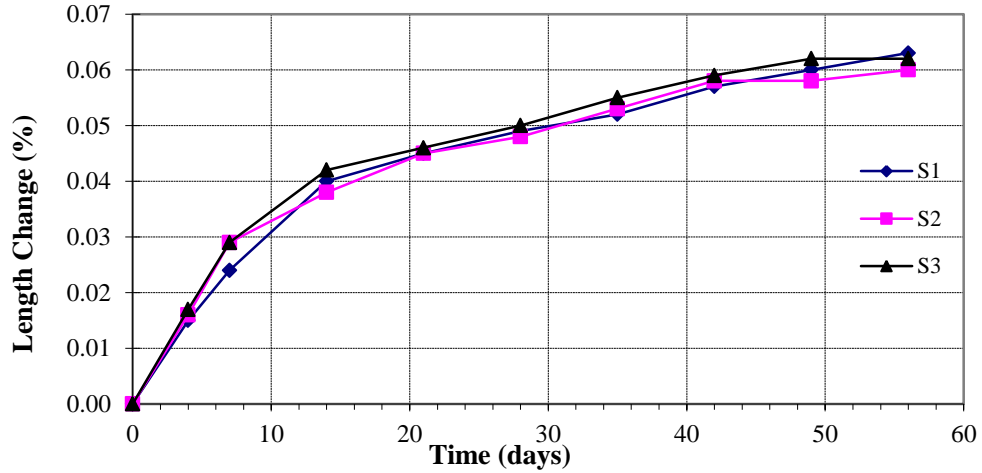


Figure 77 Mix 7 free drying shrinkage results

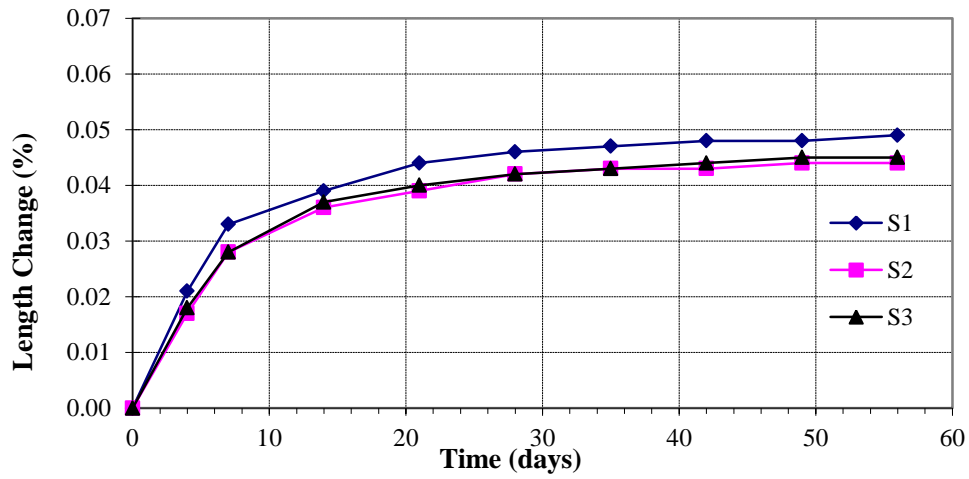


Figure 78 Mix 8 free drying shrinkage results

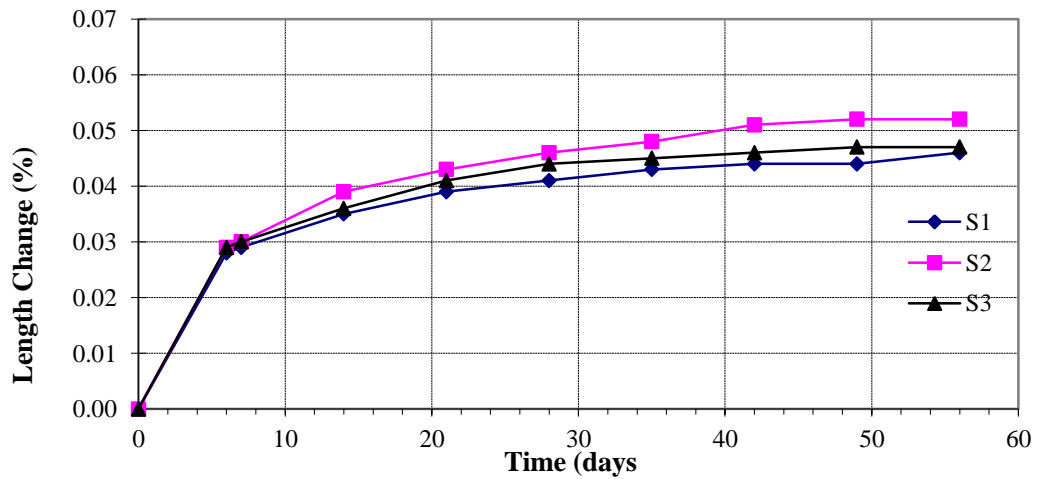


Figure 79 Mix 9 free drying shrinkage results

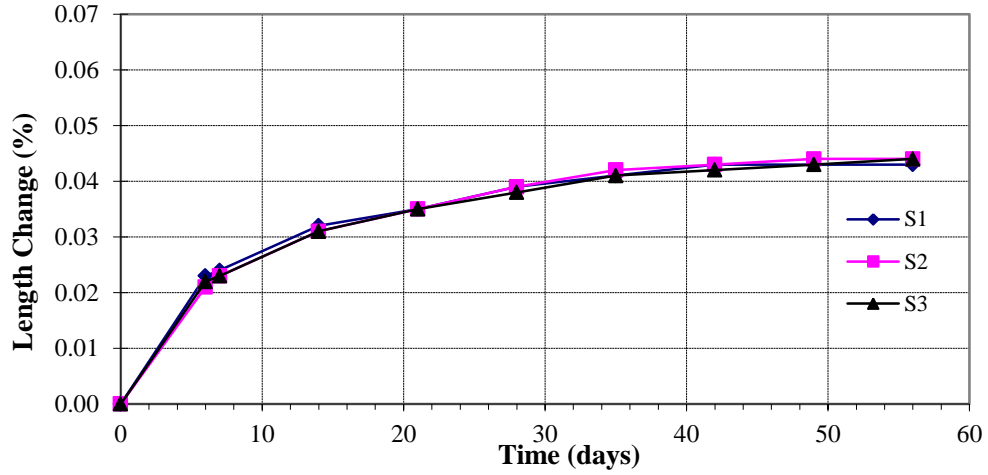


Figure 80 Mix 10 free drying shrinkage results

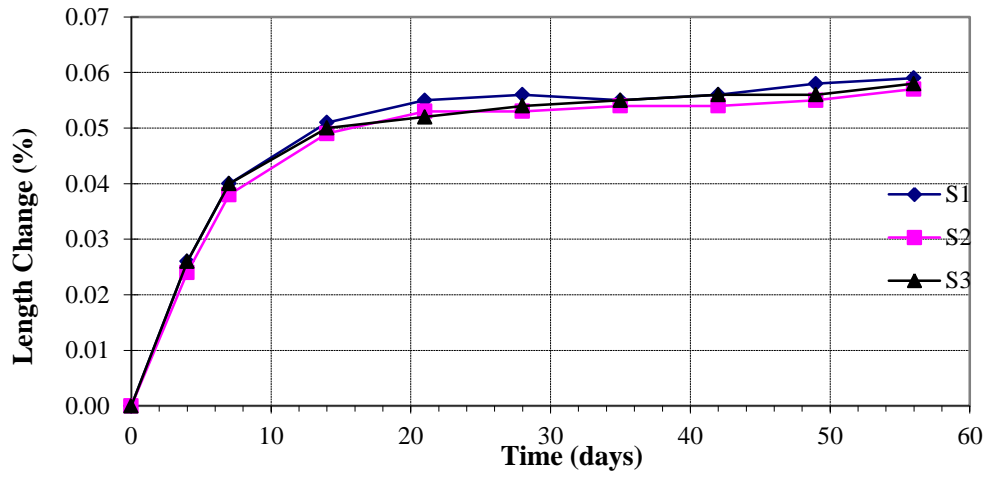


Figure 81 Mix 11 free drying shrinkage results

Restrained shrinkage measurements

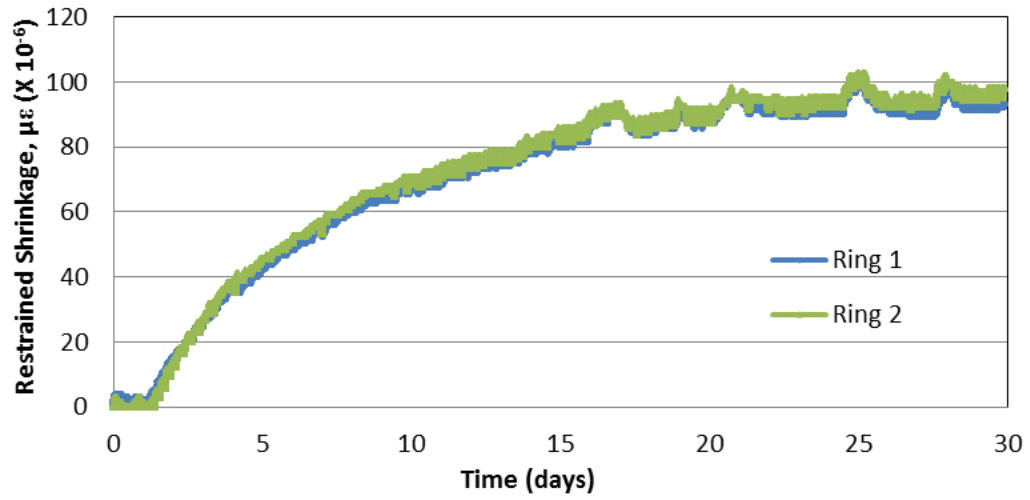


Figure 82 Mix 1 restrained shrinkage results

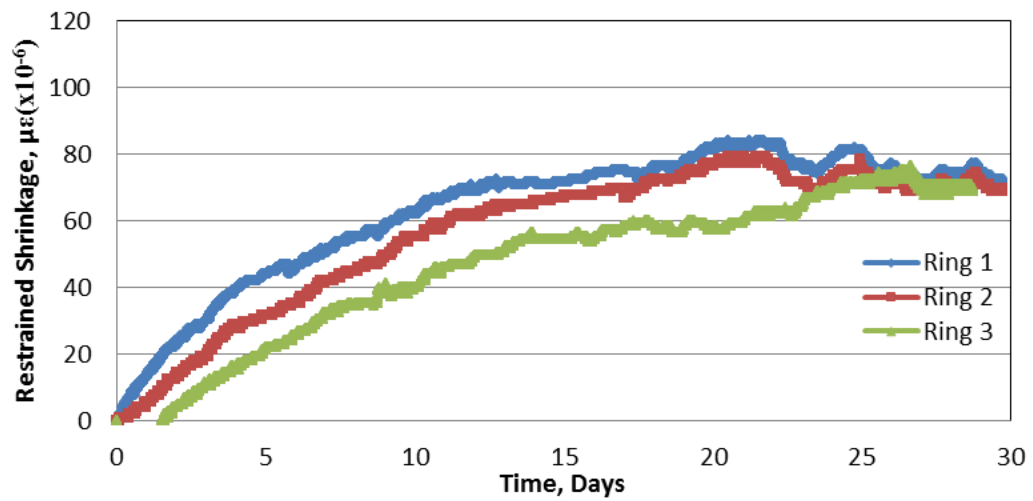


Figure 83 Mix 2 restrained shrinkage results

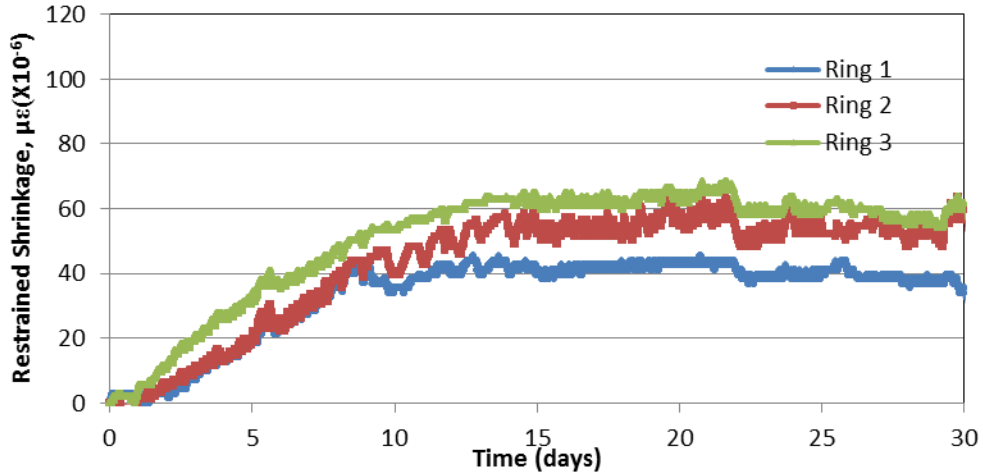


Figure 84 Mix 3 restrained shrinkage results

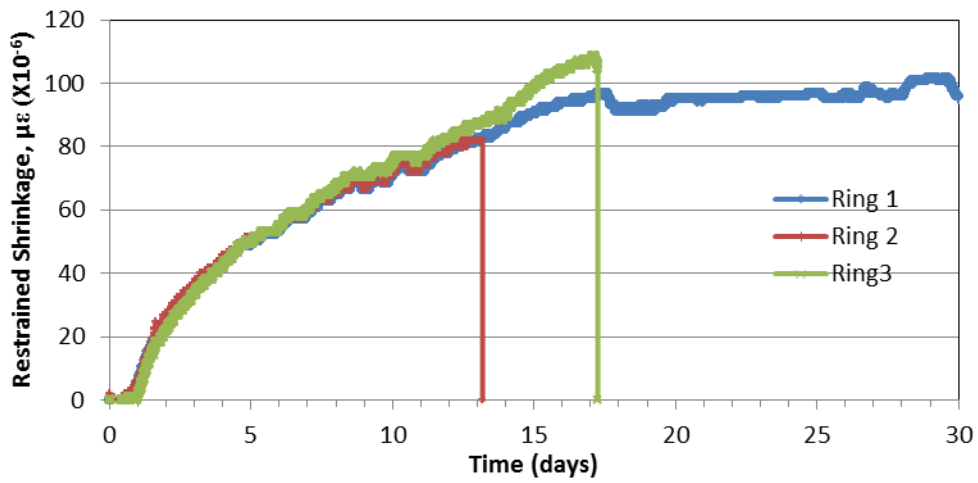


Figure 85 Mix 4 restrained shrinkage result

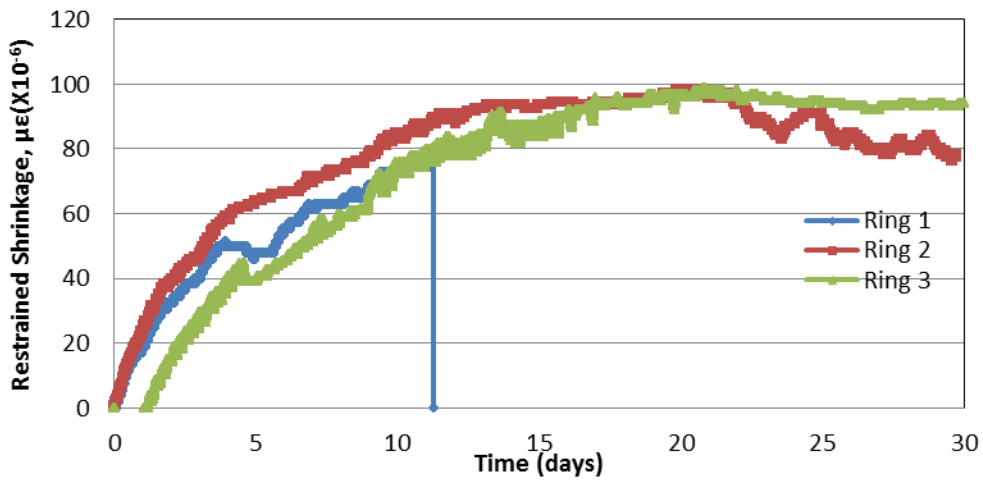


Figure 86 Mix 5 restrained shrinkage results

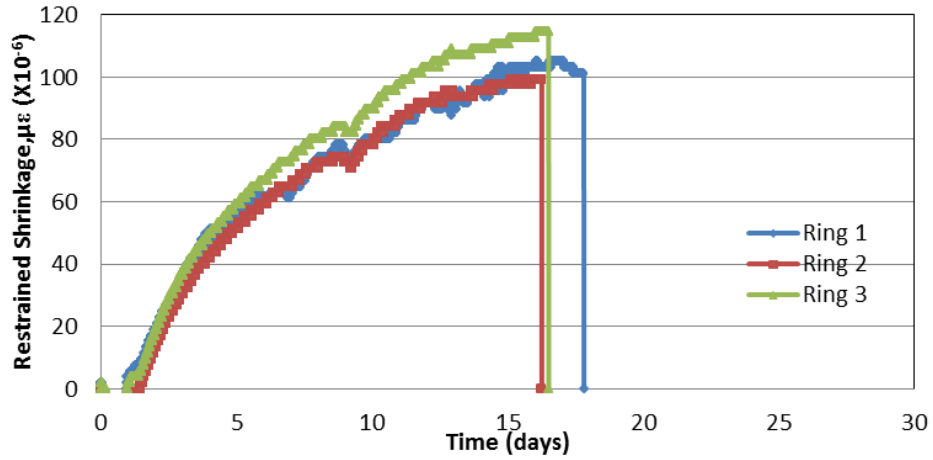


Figure 87 Mix 6 restrained shrinkage results

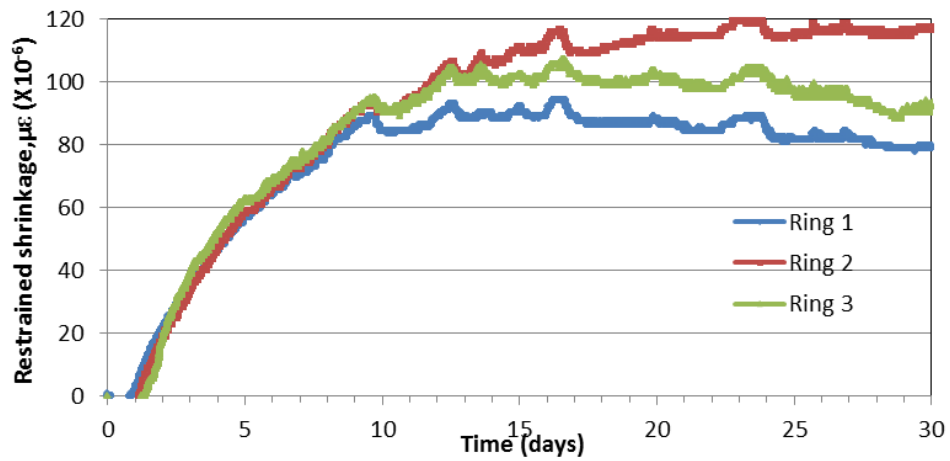


Figure 88 Mix 7 restrained shrinkage results

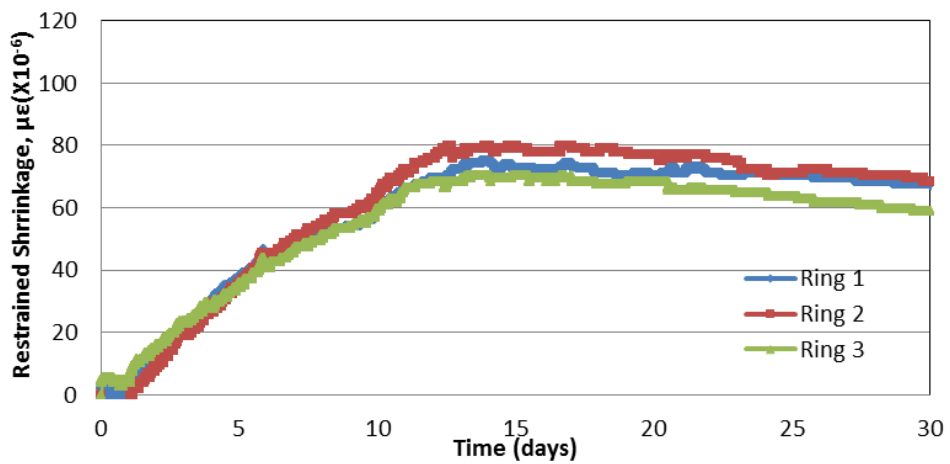


Figure 89 Mix 8 restrained shrinkage results

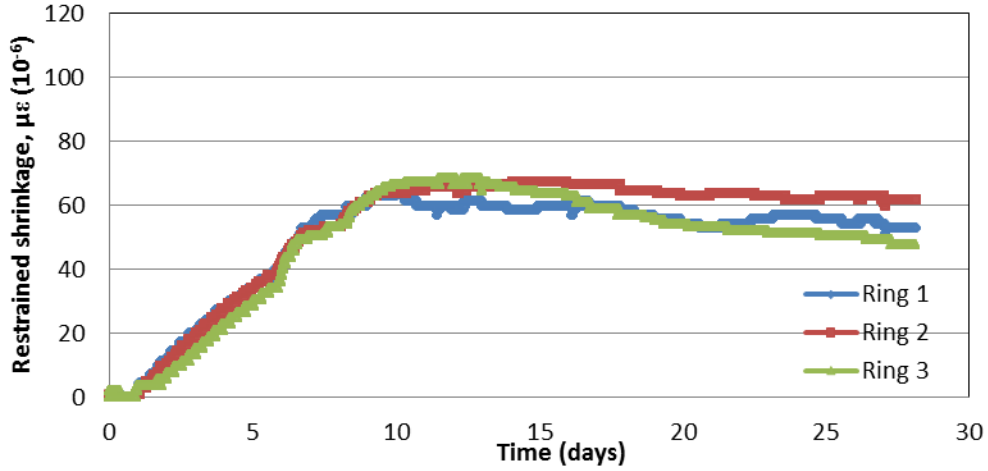


Figure 90 Mix 9 restrained shrinkage results

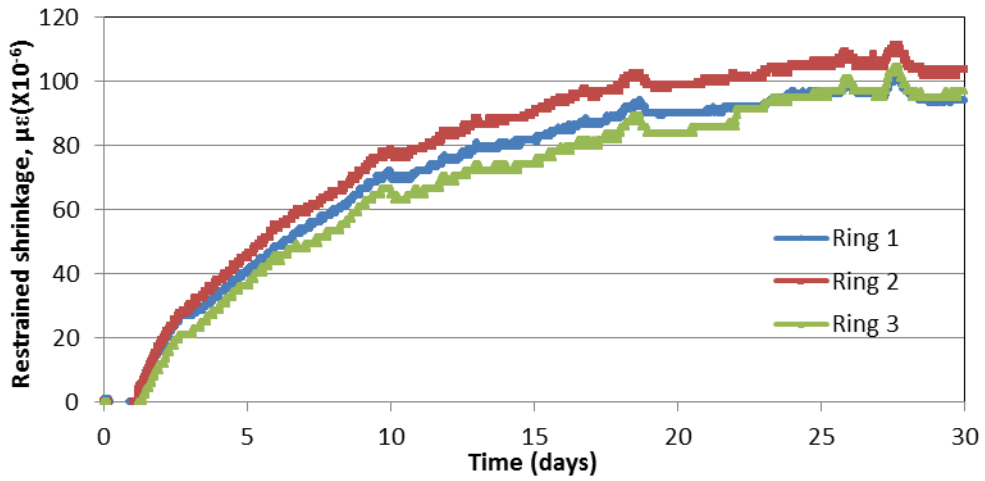


Figure 91 Mix 10 restrained shrinkage results

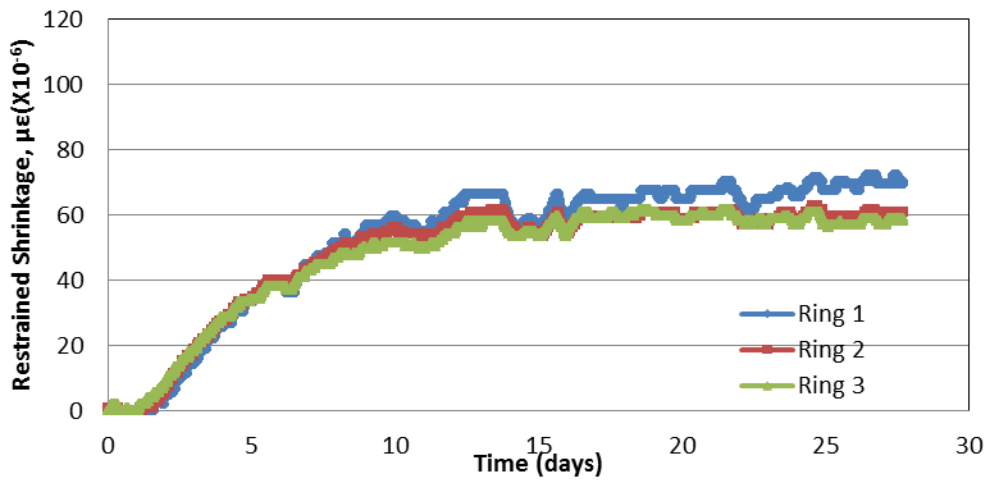


Figure 92 Mix 11 restrained shrinkage results

Compressive strength

Table 22 Results of compressive strength test

Compressive Strength (psi)												
Age (days)	Sample #	Mix 1	Mix 2	Mix 3	Mix 4	Mix 5	Mix 6	Mix 7	Mix 8	Mix 9	Mix 10	Mix 11
1	Sample 1	1273	1228	935	2418	1604	3529	1388	787	498	1401	396
	Sample 2	1328	1095	887	1959	1525	3542	1198	847	493	1358	441
3	Sample 1	1871	2570	1970	2699	2282	4150	2303	1341	952	2386	863
	Sample 2	1912	2516	2100	2757	2249	4157	2068	1387	877	2430	876
7	Sample 1	2445	3390	2564	3101	2497	4812	3043	1814	1528	3358	1808
	Sample 2	2559	3307	2608	3661	2643	4665	2866	1820	1393	3256	1884
14	Sample 1	3222	3984	2927	3684	3359	5177	3516	2549	1937	4172	2638
	Sample 2	3000	4008	3073	3690	3128	5305	3553	2536	2047	4055	2913
28	Sample 1	3864	4495	3521	4093	3654	5696	4130	3559	2856	4525	3159
	Sample 2	3716	4536	3388	4073	3684	6032	3800	3513	2733	4683	3365
56	Sample 1	3970	4698	3687	4502	4111	6988	4070	4845	3871	5038	4004
	Sample 2	4072	5151	3519	4508	3899	6488	4254	4551	4106	4932	3641

Elastic modulus

Table 23 Results of elastic modulus test

Elastic modulus (X 10 ⁶ psi)												
Age (days)	Sample #	Mix 1	Mix 2	Mix 3	Mix 4	Mix 5	Mix 6	Mix 7	Mix 8	Mix 9	Mix 10	Mix 11
1	Sample 1	2.10	1.90	1.65	3.40	3.14	4.35	3.40	2.60	1.65	2.50	1.85
	Sample 2	3.20	2.00	1.80	3.70	2.92	4.45	3.50	2.45	1.50	2.60	1.85
3	Sample 1	1.90	3.40	2.50	3.85	3.05	4.35	3.30	3.35	1.95	3.45	2.60
	Sample 2	3.30	3.40	2.40	3.85	3.70	4.55	3.20	2.90	1.95	3.60	2.80
7	Sample 1	3.50	3.60	3.10	4.25	4.10	4.70	3.75	3.25	3.10	3.60	3.70
	Sample 2	4.10	3.80	3.10	4.50	4.10	4.50	3.70	3.20	3.50	3.20	3.55
14	Sample 1	3.95	3.75	3.40	4.40	4.20	4.70	4.00	3.50	3.35	3.60	3.70
	Sample 2	4.00	3.75	3.60	4.30	4.35	4.60	3.94	3.70	3.40	3.70	3.90
28	Sample 1	3.90	3.70	3.60	4.35	4.40	5.20	3.90	4.00	3.60	3.80	3.80
	Sample 2	3.95	4.00	3.80	4.30	4.90	5.05	4.00	4.05	3.45	3.90	3.90
56	Sample 1	4.30	3.90	3.90	4.60	4.80	5.55	3.85	4.25	3.80	3.85	3.90
	Sample 2	3.90	3.80	3.95	4.50	4.70	5.35	4.05	4.20	3.85	3.95	4.00

Split tensile strength

Table 24 Results of Split tensile strength test

Split Tensile strength (psi)											
Age (days)	Mix 1	Mix 2	Mix 3	Mix 4	Mix 5	Mix 6	Mix 7	Mix 8	Mix 9	Mix 10	Mix 11
1	188	171	140	246	128	350	133	109	40	153	65
3	287	292	219	290	199	400	243	196	89	243	104
7	303	319	289	301	279	391	287	229	210	310	274
14	338	352	337	322	318	439	392	289	281	406	363
28	420	427	384	353	352	469	441	356	383	504	372
56	430	532	408	361	428	518	465	366	460	524	421

Prediction Models for Creep

Creep is the increase in strain of a solid under a sustained stress with time. Creep strain includes two components: a basic creep and a drying creep. The basic creep, C_0 , is the creep occurring when there is no moisture exchange between the concrete and the ambient medium. Drying creep, C_d , is the additional creep experienced when the concrete is allowed to dry while under sustained load. The sum of basic and drying creep is referred to as the total creep. The creep strain per unit of applied stress is defined as specific creep. The ratio between the creep strain (C) and the instantaneous or elastic strain due to the stress (q_1) is defined as creep coefficient (ϕ).

B3 Model

Among many models, the RILEM B3 model is considered in this study because of its simplicity and effectiveness (Bazant and Baweja 1995, 2000). The model is based on a systematic theoretical formulation of the basic physical phenomena involved, couples creep and shrinkage, and agrees better with the most of the test data that exist in the literature.

The B3 model is often applied for portland cement concrete with the following property range:

$$0.35 \leq w/c \leq 0.85, 2.5 \leq a/c \leq 13.5$$

$$2,500 \text{ psi} \leq f_c \leq 10,000 \text{ psi}, 10 \text{ lb/ft}^3 \leq c \leq 45 \text{ lb/ft}^3$$

where: w is water content in lb/ft^3 , c is cement content in lb/ft^3 , a is total aggregate content in lb/ft^3 , and f_c is the 28 day compressive strength of concrete in psi or MPa.

The model gives the compliance function for strain (creep and elastic strain) at time t due to a unit uniaxial constant stress applied at the age of t' as follows:

$$J(t, t') = q_1 + C_0(t, t') + C_d(t, t', t_0)$$

where: q_1 is the instantaneous or elastic strain due to the stress; $C_0(t, t')$ is basic creep (no moisture movement); and $C_d(t, t', t_0)$ is drying creep.

Creep coefficient $\phi(t, t')$ calculated from the compliance function:

$$\phi(t, t') = E(t') J(t, t') - 1$$

where: $E(t')$ is the static modulus of elasticity at load age of t' .

The calculation of the basic creep derived from the time rate of basic creep. The derived equation for normal concrete is as follows.

$$C_0 = q_2 Q(t, t') + q_3 \ln[1 + (t - t')^n] + q_4 \ln(t/t')$$

where: $Q(t, t')$ is a given in Table 25, where $n=0.1$, q_2 , q_3 and q_4 are empirical constitutive parameters. The parameters q_2 , q_3 and q_4 represent aging viscoelastic compliance, non-aging viscoelastic compliance and flow compliance respectively.

$$q_1 = 0.6 \times 10^6 / E_{28}, E_{28} = 57000 \sqrt{f_c} \text{ (fc psi)}$$

$$q_2 = 451.1 c^{0.5} f_c^{-0.9}, q_3 = 0.29 (w/c)^4, q_4 = 0.14 (a/c)^{-0.7}$$

Table 25 Values of function $Q(t, t')$ for $m = 0.5$ and $n = 0.1$

log (t-t')	log t'								
	0.0	0.5	1.0	1.5	2.0	2.5	3.0	3.5	4.0
-2.0	0.4890	0.2750	0.1547	0.08677	0.04892	0.02751	0.01547	0.008699	0.004892
-1.5	0.5347	0.3009	0.1693	0.09519	0.05353	0.03010	0.01693	0.009519	0.005353
-1.0	0.5586	0.3284	0.1848	0.1040	0.05846	0.03288	0.01849	0.01040	0.005846
-0.5	0.6309	0.3571	0.2013	0.1133	0.06372	0.03583	0.02015	0.01133	0.006372
0.0	0.6754	0.3860	0.2185	0.1231	0.06929	0.03897	0.02192	0.01233	0.006931
0.5	0.7108	0.4125	0.2357	0.1334	0.07516	0.04229	0.02379	0.01338	0.007524
1.0	0.7352	0.4335	0.2514	0.1436	0.08123	0.04578	0.02576	0.01449	0.008149
1.5	0.7505	0.4480	0.2638	0.1529	0.08727	0.04397	0.02782	0.01566	0.008806
2.0	0.7597	0.4570	0.2724	0.1602	0.09276	0.05239	0.02994	0.01687	0.009494
2.5	0.7652	0.4624	0.2777	0.1652	0.09708	0.05616	0.03284	0.01812	0.01021
3.0	0.7684	0.4656	0.2808	0.1683	0.1000	0.05869	0.03393	0.01935	0.01094
3.5	0.7703	0.4675	0.2827	0.1702	0.1018	0.06041	0.03541	0.02045	0.01166
4.0	0.7714	0.4686	0.2838	0.1713	0.1029	0.06147	0.03641	0.02131	0.01230
4.5	0.7720	0.4692	0.2844	0.1719	0.1036	0.06210	0.03702	0.02190	0.01280
5.0	0.7724	0.4696	0.2848	0.1723	0.1038	0.06247	0.03739	0.02225	0.01314

Shrinkage:

$$\varepsilon_{s\infty} = -\alpha_1 \cdot \alpha_2 \cdot [26w^{2.1} f_c^{-0.28} + 270] \text{ (in } 10^{-6}\text{)}$$

$$k_t = 190.8t_0^{-0.08} \cdot f_c^{-1/4} \text{ days/in}^2$$

where: α_1 is 1.0 for Type I cement, 0.85 for Type II cement and 1.1 for Type III cement, α_2 is 0.75 for steam curing, 1.2 for sealed or normal curing in air with protection against drying 1.0 for curing in water or at 100% relative humidity.

$$q_5 = 7.57 \times 10^5 f_c^{-1} |\varepsilon_{sh\infty}|^{-0.6}$$

Humidity dependence:

$$k_h = (1 - h^3) \text{ for } h \leq 0.98$$

$$k_h = -0.2 \text{ for } h = 1, \text{ interpolate for } 0.98 \leq h \leq 1$$

Size dependence:

$$\tau_{sh} = k_t (k_s D)^2, D = 2v/s$$

where: $k_s = 1.00$ for and infinite slab, 1.15 for an infinite cylinder, 1.25 for an infinite square prism, 1.30 for a sphere, and 1.55 for a cube.

Sample Calculation

The input data used is for the sample calculation is from Mix 1 for the 28th day of drying at 50% relative humidity after 7 days of 100% relative humidity curing.

Relative humidity	= 50%
Volume/surface ratio (Prismatic specimen)	= 0.662
Cementitious material content	= 24.7 lb/ft ³
Water content	= 10.7 lb/ft ³
Total aggregate content	= 104.3 lb/ft ³
Water/cementitious material ratio	= 0.43
Aggregate/cement ratio	= 4.22
Compressive strength at 28 days	= 3790 psi
Relative humidity factor (h)	= 0.50
Estimated elastic modulus (6)E ₂₈	= 57000* $\sqrt{f_c}$ = <u>3,509,090 psi</u>
q ₁	= 0.6*10 ⁶ /E ₂₈ = 0.6*10 ⁶ /3.5*10 ⁶ = <u>0.171</u>

$$\begin{aligned}
 q_2 &= 451.1c^{0.5}f_c^{-0.9} \\
 &= 451.1*24.7^{0.5}*3790^{-0.9} \\
 &= \underline{1.348} \\
 q_3 &= 0.29 (w/c)^4 q_2 \\
 &= 0.29 *(0.433)^4 * 1.348 \\
 &= \underline{0.01376} \\
 \text{By interpolation from Table A.1, } Q(t,t') &= 0.3784 \\
 \alpha_1 = 1 \text{ (Type 1 cement)} & \\
 \alpha_2 = 1 \text{ (curing under 100\% relative humidity)} & \\
 \epsilon_{sh\infty} &= -\alpha_1 \cdot \alpha_2 \cdot [26w^{2.1}f_c^{-0.28} + 270] \\
 &= 1*1*(26*10.7^{2.1}3790^{-0.28} + 270) \\
 &= \underline{775.68 \text{ (in} * 10^{-6})} = \epsilon_{sh\infty} \\
 q_5 &= 7.57 \times 10^5 f_c^{-1} |\epsilon_{sh\infty}|^{-0.6} \\
 &= 7.57 * 10^5 * 3790^{-1} |775.68|^{-0.6} \\
 &= \underline{10.74} \\
 k_s \text{ (shape factor)} &= 1.25 \text{ (infinite square prism)} \\
 k_t &= 190.8t_0^{-0.08} \cdot f_c^{-1/4} \\
 &= 190.8*7^{-0.08} \cdot 3790^{-1/4} \\
 &= \underline{27.19 \text{ days/in}^2} \\
 \tau_{sh} &= k_t (k_s D)^2 \\
 &= 27.19*(1*2*0.6617)^2 \\
 &= \underline{74.41} \\
 S(t) &= \tanh [(t - t_0) / \tau_{sh}]^{0.5} \\
 &= \underline{0.605} \\
 S(t') &= \tanh [(t' - t_0) / \tau_{sh}]^{0.5} \\
 &= \underline{0} \\
 H(t) &= 1 - (1-h)*S(t) \\
 &= \underline{0.697} \\
 H(t') &= 1 - (1-h)*S(t') \\
 &= \underline{1} \\
 C_o(t,t') &= q_2 * Q(t,t') + q_3 * \ln[1 + (t/t')^n] + q_4 \ln(t/t') \\
 &= \underline{0.546}
 \end{aligned}$$

$$\begin{aligned}
C_d(t,t',t_0) &= q_5 * [\exp\{-8H(t)\} - \exp\{-H(t')\}]^{1/2} \\
C_d(t,t',t_0) &= 0.2415 \\
J(t,t') &= q_1 + C_o(t,t') + C_d(t,t',t_0) \\
&= \underline{0.958} \\
\emptyset(t,t') &= E(t') * J(t,t') - 1 \\
&= 3.50 * 0.958 - 1 \\
&= \underline{2.363}
\end{aligned}$$

Modified NCHRP 496 Model

The NCHRP model has been modified for high strength concrete. These equations were developed because the existing LRDF provisions for estimation of creep did not provide a reliable estimate for high strength concrete.

$$\phi(t,t_i) = 1.9 k_{td} k_{vs} k_f k_{hc} t_i^{-0.118}$$

Ambient Relative humidity correction factor k_{hc} :

$$k_{hc} = 1.56 - 0.008RH$$

Size Correction factor k_{vs} :

$$k_{vs} = 1.45 - 0.13\left(\frac{v}{s}\right)$$

Strength correction factor k_f :

$$k_f = \frac{5}{(1 + f'_{ci})}, \text{ where } f'_{ci} = 0.8f'_c$$

Time development factor k_{td} :

$$k_{td} = \frac{t}{(61 - 4f'_{ci} + t)}, \text{ where } t \text{ is the time for loading}$$

Sample Calculation

The input data used is for the sample calculation is from Mix 1 for the 28th day of drying at 50% relative humidity after 7 days of 100% relative humidity curing.

$$\begin{aligned}
k_{vs} &= 1.45 - 0.13(v/s) \\
&= 1.45 - 0.13 * 0.6617 \\
&= \underline{1.364} \\
k_{hc} &= 1.56 - 0.008RH \\
&= 1.56 - 0.008 * 50 \\
&= \underline{1.16} \\
k_f &= 5 / (1 + f'_{ci})
\end{aligned}$$

$$\begin{aligned}
 &= 5/(1 + 0.8*3.79) \\
 &= \underline{1.24} \\
 \text{For ultimate creep coefficient, } k_{td} &= 1.00 \\
 \varphi(t, t_i) &= 1.9 k_{td} k_{vs} k_f k_{hc} t_i^{-0.118} \\
 &= \underline{\underline{2.515}}
 \end{aligned}$$

Table 26 Summary of calculated creep coefficient

Mix #	Creep Coefficient (28day)		
	B3 model	NCHRP model	Average
1	2.36	2.52	2.44
2	2.19	2.34	2.26
3	2.40	2.87	2.63
4	2.31	2.38	2.35
5	2.36	2.56	2.46
6	2.08	1.80	1.94
7	2.33	2.43	2.38
8	2.45	2.67	2.56
9	2.64	3.14	2.89
10	2.18	2.17	2.17
11	2.47	2.81	2.64

Developing the finite element model in MIDAS 2013

The following steps were followed to develop the finite element model of the deck and overlay.

- Tools > Unit System >
 - Length – inch,
 - Force – kips,
 - Heat – Btu

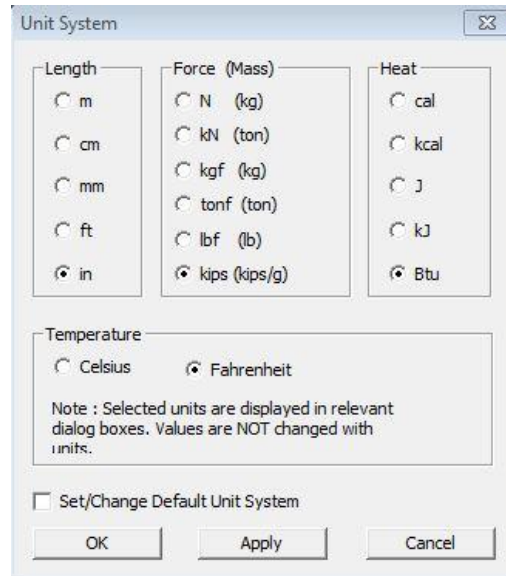


Figure 93 Define unit system

- Properties > Material Properties > Add >
 - Name – Deck,
 - Type of design – Concrete,
 - Standard – ASTM (RC),
 - DB – Grade 6000

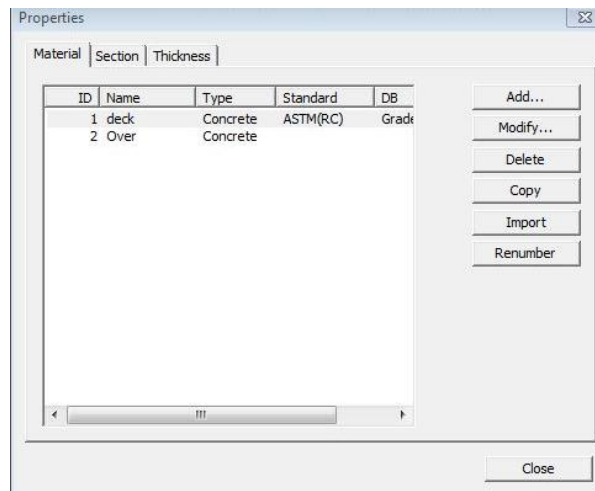


Figure 94 Material property input window

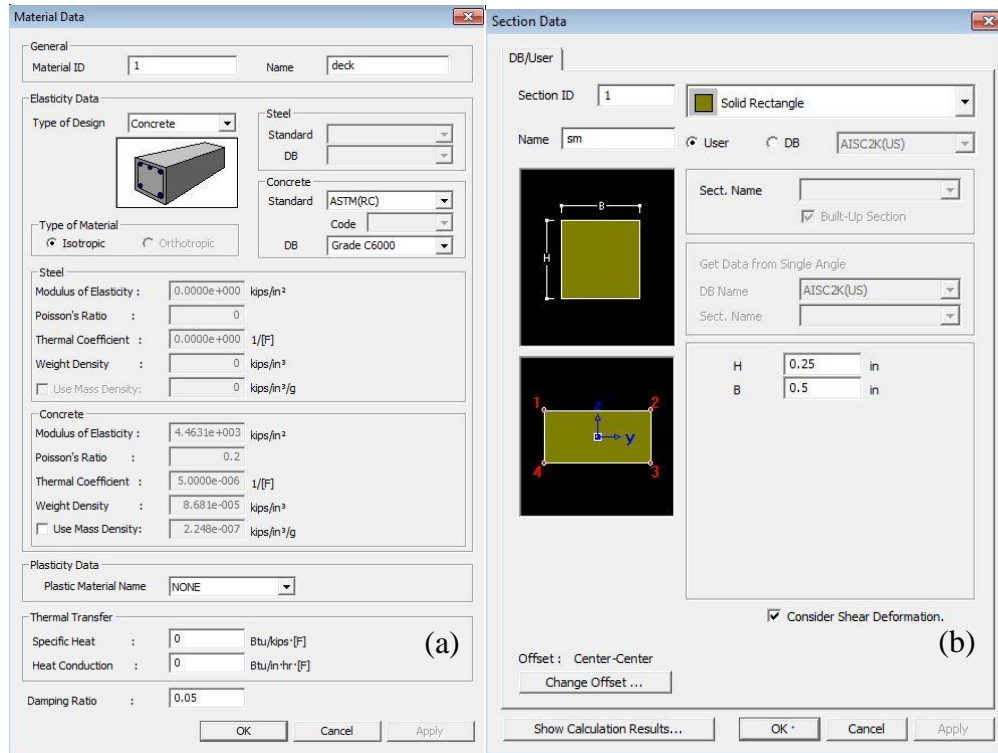


Figure 95 Define (a) material and (b) section data

- Properties > Material Properties > Add >
 - Name – Overlay,
 - Type of design – Concrete,
 - Standard – None,
 - Modulus of Elasticity – Input 28day modulus of elasticity value for specific mix
 - Poisson's ratio – 0.2
- Properties > Section Properties > Add > DB/ User
 - Name – Section 1
 - Section – Solid Rectangle
 - Select user defined tab
 - H – 0.25 in., B – 0.50 in.
- Properties > Compressive Strength > Add
 - Name – Deck
 - Type > Code
 - Code – CEB-FIP

- Mean compressive strength of concrete at the age of 28 days – 6 kips
- Cement type – N, R : 0.25
- Click redraw graph

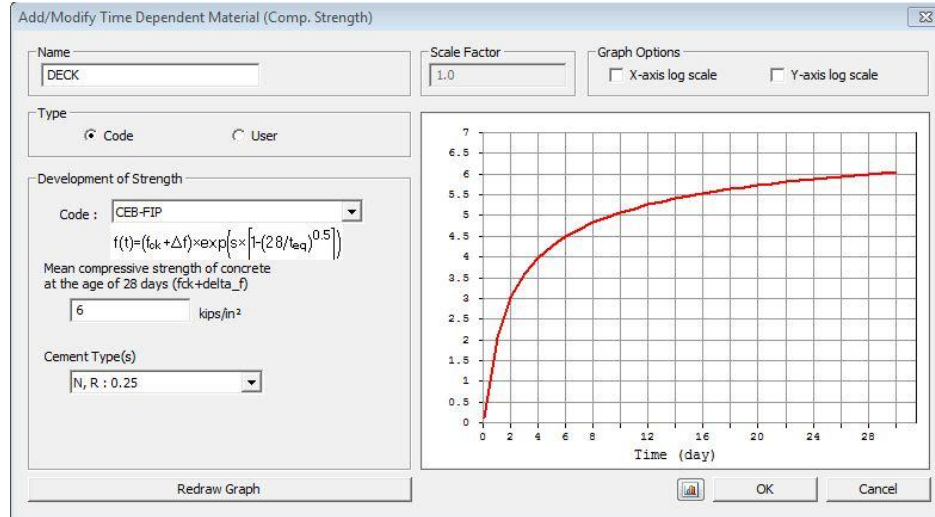


Figure 96 Time dependent material property: compressive strength

- Properties > Compressive Strength – Add
 - Name – Overlay
 - Type – User
 - Input the data for compressive strength, elastic modulus and tensile strength in kips
- Properties > Creep/Shrinkage > Add
 - Name – Deck
 - Code – CEB-FIP (1990)
 - Characteristic compressive strength of concrete at 28 days – 6 kips/in²
 - Relative humidity –50%
 - Notional size of member – 0.25 in
 - Type of cement – normal or rapid hardening cement (N, R)
 - Age of concrete at the beginning of shrinkage – 7 day
 - Click show result to check the creep and shrinkage of the concrete.
- Properties > Creep/Shrinkage > Add
 - Name – Deck
 - Code – User Defined

- Creep Function > Click on the dotted button to add the used defined creep function
- Click Add in the new dialog box that opens
- Function name – Overlay
- Creep function data type – Creep coefficient
- Elasticity – add the elasticity corresponding to the 28 day modulus of elasticity (e.g. 4000 kips/in²)
- Input the values of the average creep coefficient calculated in the table and click ok
- Select the Shrinkage Strain tab > Add
- Function Name – Overlay
- Input the measured values of shrinkage with age of the concrete in the table (e.g. 500 * 10⁻⁶)
- Click ok and close the dialog box that was used to add the creep function
- Select the creep function and add the age at loading. Then click add creep function.
- Tick the shrinkage strain function and select the shrinkage strain function for the selected mix. Click ok to apply the selected creep and shrinkage and close the dialog box.

Add/Modify Time Dependent Material (Creep / Shrinkage)

Name : Code :

CEB-FIP(1990)

Characteristic compressive strength of concrete at the age of 28 days (fck) : kips/in²

Relative Humidity of ambient environment (40 - 99) : %

Notational size of member : in

$h = 2 * A_c / u$ (A_c : Section Area, u : Perimeter in contact with atmosphere)

Type of cement

Rapid hardening high strength cement (RS)

Normal or rapid hardening cement (N, R)

Slowly hardening cement (SL)

Age of concrete at the beginning of shrinkage : day

Show Result... OK Cancel Apply

Figure 97 Time dependent material property: creep and shrinkage

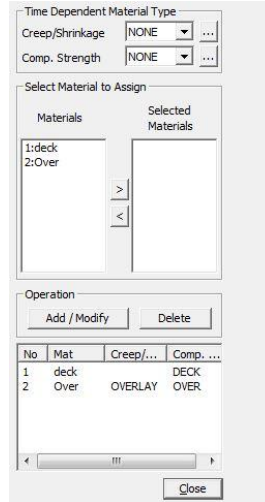


Figure 98 Material link

- Properties > Material Link
- Time dependent material property > Creep/Shrinkage – deck, compressive strength – deck
- Select material Deck and move it to the selected material column using the “>” symbol.
- Click Add/Modify to combine the time dependent material properties to the deck concrete.
- Similarly select the properties for the overlay concrete and combine their effects to the overlay material

Note: the creep and shrinkage of the deck concrete was removed from the groups tab subsequent to the material link function. This was done to eliminate the effects of the deck structure to not affect the stress levels observed in the overlay.

- Node/Element > Create Nodes > Create nodes
 - Coordinates – 0, 0, 0
 - Copy – 0
 - Distance – 0, 0, 0
 - Click Apply

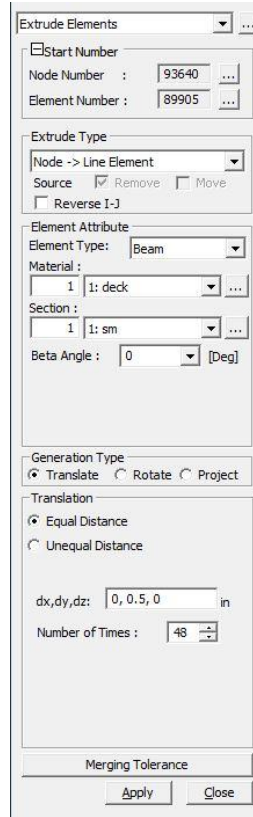



Figure 99 Extrude elements

- Node/Element > Extrude
 - Extrude type > None → Line element
 - Extrude attribute – Element type > Beam, Material – Deck, Section – Section 1
 - General type – Translate
 - Translation – Equal distance, [dx, dy,dz]: (0.5, 0, 0), Number of times – 48, Click Apply
- Node/Element > Extrude
 - Extrude type > Line element → Planar element
 - Extrude attribute – Element type > Plate, Material – Deck,
 - General type – Translate
 - Translation – Equal distance, [dx, dy,dz]: (0, 0.5, 0), Number of times – 48, Click Apply
- Node/Element > Extrude
 - Extrude type > Planar element → Solid element

- Extrude attribute –Element type > Solid, Material – Deck,
- General type – Translate
- Translation – Equal distance, [dx, dy,dz]: (0, 0, 0.25), Number of times – 38, Click Apply

Get the right view by simultaneously pressing Ctrl+Shift+R and select the top 7 layers of the model (Figure 2) using the select nodes icon . Go to the works tab in the tree menu and expand the material tab by clicking on the “+” sign. Drag and drop the material “Overlay” to the model view plane. Once applied successfully the selected nodes will return the original light blue color.

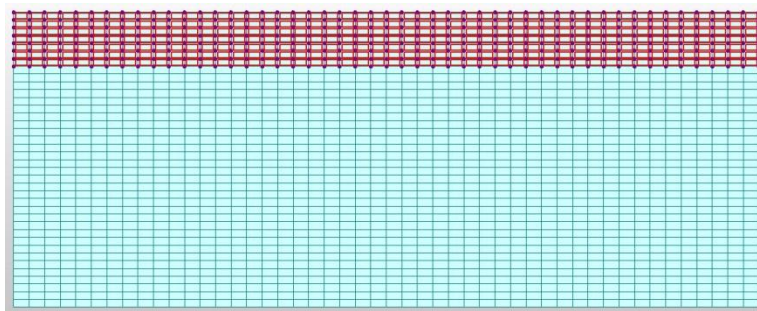



Figure 100 Overlay selected

- Boundary > Define Supports
 - Select the top view by pressing Ctrl+Shift+T simultaneously
 - Use the select nodes icon  and select all the nodes parallel to x and y axes (Figure 3)

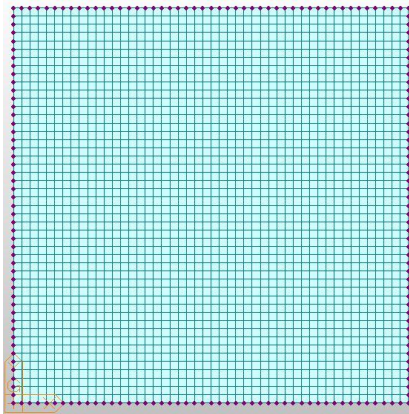


Figure 101 All nodes parallel to x and y axes selected

- Boundary group name – Default, Options – Add

- Support type – Select both D-All and R-All, and click apply

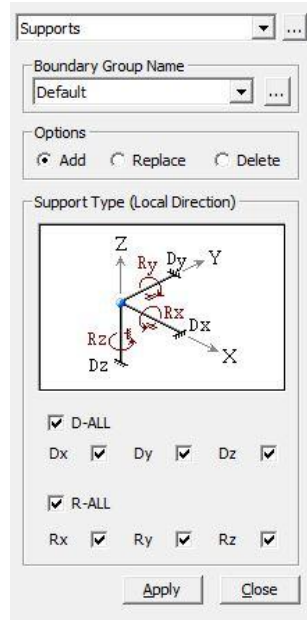


Figure 102 Define supports

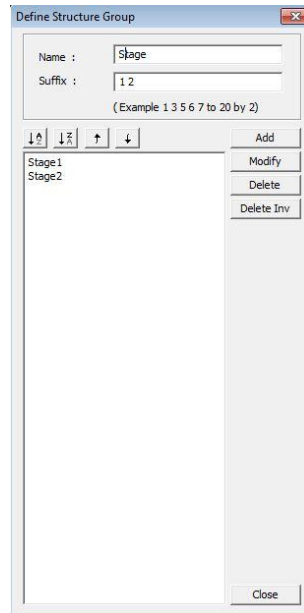
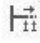


Figure 103 Define structure groups

Use the group tab in the tree menu to create structure and boundary groups

- Tree menu > Groups> Structure group> New
 - Name – Stage
 - Suffix – 1to2, Click add and close the window
 - Press Ctrl+Shift+R simultaneously to get the right view and select the bottom 31 elements (Deck). Drag and drop the Structure group Stage 1 to the Model view plane. Select the top 7 layers and Drag and drop the Stage 2 of structure groups to the model view plane.
 - Follow the same procedure for boundary groups by creating Stage 1 and Stage 2.
- Select the Define Construction Stage tab  and click Generate.
 - Click Generate in the window that opens
 - Name – Stage
 - Suffix – 1to2
 - Save result – tick both stage and additional steps, click apply and close the window.
 - Select stage 1 in the window and click modify
 - Define duration as 9000 days
 - Under the element tab select Stage 1 and under the activation tab type 7 days. Then click add.
 - In the boundary tab select Stage 1 and deformed in the activation section. Then click add. Click ok in the main window to return to the original window and select Stage 2
 - Define duration as 56days under additional steps type 1, 3, 7, 14, 28 and click add. Five additional steps will appear in the window.
 - Follow similar steps for element and boundary group as in Stage 1. Activation age for the Stage 2 is 3 days.
 - Click ok and close the original window.

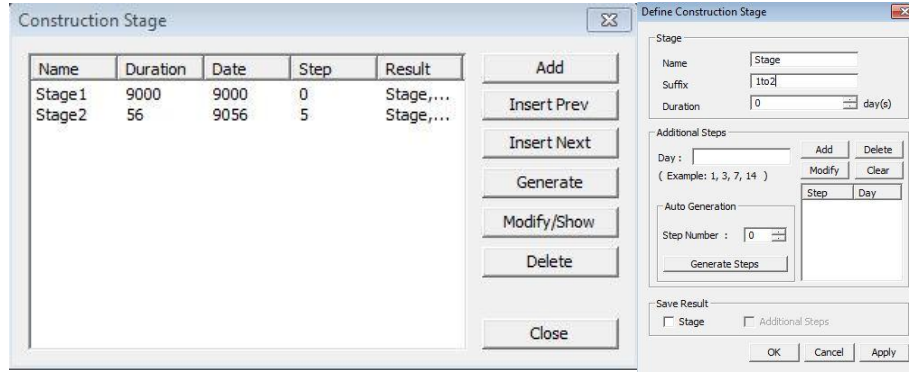


Figure 104 Define construction stages

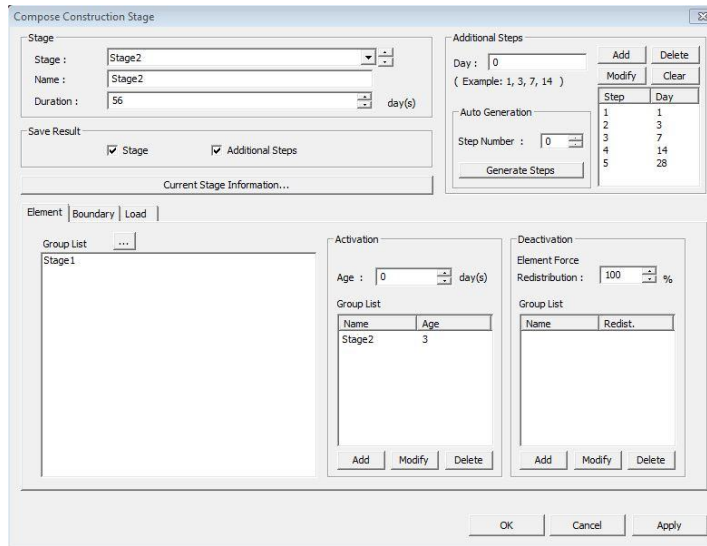
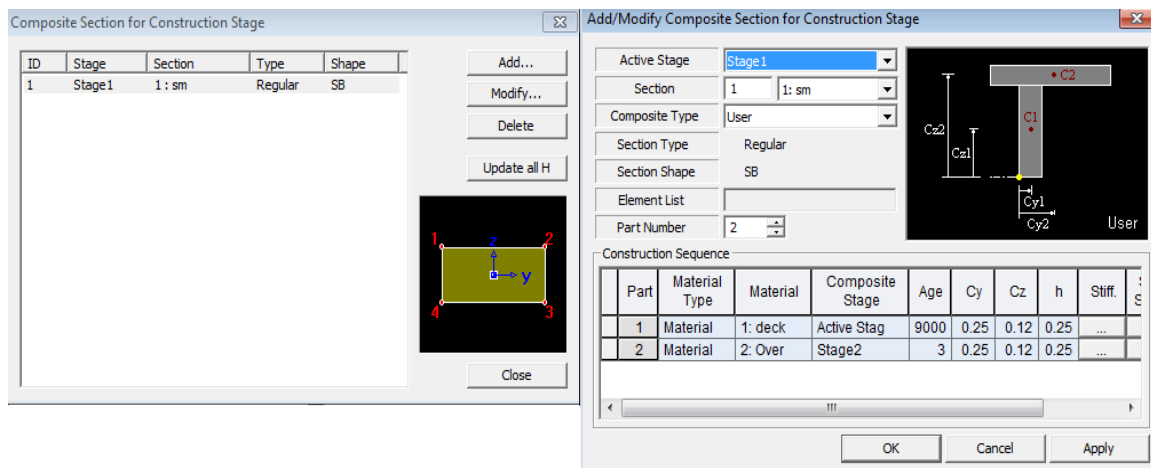



Figure 105 Compose construction stages



- Click composite section for construction stage icon  in the model view plane.
 - Click add, in the new dialog box input Part Number 2
 - For part one select material type and find material in the drop down menu.
 - Under the material section select 1:Deck.in the drop down menu.
 - Composite stage – Active Stage
 - Age – 9000
 - $C_y = 0.25$, $C_z = 0.125$, $h = 0.25$, click the stiffness section to import the section and select Section 1
 - For part 2 select material under material type, then Overlay under material and Stage 2 under composite stage.
 - Age – 3
 - $C_y = 0.25$, $C_z = 0.125$, $h = 0.25$, click the stiffness section to import the section and select Section 1
 - Click ok and close the main window
- Analysis> Construction Stage
 - Select last stage
 - Tick time dependent effect and open the time dependent effect control. Under type select creep and shrinkage. Select Auto time step generation for large time gap, tendon tension loss effect, variation of compressive strength, apply time dependent effect elastic modulus to post C.S. and click ok.
 - Select calculate output for each composite section under frame output and save output for construction stage and click ok.
- Click perform analysis for the program to execute the analysis
- After the MIDAS civil has finished its analysis go to: Results > Stresses > Solid Stresses
- Select the construction stage in the drop down menu in the model view to Stage 2
- Select secondary shrinkage under load combination to find the restrained shrinkage effect the structure.

- Under steps select user step 1 and under components select Sig-xx and for type of display select contour and legend. Click apply for the results to appear in the model view plane.

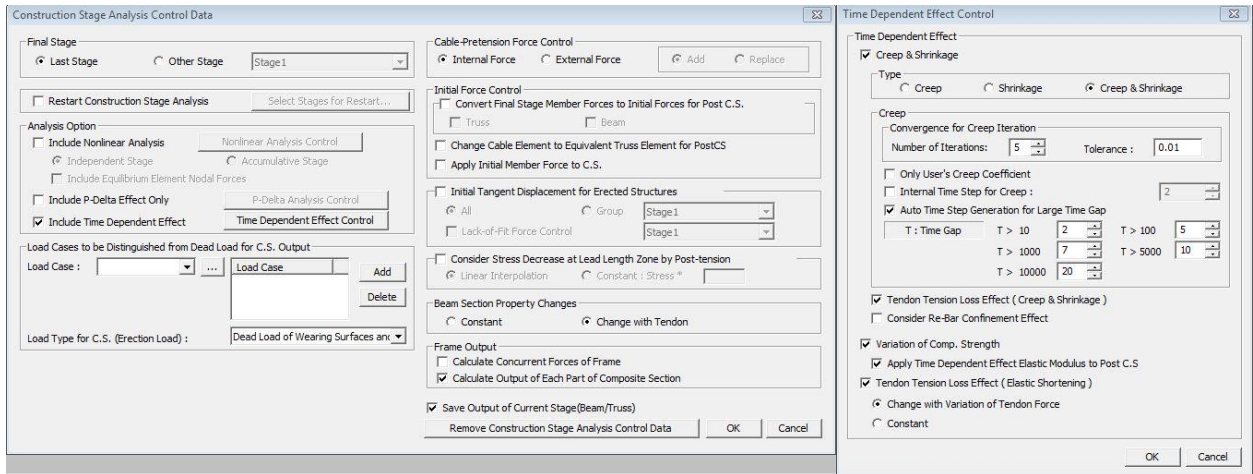


Figure 107 Construction stage analysis control data